NBER WORKING PAPER SERIES

THE DEATH AND LIFE OF GREAT BRITISH CITIES

Stephan Heblich
Dávid Krisztián Nagy
Alex Trew
Yanos Zylberberg

Working Paper 34029
http://www.nber.org/papers/w34029

NATIONAL BUREAU OF ECONOMIC RESEARCH
1050 Massachusetts Avenue
Cambridge, MA 02138
July 2025, Revised June 2026

We thank Gabriel Ahlfeldt, Pierre-Philippe Combes, Kerem Cosar, Don Davis, Jonathan Dingel, Gilles Duranton, Fabian Eckert, Pablo Fajgelbaum, James Feigenbaum, Ed Glaeser, Laurent Gobillon, Gordon Hanson, Miklos Koren, Hans Koster, Oleg Itskhoki, Guy Michaels, Eduardo Morales, Henry Overman, Javier Quintana, Steve Redding, Jean-Marc Robin, Michele Rosenberg, Esteban Rossi-Hansberg, Olmo Silva, Robert Staiger, Daniel Sturm, Lin Tian, Elisabet Viladecans-Marsal, Pablo Warnes, David Weinstein, as well as participants in seminars and conferences at Birmingham, Bocconi, Bologna, Bristol, BU, CERGE-EI, Chicago Fed, Cologne, CRED, CREi, CURE, Dortmund, the EEA meetings, ENS-Lyon, FREIT, Georgetown, HEC, Helsinki, HU Berlin, IAB Urban Labor Markets and Local Income Inequality workshop, INSEAD, LSE, McGill, NBER SI, Oregon, Oslo, Penn State, Philadelphia Fed, Princeton, Paris 1, PSE, Reading, Richmond Fed, RWI, Sciences-Po, SED, Sheffield, SMU, Toronto, Tufts, UCL, UCLA, UEA, UPF, USC, Virginia, Washington, Warwick, Wilfrid Laurier University, the World Bank, and York for useful comments. We would also like to thank Clement Gorin for invaluable advice and the Cambridge Group for the History of Population and Social Structure, the British Library, Alexis Litvine and Gethin Rees for their help with data. Heblich and Zylberberg acknowledge support from the ANR/ESRC/SSHRC, through the ORA grant ES/V013602/1 (MAPHIS: Mapping History). The views expressed herein are those of the authors and do not necessarily reflect the views of the National Bureau of Economic Research.

The Death and Life of Great British Cities
Stephan Heblich, Dávid Krisztián Nagy, Alex Trew, and Yanos Zylberberg
NBER Working Paper No. 34029
July 2025, Revised June 2026
JEL No. F63, N93, O14, R13

ABSTRACT

Does industrial concentration shape the life and death of cities? Using newly constructed data that identify and track English and Welsh cities from the early nineteenth century to the present, we estimate the causal effects of industrial concentration and city size on urban dynamics. We show that greater industrial concentration reduces long-run productivity, conditional on industry-specific trends, consistent with the presence of cross-industry (Jacobs) externalities. We embed these dynamic city-level externalities in a quantitative multi-sector spatial model to evaluate their aggregate and distributional implications. Shutting down Jacobs externalities would reduce today's North-South productivity divide by over 40%. The model also reveals a dynamic trade-off in the design of spatial clusters: patient policymakers favor diversification, whereas those prioritizing short-run gains favor concentration.

Stephan Heblich
University of Toronto
Department of Economics
and NBER
stephan.heblich@utoronto.ca

Dávid Krisztián Nagy
Centre de Recerca en Economia
Internacional (CREI)
dnagy@crei.cat

Alex Trew
University of Glasgow
Adam Smith Business School
alex.trew@glasgow.ac.uk

Yanos Zylberberg
University of Bristol
yanos.zylberberg@bristol.ac.uk

Many of the cities and regions that drove the industrial transformation of the nineteenth century declined during the twentieth century. Formerly thriving areas—such as the towns of Lancashire, the Rust Belt cities of the northeastern United States, and the Ruhr Valley in Germany—grew rapidly and employed generations of workers, yet later struggled to sustain long-run economic success. One explanation is *external* to cities: macroeconomic forces of demand and technological change shape industry dynamics at the national level, and urban fortunes are tied to the aggregate trajectories of the industries in which cities hold a comparative advantage. A second explanation is *internal* to the city: a city's industrial portfolio may influence its long-run development even after accounting for external industry trends. The important role of long-run, between-industry externalities in driving urban growth was formalized in the influential contribution of Glaeser et al. (1992), building on the seminal insights of Jacobs (1961, 1969) in *The Death and Life of Great American Cities*.

This paper focuses on (i) identifying the strength of these within-city drivers and (ii) quantifying their consequences for the spatial dynamics of economic activity. Our analysis draws on unique data tracing the evolution of employment and industrial structure across England and Wales over two centuries. Specifically, we delineate the footprint of potential cities in the early nineteenth century using historical maps; track their growth during the period of rapid urban and industrial expansion using a "quasi-census" based on baptism records around 1817 and a full micro-census in 1881, by which time urban structures had largely stabilized; and measure long-run performance using a rich set of contemporary outcomes, including firm-level production data. In the first step, our reduced-form analysis provides evidence of long-run between-industry externalities: higher industrial concentration in 1881 has a strong negative effect on subsequent city productivity, independent of secular industry trends. In the second step, we develop and estimate a multi-sector spatial model in which heterogeneous cities produce and trade goods, and dynamics are shaped by city-specific externalities (including Jacobs externalities) and exogenous industry-wide trends. We show that the industrial concentration patterns that emerged in nineteenth-century Britain play a persistent role in regional disparities: absent long-run Jacobs externalities, the present-day North-South productivity gap would be roughly 40% smaller.

Britain provides an ideal setting for this analysis. Over the nineteenth century, the adoption of labor-saving technologies, the shift toward large-scale steam-powered production, and the rapid expansion of domestic and international trade fundamentally reshaped the economy. These forces transformed both the scale and structure of cities and industries: the predominantly small, mixed settlements of the early nineteenth century gave way to a dense network of larger industrial cities. By the end of the century, cities

in England and Wales had emerged into markedly different economic structures—some developed diversified industrial bases, others specialized in a narrow set of activities; some sustained long-run growth, others stagnated. The neighboring cities of Bradford and Leeds illustrate this divergence. Similar in size and economic structure around 1800, both cities expanded rapidly during the nineteenth century as industrialization transformed northern England. Bradford—known as "Worstedopolis"—specialized heavily in worsted wool production and became one of the world's leading textile centers, whereas nearby Leeds developed a more diversified industrial base spanning textiles, engineering, machinery, and commercial services. Over time, these differences translated into divergent economic trajectories: Leeds emerged as Yorkshire's economic center, while Bradford experienced relative economic decline.

Our analysis extends the example of Bradford and Leeds to England and Wales as a whole, exploiting a newly constructed spatial dataset that identifies early nineteenth-century settlements from historical maps and follows their evolution over two centuries. To locate and delineate potential cities in the early nineteenth century, we assemble historical maps from around 1790–1820, develop a machine-learning algorithm to detect buildings, and apply a delineation procedure that identifies urban settlements as sufficiently large clusters of built-up areas (De Bellefon et al., 2021). This approach yields a dataset of roughly 400 early settlements and their boundaries—each a potential city by the late nineteenth century. We then nest economic activity within these evolving geographies throughout the nineteenth century and into the present.

The first step of our analysis assesses the strength of long-run Jacobs externalities using a *reduced-form specification* that accounts for agglomeration economies and industry trends. The key challenge is to isolate exogenous variation in industrial concentration around 1881, independently of city size. We separately estimate the effects of industrial diversity and city size on long-run urban dynamics using two distinct instruments. To predict late nineteenth-century industrial concentration, we construct a *shift-share* industrial Herfindahl index that combines (i) aggregate, exogenous variation in labor demand across sectors (the "shifts") with (ii) initial location advantages (the "shares"), measured by the two-digit industrial composition of early settlements in 1817. Settlements with different initial portfolios of comparative advantage were differentially exposed to subsequent changes in global demand and production costs across industries, generating plausibly exogenous variation in later specialization patterns over and above their effect on city size. To instrument for city size, we instead build on the idea that geographic constraints on urban expansion shape local land supply elasticities (Saiz, 2010). Specifically, we draw on the historical insight that land ownership fragmentation at the urban fringe constrained urban expansion during industrialization. This mechanism lies

at the core of the land assembly problem (see, e.g., Eckart, 1985; Strange, 1995): greater fragmentation increases the costs of assembling land for urban use. Because observed land ownership patterns were partly shaped by local institutions (Heldring et al., 2022), we develop an algorithm to predict *natural* boundaries between agricultural land parcels, defined by multidimensional discontinuities in soil characteristics and topography. Our instrument for nineteenth-century city size is the density of such *natural* parcels around early settlements, measured within a buffer corresponding to their expected growth, following related approaches in Saiz (2010) and Harari (2020).[1]

Identification rests on two conditions: (H1) relevance and (H2) exogeneity. The relevance condition motivates our search for independent sources of variation with sufficient explanatory power: *natural* land fragmentation constrains city growth without directly affecting industrial diversity, while the shift-share Herfindahl index primarily predicts industrial concentration. Exogeneity of the industrial concentration instrument builds on recent advances in the identification of shift-share designs (Borusyak et al., 2022): our empirical strategy isolates quasi-random variation in aggregate industrial dynamics (the "shifts") that is plausibly independent of local conditions. The exclusion restriction for the land-fragmentation instrument requires that it has no direct effect on subsequent city dynamics from the early twentieth century onward. To support these (conditional) exogeneity assumptions, we control for employment levels, industrial concentration, and agricultural employment shares in 1817, and account for aggregate industry trends during the twentieth century. The empirical analysis further includes extensive controls for first-nature geography (topography, agricultural productivity, latitude and longitude, waterways) and second-nature geography (transport infrastructure, market access, and travel time to resources), as well as measures of *natural* ownership fragmentation relevant during the twentieth-century.

Our reduced-form results reveal that cities that were more specialized in 1881 are substantially less productive in the long run. A 0.10 increase in the two-digit industrial Herfindahl index—approximately 60% of a standard deviation—reduces labor returns by 23% and firm productivity by 24% around 2020, with the latter estimate conditioning on four-digit industry fixed effects, local industry shares, and firm-level factor inputs. By contrast, city size in 1881 has limited predictive power for long-run outcomes, consistent with Gibrat's law. A wide range of robustness checks confirms that these findings are not driven by differential agricultural productivity (Coeurdacier et al., 2022), exposure to the Grain Invasion (Heblich et al., 2024), parliamentary enclosures (Heldring et al., 2022), broad sectoral dynamics, or any specific two-digit industries. Finally, the es-

[1]We validate the predictive power of *natural* land fragmentation by comparing it to the actual concentration of ownership in micro-census records that report land acreage by owner.

timated Jacobs externalities appear spatially localized and exhibit limited heterogeneity across aggregate industrial compositions.

The long-run impact of industrial concentration on local productivity may operate through several channels. A central mechanism, emphasized by Jane Jacobs, concerns knowledge externalities and cross-industry spillovers in innovative activity. We leverage the recent digitization of British patent records to estimate the causal negative effect of industrial concentration on innovation *intensity*, innovation *diversity*, and its *cross-industry* nature (see Boeri and Silva, 2025, for in-depth evidence on spillovers in Britain, 1851–1911). This pattern mirrors the historical contrast between Bradford and Leeds: specialized Bradford exhibited concentrated patenting in textiles, whereas diversified Leeds generated a broader range of innovations, including general-purpose technologies (e.g., power transmission systems) and adapting textile machinery innovations to locomotives, traction engines, and agricultural equipment. A century later, Leeds is widely regarded as Yorkshire's economic center, whereas Bradford's productivity stands roughly 40 percent below the national average.

The second step of our analysis integrates these dynamic forces into a multi-sector spatial model to study the evolution of industries across cities over time. The model features a set of cities that trade the outputs of a finite set of industries. At any point in time, cities may differ in sectoral productivity, amenities, land supply elasticity, and bilateral trade costs. The framework accommodates three types of externalities: (i) contemporaneous agglomeration externalities; (ii) long-run effects related to city size; and, (iii) long-run Jacobs externalities related to industrial diversity. The latter two stem from random meetings among local workers that generate new ideas, in the spirit of Buera and Lucas (2018). In our quantification, we credibly estimate long-run Jacobs externalities, while conditioning on contemporaneous and long-run Marshall–Arrow–Romer effects (see Carlino and Kerr, 2015, for a review about important determinants of city growth), and we parameterize contemporaneous agglomeration spillovers. The model rationalizes the spatial distribution of economic activity in the late nineteenth century: low trade costs encouraged specialization according to comparative advantage, while land availability shaped the extent of urban expansion. Because of aggregate industry trends and long-run Jacobs externalities, this nineteenth-century heterogeneity produced sharply divergent city trajectories into the twentieth century. Cities with a location advantage in originally flourishing but later floundering industries suffer by dint of their reliance on that sector (due to structural change or international competition, see Ngai and Pissarides, 2007; Pierce and Schott, 2016), while long-run Jacobs externalities generate persistent productivity gains in historically more diverse cities. Both mechanisms can account for urban decline, but they imply distinct policy trade-offs; separating

their contributions is therefore crucial.

We estimate the quantitative model using several key inputs: city-industry employment data; trade costs and industry-specific factor shares in production; elasticities from the existing literature (including elasticities of substitution within and across industries, static agglomeration externalities, and migration elasticities); city-specific land supply elasticities (Drayton et al., 2024); and our empirical sources of exogenous variation, which identify the effect of long-run Jacobs (and agglomeration) externalities on recovered city-industry productivity. The estimated model enables two counterfactual experiments that quantify the roles of location fundamentals, industry life cycles, and *local* externalities in shaping urban dynamics. First, we assess the contribution of long-run Jacobs externalities to present-day regional inequality in England and Wales. Eliminating these externalities would reduce the North-South productivity gap by nearly half—from roughly 35% to 20%. This spatial inequality reflects the interaction between long-run Jacobs externalities and the historically high industrial concentration of the nineteenth century, amplified by trade openness and improvements in transport infrastructure. Second, we evaluate stylized place-based industrial policies that alter local industrial diversity—capturing specialization-inducing or diversification-promoting interventions—and quantify their normative implications.[2] This exercise highlights a dynamic trade-off faced by local policymakers: specialization-inducing interventions can yield short-term productivity gains by reinforcing comparative advantage, but they may weaken long-run performance by reducing industrial diversity. The strength of dynamic externalities and the policymaker's discount factor are key. In our counterfactuals, both diversification and specialization policies can be justified, but more patient policymakers—those assigning greater weight to future generations—favor diversification. In practice, however, many place-based policies emphasize specialization, reflecting the revealed preferences of policymakers who place low weight to future generations.

The main contributions of our study are to estimate long-run Jacobs externalities, to isolate their role in driving regional inequalities, and to highlight a novel trade-off in the spatial allocation of economic activity—a dynamic trade-off rooted in industrial composition (in contrast to the static trade-off between agglomeration benefits and crowding costs discussed in, e.g., Henderson, 1974; Ahlfeldt et al., 2015; Brinkman, 2016).[3] We

[2]Our theory does not aim to capture detailed innovation processes within or across industries. As a result, we are not well positioned to directly evaluate place-based industrial policies such as the *Smart Specialisation Strategy* implemented by the EU or innovation cluster policies in the US.

[3]Our focus on the long-run impact of industrial structure entails several limitations. First, while the theoretical framework incorporates dynamic spillovers across industries, it does not model detailed firm-level interactions or the full range of contemporaneous agglomeration mechanisms. This reflects a deliberate emphasis on long-run structural dynamics rather than within-period market interactions. Second, our empirical analysis identifies a reduced-form causal relationship between industrial concentration and long-run productivity. While several mechanisms may contribute to this relationship, disentangling their

relate to several strands of existing research. First, our study adds to the literature discussing industries as drivers of urban growth (Duranton, 2007; Hanlon and Miscio, 2017; Lane, 2025), and specifically to research on the negative effects of industrial concentration (Glaeser et al., 1992; Duranton and Puga, 2001; Lin, 2011; Faggio et al., 2017; Heblich et al., 2026). The closest paper to ours is Henderson et al. (1995), which discusses the interconnected life-cycle of industries and cities. One feature of our model, responsible for the negative effect of industrial concentration, is the role played by externalities à la Jacobs (1969) as drivers of knowledge development in the long run (Cai and Li, 2019). In a related application, Glaeser (2005) points to the role of human capital in reinventing Boston after periods of crisis and decline; distortion to the acquisition of human capital is also a key mechanism behind the rise and fall of cities in Franck and Galor (2021). Relative to these earlier contributions, an our empirical design causally identifies the long-run impact of industrial concentration, while also accounting for the life cycle of nationwide industries themselves.

Second, our work is inspired by theories of agglomeration economies—recently reformulated as sharing, matching, and learning effects, operating through production linkages, labor markets, or knowledge creation (Duranton and Puga, 2004)—but mostly relates to their empirics (Combes and Gobillon, 2015). Our empirical approach focusing on Jacobs externalities borrows from previous literature in its measurement of industrial concentration, but markedly differs in its time horizon: we relate contemporary productivity to industrial structure at the end of the nineteenth century, thus capturing the (very) long-run effects of localized knowledge spillovers (Carlino and Kerr, 2015).

These long-run dynamics bear directly on the normative evaluation of place-based policies, where the spatial allocation of activity is shaped by local spillovers and long-run externalities (e.g., Fajgelbaum and Gaubert, 2025; Kline and Moretti, 2014b; Gaubert et al., 2025). In their study of the Tennessee Valley Authority, Kline and Moretti (2014a) show that place-based interventions may be justified on efficiency grounds if they correct meaningful local market failures; otherwise, they risk being distortionary, with local gains offset by national losses. We complement this view by introducing an intertemporal dimension and suggest that planners must weigh not only static efficiency considerations but also long-run consequences tied to local industrial structure.

Third, we connect to a quantitative literature studying the dynamic evolution of economic activity across space. The closest contributions in this literature are Allen and Donaldson (2020), Berkes et al. (2021), Caliendo et al. (2019), Nagy (2023), Eckert and Peters (2023) and Fajgelbaum and Redding (2022), and we refer to Redding and Rossi-Hansberg (2017) and Nagy (2022) for comprehensive surveys. Our main contribution to

relative importance remains an important direction for future research.

this literature lies in proposing a multi-sector dynamic model with various dimensions of heterogeneity that can be taken to the data in a tractable way.

Finally, our period of interest includes a key transformation of Britain—the industrial revolution—accompanied by urbanization, trade, and structural transformation. Trade has been discussed as a key mechanism behind the industrial revolution (Stokey, 2001; Allen, 2009); it accelerated the transition to large-scale, export-oriented (urban) growth, and induced the invention of the labor-saving technologies that underpinned Britain's transformation. Our model has the ingredients to rationalize urban growth through both supply-side factors—productivity growth in urban industries—and demand-side factors—the decline in trade costs across cities. A macroeconomic literature studies growth and structural transformation (Herrendorf et al., 2014). Our quantitative spatial model abstracts away from the mechanisms discussed in theories of structural change and considers relative prices across industries as given (in contrast with Eckert and Peters, 2023).

The remainder of the paper is organized as follows. Section 1 presents some historical context. Section 2 describes our data. Section 3 establishes empirical facts which motivate the structure of the model, described in Section 4. Finally, Section 5 takes the model to the data and discusses mechanisms behind the long-run dynamics of cities.

1 Context and illustrative example

1.1 Context

This section provides a brief overview of the context in which cities of our sample grow over the course of the nineteenth century: the industrial revolution in Britain, its early cottage industries, and the rise of urban agglomerations from early settlements.

The industrial revolution in Britain The industrial revolution can be broadly characterized by four stylized facts: (a) the emergence of new technologies in key sectors leading to sustained increases in growth rates of income per capita; (b) a declining share of employment in agriculture; (c) the growth in domestic and international trade; and (d) an increasing share of the population living in cities. How each of these fit together, and what are the factors that caused Britain to industrialize first, is not completely settled (see, e.g., the survey in Clark, 2014).[4]

[4]Two highly influential hypotheses on the causes of the industrial revolution are formulated in Mokyr (2009) and Allen (2009). In Mokyr (2009), the industrial revolution is driven by the emergence of "attitudes" (a respect for entrepreneurs and inventors) and "aptitudes" (the growth of useful human capital, see Mokyr, 2021). Kelly et al. (2023) and Hanlon (2022) corroborate this view with a focus on mechanical workers and the professionalization of invention through the emergence of engineers. By contrast, in Allen (2009), (openness to) trade changes demand for the manufactured output, causing a shift in modes of production away from rural, low-scale, domestic-oriented and water-powered production to urban, specialized,

Figure 1. The industrial revolution in Britain.

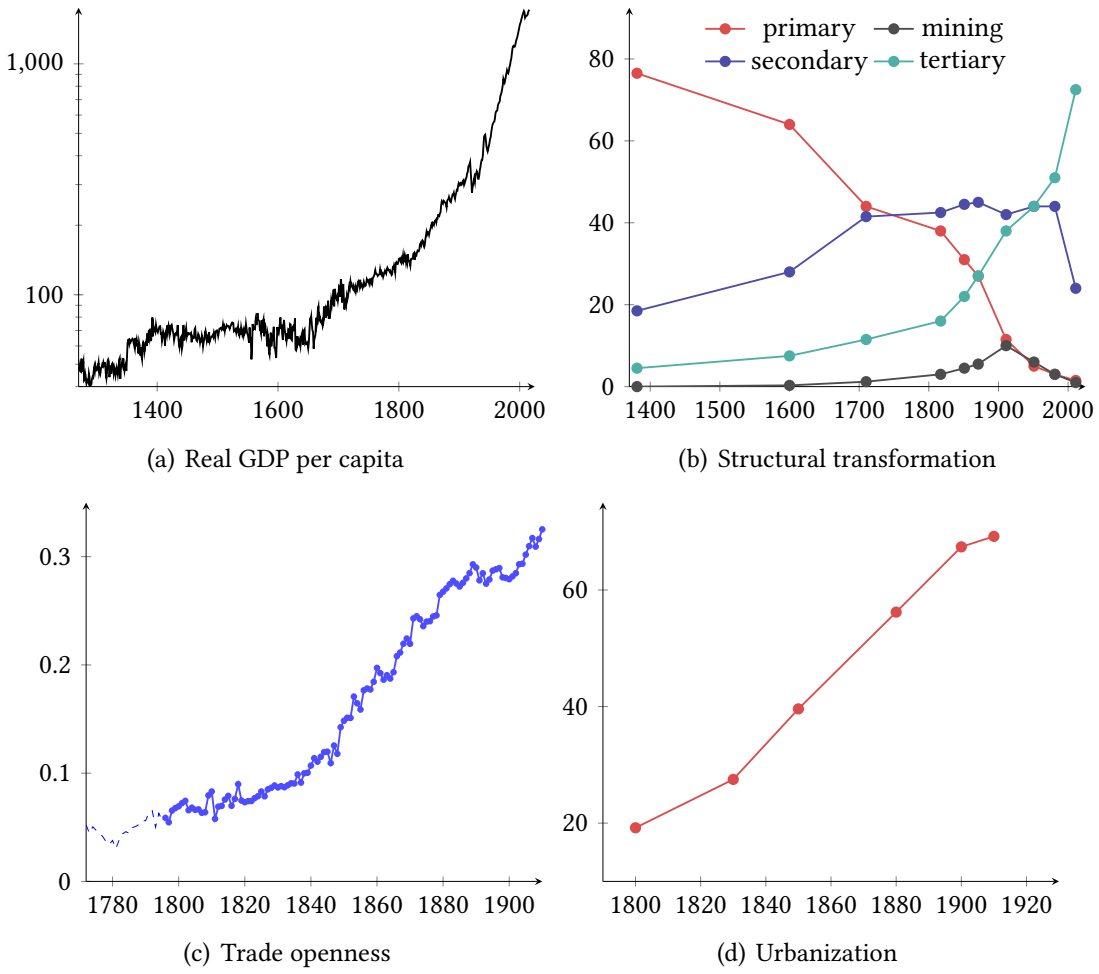

(a) Real GDP per capita

(b) Structural transformation

(c) Trade openness

(d) Urbanization

Notes: Panel **(a)** provides data on real GDP per capita from Broadberry et al. (2015) and national accounts, collated in Thomas and Dimsdale (2018). In panel **(b)**, employment shares are classified according to the PST system—primary, secondary, tertiary—described in Wrigley (2010), which are respectively (and very broadly) agriculture, manufacturing/construction and services. Note that we report available data for male adults in England and Wales and we separate out mining (Shaw-Taylor and Wrigley, 2014; Shaw-Taylor, 2019). In panel **(c)**, trade openness is defined as the sum of imports and exports as a share of GDP, using Hills et al. (2010) and Broadberry et al. (2015). In panel **(d)**, urbanization is defined as the population share in cities over 5,000 inhabitants (Bairoch and Goertz, 1986).

Figure 1 depicts trends of these four dimensions. Although many foundational industrial technologies emerged in the mid-eighteenth century, growth in output per capita accelerated markedly in the early nineteenth century (panel a), coinciding with a period of rapid population expansion. The share of employment in the secondary sector reached a peak around 1871, having only marginally grown since 1710; and structural

export-oriented and large-scale factories in which steam power dominates (a change discussed in Crafts, 1989). More specifically, high wages due to external demand drive capital-biased, labor-saving technical change which fosters the growth in export-oriented industries (Allen, 2021). Stokey (2001) finds that trade explains all the decline in agricultural production, and a significant share of the increase in manufacturing and real wages (a finding qualitatively supported by Harley and Crafts, 2000; Clark et al., 2014).

transformation then materialized in a swift rise in tertiary employment (panel b). Particularly striking are the dramatic rises in trade openness, which accelerated after 1820 (panel c), and in urbanization, which increased by nearly fifty percentage points between 1820 and 1900 (panel d). Over the nineteenth century, Britain transformed from a largely rural economy into one of the most urbanized societies.

Figure 2. The urbanization of Oldham.

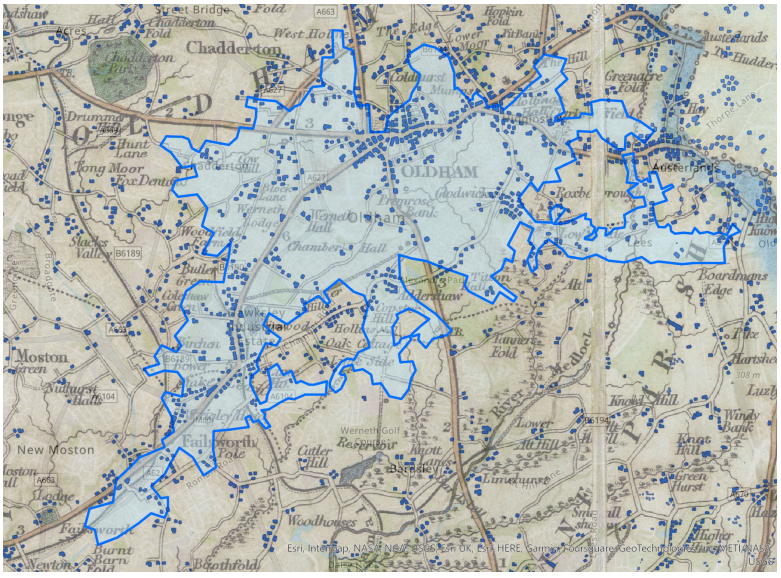

Notes: The underlying map is a county map of Lancashire around 1820 where built-up is indicated by darker blue rectangles (see Section 2 for a description of the built-up extraction process). The lighter blue area shows the urban boundaries of Oldham around 1880–1900, as defined by areas of contiguous built-up.

Proto-industrialization and urbanization The shift of industrial production from a rural to an urban setting has been studied extensively. In the early eighteenth century, the low-scale artisanal home-production of finished manufactures gave way to well-organized rural industries, some of which exported beyond the locality (Hudson, 2004; Goose, 2014). This phenomenon is sometimes labeled "proto-industrialization" and was common in Europe (Mendels, 1972; Ogilvie, 2008). The existence of extensive proto-industries rationalizes high employment shares in the secondary sector between 1700–1820 in spite of low urbanization levels (Figure 1). Factory production was, at this time, frequently rural, relying on water power and with workers housed by entrepreneurs around production facilities (Trinder, 2000). Steam engines began to emerge in the eighteenth century (Nuvolari et al., 2011), though the transition to steam as the main power source, and the associated large-scale, city-centered factory production, was not complete until the mid-nineteenth century (Musson, 1976). An illustration of the swift concentration of manufacturing production in urban centers is Oldham (north-

east of Manchester). At the end of the eighteenth century, Oldham does not exist yet as a town: there are numerous hamlets where cottage industry takes place, including one called Oldham. By the end of the nineteenth century, Oldham is a factory town of about 140,000 inhabitants which produces a significant share of the national output (a quarter of cotton production in 1911). Figure 2 provides the geographical illustration of this rapid urbanization: the underlying map is from around 1820, with the 1820 built-up areas (dark blue polygons) overlaid with the urban boundary of Oldham around 1880–1900.

Figure 3. The geography of employment and growth in Britain.

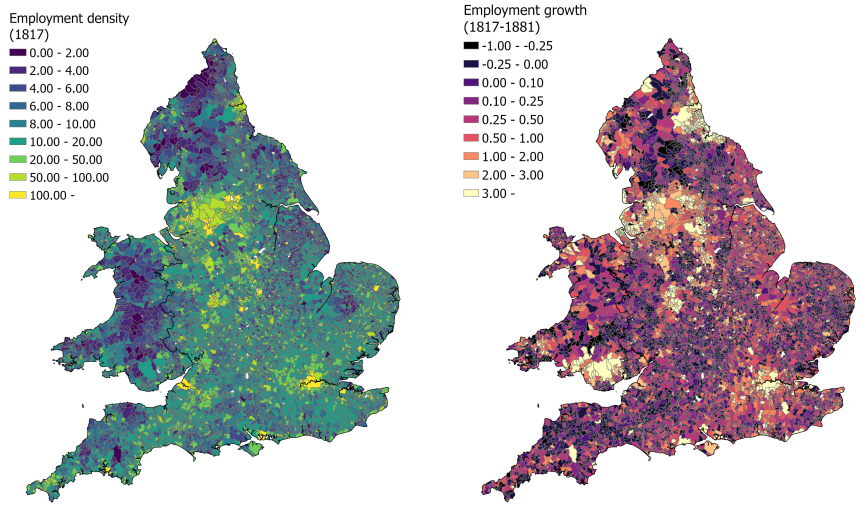

(a) Employment density (1817) (b) Employment growth (1817–1881)

Notes: These maps represent employment density in 1817 (panel **a**, as computed from a quasi-census of baptism records conducted between 1813–1820, and in number of workers per square kilometers) and employment growth between 1817–1881 (panel **b**, where population in 1881 is calculated using micro-census records). The geographic unit is a parish (see Section 2).

The example of Oldham is typical of a phenomenon whereby smaller settlements consolidated into towns, and small towns grew into cities with a high concentration of industries. In other words, settlements of the early nineteenth century gave way to a dense network of cities by the end of the century. Figure 3 illustrates the geographic patterns of this process. As shown in panel (a), early nineteenth century employment is concentrated in regions such as Lancashire, North Yorkshire, the West Midlands, Northumberland, London and a few isolated cities (e.g., Bristol). The geography of employment growth during the century is more balanced across space, but highly correlated with this initial distribution of employment (panel b). We shed further light on the extent and nature of this growth in Figure 4. In panel (a), we show the distribution of employment across cities in 1817 and in 1881: cities grow by a factor of 4 on average (while overall population increases by about 80% during the same period). In panel (b), we show the dis-

tribution of industrial concentration, as captured by a 2-digit industry-based Herfindahl index of employment. Cities are mechanically more specialized than the overall economy, but there exists large variation in the degree to which they specialize. We will see later that this variation is tied to the portfolio of location advantages that they hold across the different industries.

Figure 4. Specialization and growth in cities.

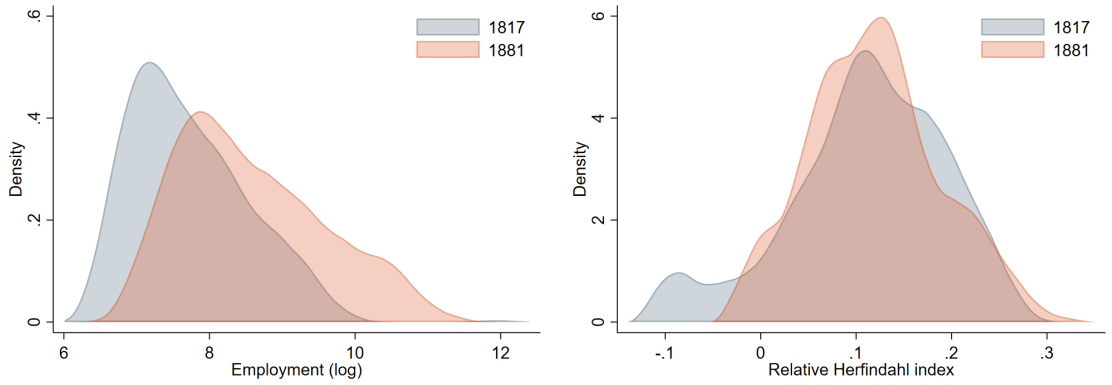

(a) Employment (b) Herfindahl index

Notes: These two figures represent the distribution of employment (panel **a**) and industrial concentration (panel **b**) across 435 potential cities of England and Wales (see Section 2 for a definition of these potential cities and their boundaries). The distributions are shown in 1817 (blue) and in 1881 (orange). Specialization is captured by a Herfindahl index calculated as the difference between the city-specific Herfindahl index and a national one, $\widetilde{h}_c = \sum_j s_{jc}^2 - \sum_j s_j^2$, where s_{ic} is the employment share in city c and industry i and s_i is the nationwide employment share in industry i. Industries are captured at the 2-digit level, based on the PST system—primary, secondary, tertiary—described in Wrigley (2010).

Land supply and local growth constraints During the nineteenth century, industrialization led to rising demand for space within, then around, cities.[5] While factory production using new technologies concentrated in growing cities (see, e.g., Trew, 2014), some locations faced difficulties in meeting the accelerating external demand after the 1820s, because of land constraints. Such constraints could be geographic but they could also be the remnants of historical property rights that presented a land assembly-type problem (Hoskins, 1988; Eckart, 1985; Strange, 1995; Neeson, 1996; Hudson, 2004). As Trinder (2000) notes, the "pattern of urban industrial growth in Britain before 1840 was untidy" (p.827). Where possible, towns were laid out in a grid pattern and experienced rapid growth. Where it was not, "[p]atterns of housing were dispersed, following patterns set by pre-existing fields and property boundaries rather than those of order and

[5] "Land inside the older towns was acquiring a scarcity value [...] Open spaces inside the older towns vanished rapidly..." (Hoskins, 1988, p.185); "Manufactures ran up their mills, factories and works on the edge of existing towns[...]" (Hoskins, 1988, p.183).

convenience" (p.820). Our empirical strategy will exploit how land ownership patterns shape the potential for urban expansion.

1.2 A tale of two cities

The rise Bradford and Leeds, two towns in the West Riding of Yorkshire located 10 kilometers apart, illustrate the short-run gains and long-run costs of industrial concentration. In the early nineteenth century, the towns were comparable in size (Leeds with around 11,600 workers in 1817; Bradford with 7,800), in sectoral composition (approximately 65% of employment in manufacturing), and in their integration within the regional economy. Yet their development paths diverged. Leeds expanded across a range of activities—combining textiles with finished clothing, iron, engineering, printing, and pottery—whereas Bradford specialized in a single product: worsted wool. The returns to industrial concentration were for a time spectacular. Between 1800 and 1850, Bradford's population grew from roughly 13,000 to over 100,000, making it among the fastest-growing towns in Britain. By 1900, it housed 350 mills, processed two-thirds of national wool output (Ittmann, 1995), and had earned the nickname "Worstedopolis."

Figure 5. A story of two cities—Bradford and Leeds.

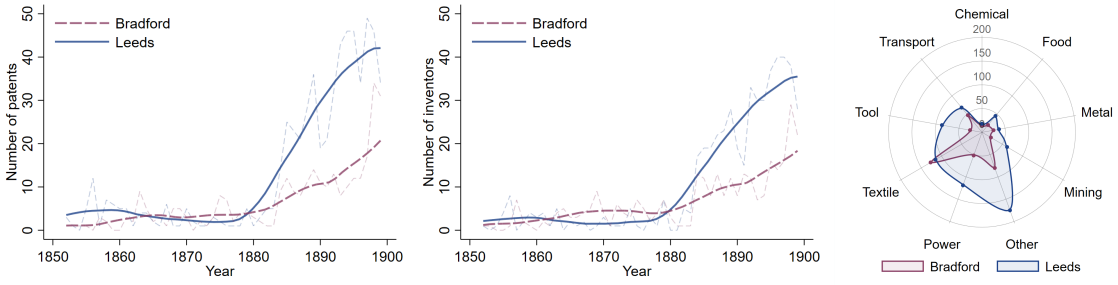

(a) Patents (b) Innovators (c) Industries

Notes: Panels **(a)** and **(b)** display the annual number of unique patents and inventors in Leeds (blue solid line) and Bradford (claret dashed line). The data are drawn from British patent records covering 1617–1899 (Berkes et al., 2026). We classify patents granted between 1852 and 1899 using their technical specifications, assigning them to approximately 10 industries and 45 sub-industries. Inventors are geolocated using linked address information—sometimes corresponding to the address of their factory—allowing us to assign patents to settlements (see Section 2). Panel **(c)** reports the distribution of patents across industries, grouped as follows: *Chemical* (chemicals; medical and health); *Mining* (mining and minerals; construction); *Power* (power and general machinery; electrical and communications); *Food* (food and agriculture); *Tool* (instrument making; household appliances); *Metallurgy*; *Textile*; *Transport*; and *Other*.

The distinct trajectories of the two cities are reflected in their flagship factories. In rapidly expanding Bradford, Samuel Lister founded Lister Mills, which became the largest silk factory in the world and one of the largest textile mills. Operating from the early nineteenth century until the 1980s, it produced high-quality velvet and silk, including parachute and flame-resistant fabrics during the Second World War. In Leeds,

Armley Mills and Marshall's Mill were major flax and woollen producers; however, by the late nineteenth century the city also supported soap, glass, and chemical manufacturers, alongside specialized engineering firms.

The divergence The industrial composition of the two cities had both immediate and delayed consequences for their economic trajectories. The immediate effects are visible in Figure 5. Using the universe of patent applications and their geolocated inventors, we show that Bradford generated patents and inventors, but far fewer by the end of the century (panels a and b), and almost exclusively in textiles (panel c). In contrast, Leeds patented increasingly across a broad range of industries.

Bradford-based Samuel Lister developed the Lister nip comb, exemplifying innovation concentrated in fiber treatment, spinning, yarn, and finishing. By contrast, firms such as the Hunslet Engine Company, Greenwood & Batley, and Whitehouse Engineering Works in Leeds patented improvements in valves, narrow-gauge design, traction engines, locomotives for collieries, agricultural machinery (e.g., plowing engines and steamrollers), and textile machinery—including power transmission systems and mechanized spinning—partly driven by the rise of engineers documented in Hanlon (2025).

Over time, these diverging innovation trajectories translated into different economic dynamics. Today, Leeds is widely regarded as Yorkshire's economic "powerhouse," with gross value added per head roughly 25% above the national average. Bradford, by contrast, has nearly a quarter of its working-age population economically inactive and a gross value added per head approximately 40% below the national average. The contrast motivates the central question of this paper: whether Bradford's early depth of specialization, despite its short-run returns, foreclosed the cross-industry interactions that sustained Leeds's longer-run relative success.

2 Data and empirical strategy

This paper combines data on the evolving economic geography of England and Wales over 200 years. In this section, we present our data sources, describe the dynamics of urban settlements over the nineteenth century, and discuss our empirical strategy.

2.1 Data sources

Census of England and Wales The main data source for population and employment is the Census of England and Wales, which provides a highly detailed characterization of population and industrial composition at the level of about 11,500 parishes over the course of two centuries (1801–1911, 1971–2011). The census provides population counts

from 1801 onward, but a precise decomposition of the labor force across occupations only after 1851—when the micro-census records become available. We thus rely on a quasi-census based on (adult male) Anglican baptism records collected between 1813 and 1820 (referred to below as 1817) in order to retrieve consistent 2-digit industrial composition at the parish level before the time of rapid industrialization (Shaw-Taylor and Wrigley, 2014). One issue with census data is that the smallest administrative units—the parishes—are regularly redefined, merged or split over the course of the nineteenth century. We thus apply an "envelope" algorithm which considers the transitive closure of the different parishes covering the same points over time (see Appendix A.1).

Registered patents in 1852–1899 Our evidence on spatial patterns of innovation in the nineteenth century draws on the recent digitization of British patent records (1617–1899) and their linked inventors (Berkes et al., 2026). We use the technical specifications of patents granted after the Patent Law Amendment Act (1852–1899) to classify them into industries (e.g., "Electrical and communications") and sub-industries (e.g., "Motors, dynamos, and generators"). These 450,000 patents are then assigned to settlements based on the geolocated residential or workplace addresses of their inventors.

Firm data We access—through a secure server—high-quality contemporary data, most notably firm-level production information: the Annual Business Survey (ABS), which reports turnover, purchases, employment costs, capital expenditure, stocks, and, value added for a representative selection of firms (about 2.5% of all firms); the Business Register and Employment Survey (BRES), which reports detailed employment for a representative selection of firms (about 4% of all firms); and, the Business Structure Database (BSD), which reports aggregate employment and turnover for all businesses. A challenge is that these firms are nested within geographies (NUTS-3 or local authority) and industries (4-digit SIC) which differ from the nineteenth century data. A corollary is that we will lose some geographic granularity in analyzing firm productivity and that we will not be able to map industrial codes in earlier censuses with later industry classifications—which does not prevent us from controlling for *contemporaneous* Marshall-Arrow-Romer externalities and demand shifters at the level of 4-digit industries.

Geography, land ownership, and transportation To characterize the immediate neighborhood of cities and the local, temporary drivers of urban land supply, we gather high-quality raster maps at a disaggregated level: elevation (Open Land Map, 30m resolution); soil organic carbon content (Open Land Map, 250m); soil bulk density (Open Land Map, 250m); and detailed soil classification (National Soil Resources Institute).

A crucial component of the empirical analysis consists in the construction of an exogenous measure of land fragmentation based on topography and soil characteristics (i.e., natural breaks between agricultural land parcels). Such natural land fragmentation may restrain city growth if it leads to fragmented land ownership. To validate this channel, we collect measures of land ownership fragmentation from censuses (in 1851 and 1861) where land acreage is reported by landowners. Inferring land ownership fragmentation from micro-census records requires textual analysis.[6]

We complement the data on population, occupations and geography with a dataset of all rivers and smaller streams in England and Wales (OS Open Rivers) and a panel dataset of transportation infrastructure (main roads, navigable waterways, train lines and train stations) from Alvarez-Palau et al. (2025) and Gregory and Henneberg (2010), allowing us to measure access to resources and trading costs in different cities over time (see Appendix A.1).

2.2 The dynamics of cities over the nineteenth century

Urban settlements at the onset of industrialization In the early nineteenth century, the population of Britain mostly lives in rural settlements or small towns. That starting point allows for a significant reshaping of the urban network, with the rise of new cities sprawling around existing hamlets. This also represents a challenge: how can we identify potential cities and their boundaries?

Figure 6. A rich set of Ordnance Survey drawings and county maps (1790–1830).

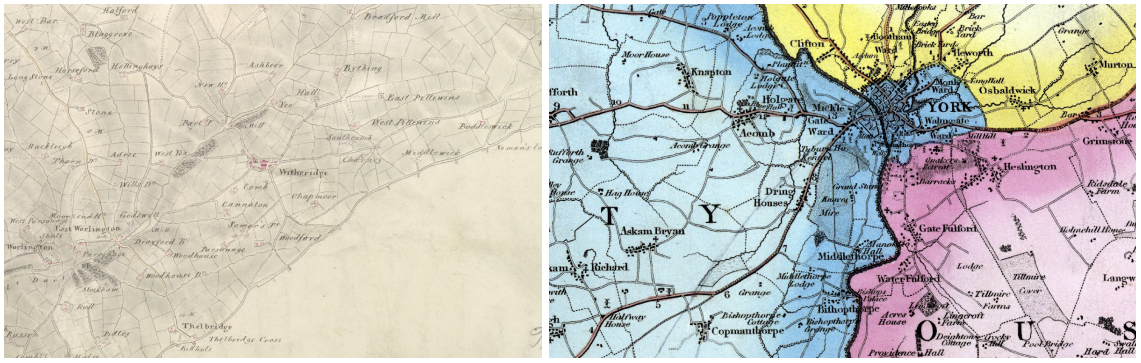

(a) South Molton (Devon) (b) York (Yorkshire)

Note: Panel **(a)** displays the surroundings of South Molton in Devon, a typical example of Ordnance Survey drawings (2 inches to the mile, 1804). Panel **(b)** displays the surroundings of York in Yorkshire, a typical example of county maps (4/5-inches to the mile, 1828). While built-up tends to be indicated with red in Ordnance Survey drawings, it is typically represented as dark rectangles and gray blocks in county maps. See Appendix A.1 for a description of these maps.

[6]In particular, the occupational category in micro-censuses provided by I-CeM is extracted from a free text entry detailing occupations, such as "Farmer, 5 acres, 4 men, 2 boys". We use this free text to systematically collect information about farm acreage and employment.

Our approach exploits early county maps and Ordnance Survey drawings, mostly produced between 1790–1830, that cover the whole territory of England and Wales. We digitize, geo-reference and process these maps through computer vision.[7] We provide illustrations in Figure 6 centered around South Molton (Devon, Ordnance Survey drawing) and York (Yorkshire, county map). Identifying objects of interest on these maps is challenging (see, e.g., Combes et al., 2022, for a discussion of map digitization through machine learning). We briefly describe our approach to identifying built-up areas, leaving further details to Appendix A.1. We train a U-Net—a neural network commonly used to detect objects of interest within images—by manually labeling built-up areas across different map tiles and drawings, and validate it through the use of a validation sample. Due to the large sample of labeled buildings and their heterogeneity, overfitting is a second-order concern; we however apply various transformations (i.e., flipping, zooms, rotations) to each training batch, which allows us to impose invariance properties to these transformations. Our procedure leads to a good classification of built-up areas (our main object of interest), with a precision of 0.96—the resulting polygons are illustrated in Figure 2 for instance.

Figure 7. Clustering procedure.

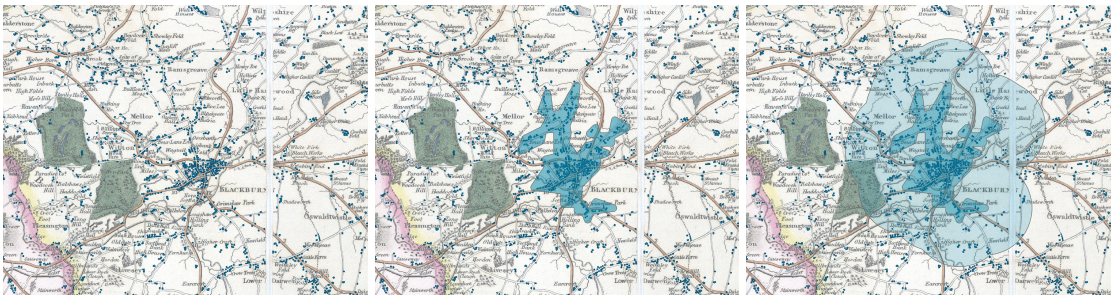

(a) Detecting built-up areas (b) Clusters and city boundaries (c) Predicted sprawl

Notes: The underlying map is the county map of Lancashire drawn by G. Hennet. The blue rectangles are built-up areas detected by our algorithm; the blue area in panel **(b)** is the outcome of our clustering algorithm adapting De Bellefon et al. (2021). In panel **(c)**, the lighter blue area is predicted urban sprawl based on average urban sprawl across all towns. While these areas can overlap, at least in principle, we record no such overlaps for our baseline sample of 435 cities.

Next, we need to select clusters of built-up areas as candidate cities. At the turn of the nineteenth century, some of the settlements that would later consolidate into towns and grow into cities are large and dense, others are spread across contiguous hamlets. To identify future cities, we rely on a procedure to select urban settlements as sufficiently

[7]We rely on about 350 Ordnance Survey drawings (covering Southern England and Wales) and 10 larger county maps (covering Chester, Cumberland, Derbyshire, Durham, Lancashire, Lincolnshire Northumberland, Nottinghamshire, Westmoreland, and Yorkshire). These collections markedly differ in their display of built-up areas; they also use different symbols and colors within collections.

large clusters of built-up areas. Figure 7 illustrates our approach with the city of Blackburn. We first detect built-up areas on the raw map with the previous algorithm (panel a). We then follow the procedure developed in De Bellefon et al. (2021) to identify a nucleus of high density and contiguous areas of excess building density (panel b).[8] We finally construct predicted boundaries for these cities at the end of the nineteenth century by assuming that towns and cities all grow at the same proportional rate across the country and do so homogeneously in any direction (panel c). In practice, towns and cities all expand to some degree, but this expansion is not homogeneous across all directions and not homogeneous across cities. We discuss in Section 2.3 how we predict the extent of such expansion—and therefore cities' late-nineteenth century population—with land ownership fragmentation.

The heterogeneous rise of Great British cities Our procedure to detect urban settlements around 1790–1820 identifies more than 800 clusters and their initial boundaries. Throughout the paper, we consider a sample of settlements excluding those with an agricultural share of employment in the top quartile (above 60%) and a population below 3,000 inhabitants in 1817.[9] We are left with 435 potential cities, 7 of those being isolated in their county. By the end of the nineteenth century in Britain, as urbanization growth slows, some of these cities are specialized in a few industries while others are more diverse. This process is disciplined by geography, trade and the distribution of location advantages, as we describe next.[10]

Late-nineteenth century population and industrial concentration are primarily explained by geography, and the initial distribution of location advantages. To quantify the respective role of initial industrial mix and geography in predicting urban dynamics across urban settlements, we conduct a simple variance decomposition exercise explaining industrial concentration in 1881—constructed from employment shares in 1881, s_{ic}^{81}, in city c and 2-digit industry i, as $h_c = \sum_j \left(s_{jc}^{81}\right)^2$—and employment growth between 1817 and 1881. We first control for initial industries; we then add a large set of geographic indicators (topography, market access, transportation, agricultural potential, built-up

[8] An alternative procedure is described in Arribas-Bel et al. (2021).

[9] We provide robustness checks showing that this selection does not affect our headline estimates for the long-run impact of industrial concentration. Note that boundaries of urban settlements change during the period, and they do so endogenously. To strike a balance between comparing employment numbers within similar areas across time and dealing with endogenous urban sprawl, we associate employment within each 2-digit industry in 1817 and in 1851–1911 (and in 1971–2020) to a city c by intersecting the predicted boundaries around 1880–1900 with parish boundaries, allocating employment using the area share of the intersection. Predicted boundaries are calculated by assuming a homogeneous, proportional growth of all urban areas in every direction between 1817–1881. In summary, we construct all our employment/population variables within predicted expanded cities as of the end of the nineteenth century.

[10] In Appendix A.3, we illustrate the role of initial industries in shaping the industrial structure of cities, and we discuss two empirical regularities of urban development: Gibrat's law and Zipf's law.

Table 1. The role of initial industries and geography.

Adjusted R-squared	Herfindahl index (1881)	Employment (1881)
Initial industrial mix (1817)	0.778	0.489
+ Geography	0.841	0.762
Observations	435	435

Notes: The Herfindahl index (1881) is constructed from industrial employment shares (s_{ic}^{81} for city c and industry i) in 1881 as $\sum_j \left(s_{jc}^{81}\right)^2$. Employment (1881) is the (log) employment growth between 1817 and 1881, $\ln\left(L_c^{81}\right) - \ln\left(L_c^{17}\right)$. *Initial industrial mix (1817)* includes: dummies corresponding to deciles of employment in 1817, deciles of industrial concentration in 1817, and deciles of agricultural employment and public employment shares in 1817; and the industry-based shift-shares, g_c and χ_c, later described in this Section 2.3. *Geography* includes: (log) area of the initial city outline; topography indices (maximum elevation, slope, mTPI†); soil bulk density; latitude/longitude; travel time to the closest market town, to each major port (London, Liverpool, Plymouth, Portsmouth), and to coal; distance to the shore; density of roads (1830), train lines (1851), and waterways; suitability to grow wheat, barley, oat, grass, and rye; share of heavy soil and clay (NSRI); built-up density and the predicted natural land fragmentation, both within the contours of the settlement around 1800 and within a 10-kilometer buffer. Note that the Adjusted R-squared with only geographic variables are respectively 0.708 (Herfindahl index, 1881) and 0.669 (Employment, 1881). †: mTPI is a Multi-Scale Topographic Position Index, capturing local elevation in comparison with mean elevation within a neighborhood (i.e., identifying ridges or valleys).

density at the city fringe). Table 1 shows that initial industries are much more important in explaining industrial concentration than growth: the set of "initial industries" variables explains 78% of the variation in industrial concentration across cities in 1881. By contrast, the same set of variables only explains 49% of the variation in growth across cities. The additional factor explaining urban growth through the nineteenth century is geography: adding geographic factors to the previous regressions raises the adjusted R-squared from 0.49 to 0.76. There are two types of geographic factors which predict urban development: (i) market access and connectivity; and (ii) topography and factors which influence land supply at the fringe of urban settlements, e.g., agricultural conditions.[11]

In summary, the nineteenth century sees the rise of different cities, shaped by geography and the nature of local comparative advantage.

2.3 Empirical strategy

The identification of long-run externalities relies on (i) important parametric assumptions and (ii) exogenous variation in urban expansion and industrial concentration.

A parametric formulation for (Jacobs) externalities Our formulation for the effect of long-run externalities builds upon and augments a traditional framework connecting the dynamics of industries to the evolution of cities. Consider an industry i in city c at

[11] The role of agricultural hinterlands in fueling urban growth has been discussed in Matsuyama (1992), Coeurdacier et al. (2022), Nagy (2023) and Heblich et al. (2024).

time t, and let $\mathcal{T}_{ict}$ denote its total factor productivity. Ignoring local externalities and assuming a constant location advantage $\mathcal{A}_{ic}$, (revenue-based) total factor productivity can be written as,

$$\mathcal{T}_{ict} = \mathcal{A}_{ic} \cdot \mathcal{P}_{it}, \tag{1}$$

where $\mathcal{P}_{it}$ captures macroeconomic factors of demand and technological change affecting the dynamics of industries within the country. Under this formulation, the dynamics of cities, as disciplined by their portfolio of productivity across industries $\left\{\mathcal{A}_{jc}\right\}_{j\in I}$, reflects the dynamics of industries in which they have a comparative advantage. We augment this framework by introducing static and *long-run* externalities,

$$\mathcal{T}_{ict} = \mathcal{A}_{ic} \cdot \mathcal{P}_{it} \cdot f_i\left(\left\{L_{jc,t}\right\}_{j\in I}\right) \cdot g\left(\left\{L_{jc,t-1}\right\}_{j\in I}\right),$$

where the function f_i captures static spillovers and g maps the local industrial structure in $t-1$ to the distribution of productivity in period t. In practice, the data will not allow us to keep such level of generality, and we will consider externalities of the form,

$$f_i\left(\left\{L_{jc2}\right\}_{j\in I}\right) = L_{ic2}^{\mu}, \quad g\left(\left\{L_{jc1}\right\}_{j\in I}\right) = L_{c1}^{\rho} \cdot \left[\sum_{j\in I}\left(\frac{L_{jc1}}{L_{c1}}\right)^2\right]^{-\lambda},$$

where period 1 will be the year 1881 and period 2 will apply to contemporaneous outcomes. These parametric assumptions lead to the following relationship,

$$\mathcal{T}_{ic2} = \mathcal{A}_{ic} \cdot \mathcal{P}_{i2} \cdot L_{ic2}^{\mu} \cdot L_{c1}^{\rho} \cdot \left[\sum_{j\in I}\left(\frac{L_{jc1}}{L_{c1}}\right)^2\right]^{-\lambda}, \tag{2}$$

in which the term in brackets measures the impact of long-run Jacobs externalities, L_{c1}^{ρ} are long-run agglomeration spillovers, and L_{ic2}^{μ} captures static Marshall-Arrow-Romer externalities operating within industries. In effect, we will also be able to condition the estimation on *long-run* Marshall-Arrow-Romer externalities.

As Equation (2) constitutes the central dynamic mechanism of the model in Section 4, obtaining credible estimates of the key elasticities—particularly λ—is essential. Identification is challenging, however, because unobserved determinants of long-run productivity ($\mathcal{T}_{ic2}$) may be correlated with the initial industry portfolio ($\{L_{jc1}\}_{j\in I}$). The next section introduces two distinct instruments to identify the two *long-run* externalities.

Exogenous predictors for industrial concentration and city size To isolate exogenous variation in industrial concentration, we rely on recent advances in identification and inference within shift-share designs (Borusyak et al., 2022). Equation (1) implies

that—abstracting from externalities—employment in industry j and city c in 1881, L_{jc1}, is a function of $\mathcal{A}_{jc} \cdot \mathcal{P}_{j1}$. Accordingly, the Herfindahl index of industrial concentration would aggregate these terms across industries.[12]

Intuitively, the distribution of location advantages, $\{\mathcal{A}_{jc}\}_{j\in I,c}$, would then correspond to the "shares" while industry-wide shifters, $\{\mathcal{P}_{j1}\}_{j\in I,c}$, would correspond to the "shifts". We separate these components empirically by exploiting observations on economic activity in 1817 (period 0). Specifically, we proxy location advantages in city c using employment shares across two-digit sectors $j \in I$ in 1817, $s_{jc0} = L_{jc0}/L_{c0}$, and combine them with industry-wide shifters across two-digit sectors in 1881, d_j, to construct a predicted shift-share index of industrial concentration:

$$\chi_c = \frac{\sum_{j\in I} \left(s_{jc0} \cdot d_j\right)^2}{\sum_{j\in I} \left(s_{jc0}\right)^2} = \sum_{j\in I} \sigma_{jc0} \cdot d_j^2$$

where $\left\{\sigma_{jc0} = \left(s_{jc0}\right)^2 / \sum_{j\in I} \left(s_{jc0}\right)^2\right\}_{j\in I}$ are weights that sum to one. This predictor—relying on the initial distribution of cottage industries and differential demand dynamics across two-digit sectors—constitutes the first building block of our empirical strategy.

Following Borusyak et al. (2022), identification requires the *shifts* to be sufficiently numerous and quasi-random. To support this exclusion restriction and construct shifts, $\{d_j^2\}_{j\in I}$, that are plausibly related to aggregate rather than local factors, we consider several alternative specifications. We begin by defining $d_j = \ln(L_{j1}) - \ln(L_{j0})$, a leave-out measure of aggregate sectoral employment growth that excludes a "cell" of 50 kilometers around city c (using cells of 75 and 100 kilometers in robustness checks). The identifying assumption is then that *differential aggregate employment growth* across two-digit sectors $j \in I$ is orthogonal to the local dynamics of city c between periods 0 and 1.

Changes in global economic conditions across industries during the nineteenth century may have reflected both shifts in production costs and changes in global demand. We therefore consider two alternative specifications that explicitly decompose the forces affecting aggregate industrial dynamics into: (i) global supply factors operating through real input costs, and (ii) demand factors induced by trade with new partners. To generate variation in *input costs* across industries, we construct industry-level variation in commodity prices between period 0 (1817) and period 1 (1881), drawing on monthly prices for approximately 130 commodities traded in Philadelphia between 1784 and 1896 (Jacks

[12]For example, under the assumption that sectoral demand at the city level comes from a maximization program, $\max_{L_{jc1}} \mathcal{T}_{jct} L_{jc1}^{1-\alpha} - w_{c1} L_{jc1}$, the Herfindahl index of industrial concentration in period 1 would be written as:

$$\frac{\sum_{j\in I} (\mathcal{A}_{jc} \cdot \mathcal{P}_{j1})^{2/\alpha}}{\left(\sum_{j\in I} (\mathcal{A}_{jc} \cdot \mathcal{P}_{j1})^{1/\alpha}\right)^2}.$$

et al., 2011). Matching commodities to the production structure of the early nineteenth century (Shaw-Taylor and Wrigley, 2014), this source provides variation in the prices of globally traded commodities—primarily intermediate inputs—across two-digit industries. For example, leather-related industries experienced sharp increases in input costs (hides and bones), whereas the manufacture of chemical products, soap, and adhesives benefited from relatively lower prices of tallow and lard; employment growth in the latter industries exceeded that of the former by more than a factor of five.

Finally, we digitize reports from the "Secretary of the Treasury, on the Commerce and Navigation" for the years 1821 and 1862, which provide nominal values for more than 350 commodities imported into the United States. As above, this source requires a similar matching between imported final goods and two-digit British industries in the early nineteenth century; growth in overall U.S. imports between 1824 and 1862 is then used as an *industry-wide demand shifter* (in the spirit of Autor et al., 2013).

For each specification of the shifts, $\{d_j^2\}_{j \in I}$, we construct a "level" shift-share variable,

$$g_c = \sum_j s_{jc0} \cdot d_j.$$

We include this variable as a control to absorb the effect of labor demand shocks on *overall employment* in our empirical specifications. This ensures that χ_c captures variation in the *composition* of predicted employment across industries, holding fixed the *level* of predicted employment growth, and therefore prevents the concentration instrument from being mechanically correlated with city size. Exogenous variation in city size instead derives from local geography, as described below.

To isolate variation in nineteenth-century city growth that is plausibly exogenous to subsequent urban dynamics, we exploit our urban delineation before the time of rapid industrialization (Section 2.2) and identify possible constraints on settlement expansion. Land ownership fragmentation across England and Wales was instrumental to the evolution of agriculture (Heldring et al., 2022), but it also shaped patterns of urban growth. Indeed, when land markets are not perfectly competitive and land parcels and their rights of use cannot be split arbitrarily, developing land at the fringe of cities may be a challenge. For instance, a textile mill requires a large parcel of flat land to construct a factory. When a suitable location spans multiple existing parcels, the possible buyer needs to engage in multilateral bargaining in which the value of the marginal parcel increases as the buyer acquires the rights to use other parcels. The number of different parties therefore matters. This issue is a hold-up problem and has been labeled as the "land assembly problem" in this specific context (Eckart, 1985; Strange, 1995). The consequences for city growth are straightforward: high land fragmentation at the fringe of the city makes

negotiations to develop the land for urban use costly. Cities surrounded by fragmented ownership were thus less able to accommodate the rapid urban expansion induced by surges in external demand.

A concern is that the actual land ownership structure could reflect omitted variation such as agricultural productivity or local institutions, and reverse causality, whereby landowners near cities with expansion prospects held larger plots.[13] For these reasons, we would like to consider a measure of fragmentation with the following characteristics: (i) the measure, as evaluated within a neighborhood of city boundaries at the beginning of the nineteenth century, should predict city growth until the end of the nineteenth century; and, (ii) the measure should not directly affect the later evolution of cities *after* 1881, i.e., during the twentieth century, when conditioned on appropriate control variables—such as land supply elasticities evaluated in later periods, i.e., once cities have expanded beyond this early fringe and are subject to another topography at their borders.

Our approach constructs a measure of *natural* land fragmentation by delineating compact and homogeneous terrain patches defined by soil and topographic characteristics. We leave the details of the procedure to Appendix A.2 and only summarize its main steps below. First, we combine high-resolution data on elevation, slope, soil bulk density, and soil classes (e.g., calcareous soil) into a multi-band raster for England and Wales at 30 m resolution. Second, we apply an unsupervised segmentation algorithm that isolates contiguous "superpixels," each representing a homogeneous patch of land—analogous to an agricultural parcel. Third, we compute the density of such superpixels within buffer zones around historical city boundaries at the onset of industrialization. The instrument, ζ_c, uses buffer widths scaled to initial city area and calibrated to match average nineteenth-century city growth, but we also consider wider rings to control for later land supply elasticities.

Figure 8 shows that *natural* land fragmentation strongly predicts actual land ownership fragmentation in 1851 and in 1861, as retrieved from census records across all parishes of England and Wales.[14]

[13] A recent contribution discusses the role of enclosure acts on crop yields and land inequality (Heldring et al., 2022). Our source of variation to explain land fragmentation will be, in essence, orthogonal to local institutions, but we do control for the specific role of enclosures in a sensitivity analysis.

[14] This exercise shows that our land fragmentation algorithm does predict land ownership fragmentation; however, it does not rule out that the measure is related to city dynamics before industrialization. We further validate the land fragmentation measure by comparing urban settlements with different degrees of land fragmentation in the city fringe, as calculated at the onset of the nineteenth century (1817), in Appendix A.3. We do not find evidence that settlements with different degrees of land fragmentation differed in their population and industrial concentration before the era of rapid industrialization.

Figure 8. Validation of the land fragmentation prediction.

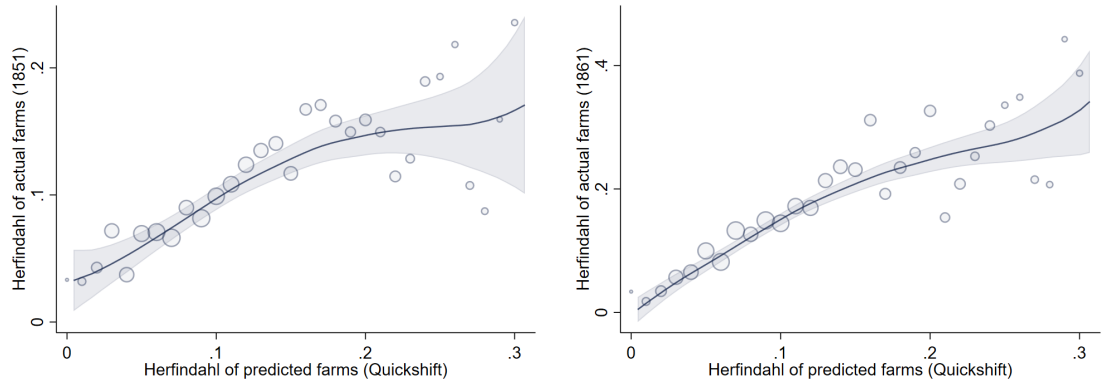

(a) Land concentration (1851)

(b) Land concentration (1861)

Notes: Panel **(a)** displays a measure of *natural* land concentration at the parish level, from predicted superpixels, versus the actual Herfindahl concentration of farm ownership as collected from micro-census records in 1851 across 11,500 parishes of England and Wales. We create about 30 bins of *natural* land concentration and the dots represent the average, actual land concentration within each bin. The lines are locally weighted regressions on all observations. Panel **(b)** repeats the same exercise with the actual Herfindahl concentration of farm ownership based on reported acres across parishes in 1861.

Identification, measurement, and sensitivity to alternative choices Our empirical strategy will consider the following specification,

$$\ln\left(\mathcal{T}_{ic2}\right) = \mu l_{ic2} + \rho l_{c1} - \lambda h_{c1} + \eta_i + \gamma \mathbf{X}_c + \varepsilon_{ic2}, \tag{3}$$

where measures of population (l_{c1}) and industrial concentration ($h_{c1} = \sum_j s_{jc1}^2$) in period 1 are instrumented by our geographic predictor of city size (ζ_c) and the shift-share specialization index (χ_c), based on location advantages and swift changes in aggregate demand; $\eta_i = \ln(\mathcal{P}_{i2})$ captures contemporary industry shifters; and our approach to further isolating city fundamentals, $\ln \mathcal{A}_{ic}$, consists in conditioning the specification on a rich set of controls capturing first-nature geography, second-nature geography, and industrial composition in 1817. In practice, we will estimate Equation (3) in its "most structural form" in the quantitative exercise of Section 5, and consider different variations of the previous equation in the reduced-form exercise of Section 3. One reason is that a few illustrative outcomes will be at the city level, thus changing our approach to controlling for industry shifters (η_i).

Identification of the parameters (ρ, λ) relies on the assumptions that (ζ_c, χ_c) predict population and industrial concentration, and that they do not have a direct effect on later productivity. The latter requires conditioning specification (3) on: granular controls for initial industries in 1817 to ensure that the variation induced by the predictor for industrial concentration (χ_c) comes from the shifts, i.e., the differential dynamics of

sectoral demand during the time of rapid industrialization and market expansion; and land supply factors that are relevant to cities *after 1881*.

The previous parametrization of externalities relies on a few important choices, e.g., related to the spatial extent of such spillovers, to treatment heterogeneity, and to the (log) linear nature of the estimated relationship (Combes and Gobillon, 2015). In the baseline specification(s), we will assume a (log) linear relationship; that the spillovers are homogeneous; and that they exclusively operate *within* cities (motivated by the localized nature of Jacobs externalities, see, e.g., Carlino and Kerr, 2015). We will relax these assumptions in a sensitivity analysis. More crucially, the literature on the empirics of agglomeration externalities usually distinguishes static and dynamic externalities. Our approach differs from the existing literature by focusing on *long-run* externalities, relating industrial structure and city size at the end of the nineteenth century to contemporary outcomes. We account for endogeneity, notably by leveraging variation from differential aggregate dynamics across industries between 1817 and 1881 and conditioning on pre-industrial conditions and city fundamentals.

The literature also discusses measurement issues: (i) how to construct an industrial concentration or diversity index; and (ii) which outcomes to consider. Our baseline measure is a Herfindahl industrial concentration index constructed from the shares of local employment within industries; we will consider alternative measures and associated instruments in robustness checks, e.g., measures of local distance to the national industrial portfolio. Regarding the choice of outcomes, our reduced-form approach will rely on (i) city-level proxies for economic development including wages, and (ii) an empirical measure of total factor productivity at the firm level; our proper quantitative exercise will use model-inferred total factor productivity at the city/industry level—relying on the model structure and the distribution of employment/wages across cities and industries.

3 Motivating facts

3.1 Long-run agglomeration and Jacobs externalities

This section assesses the strength of long-run agglomeration and Jacobs externalities within reduced-form specifications based on Equation (3).

The (exogenous) rise of different cities To establish a causal link between population, industrial concentration and the subsequent dynamics of cities, we isolate exogenous variation among the numerous factors shaping their transformation during the nineteenth century. Our empirical strategy relies on a specification with two instruments: natural land fragmentation at the fringe of urban settlements (ζ_c), intuitively

Table 2. Predicting late-nineteenth century industrial concentration and population—first stage estimates.

	Herfindahl index (1881) (1)	Employment (1881) (2)
Predicted Herfindahl index (χ_c)	0.177	-0.291
	(0.039)	(0.323)
	[**0.187**]	[**-0.047**]
Land fragmentation (ζ_c)	-0.002	-0.119
	(0.004)	(0.029)
	[**-0.014**]	[**-0.108**]
Observations	428	428

Notes: A unit of observation is a cluster of settlements around 1790-1820—following the procedure in Section 2.2. Standard errors are reported between parentheses and are clustered at the level of the closest city as of 2015 (there are 55 cities with a formal city status in England). Standardized effects are reported in square brackets. The dependent variables are the Herfindahl index of industrial concentration in 1881 (h_{c1}, column **1**) and (log) employment in 1881 (l_{c1}, column **2**). The set of baseline controls include: dummies corresponding to deciles of employment in 1817, deciles of industrial concentration in 1817, and deciles of agricultural employment and public employment shares in 1817; the industry-based shift-share, g_c; (log) area of the initial city outline; topography indices (maximum elevation, slope, mTPI†); soil bulk density; latitude/longitude; travel time to the closest market town, to each major port (London, Liverpool, Plymouth, Portsmouth), and to coal; distance to the shore; density of roads (1830), train lines (1851), and waterways; suitability to grow wheat, barley, oat, grass, and rye; share of heavy soil and clay (NSRI); built-up density and the predicted natural land fragmentation—both within the contours of the settlement around 1800 and within a 10-kilometer buffer. The specification also adds fixed-effects at the level of 39 counties and a shift-share control based on employment shares in 1881 and aggregate employment growth between 1881–1971. The two instruments are the shift-share predictor of industrial concentration (χ_c) and natural land fragmentation in the immediate fringe of urban settlements, ζ_c. †: mTPI is a Multi-Scale Topographic Position Index, capturing local elevation in comparison with mean elevation within a neighborhood (i.e., identifying ridges or valleys).

predicting (log) *population* when the structure of cities stabilizes; and our shift-share concentration index (χ_c), predicting *industrial concentration*.

We report the first stage estimates in Table 2. First, predicted industrial concentration does induce more industrial concentration in 1881. The pass-through between the shift-share index of industrial concentration (χ_c) and the actual concentration index (h_{c1}) is around 0.18, i.e., a 0.10 higher shift-share index translates into a 0.018 higher Herfindahl index in 1881. Second, we find that predicted land fragmentation impacts the capacity of cities to grow: a one standard deviation increase in land fragmentation (about 0.5) decreases employment by about 6% (0.5×0.12). Importantly, the instrument for urban growth (respectively, industrial concentration) does not significantly predict industrial concentration (respectively, city size), conditional on our controls. This conditional orthogonality between the two sources of variation is necessary to disentangle effects operating through industrial concentration from those operating through city size. In that spirit, we later report the conditional F-statistics, following Sanderson and Windmeijer (2016) and conditioning on the other endogenous variable(s).

Figure 9. Industrial concentration appears to be detrimental in the longer run.

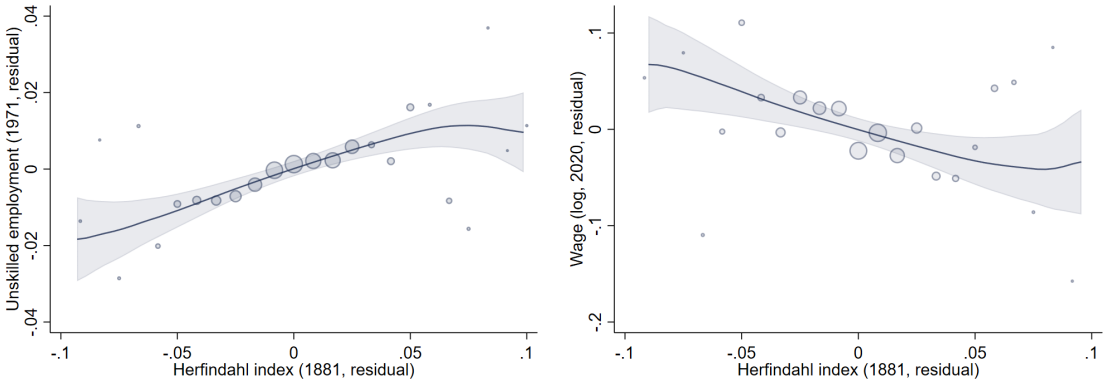

(a) Unskilled employment (1971)

(b) Wage (2020)

Notes: Panel **(a)** displays the relationship between industrial concentration in 1881 and the share of unskilled workers in 1971 (following the definition used in Heblich et al., 2021) across our 435 cities; both measures are cleaned for all controls used in Table 2. The dots represent the average residualized share of unskilled workers in 1971 within each of 20 bins grouping residualized Herfindahl index across cities, and the line is a locally weighted regression on all observations. Panel **(b)** displays the relationship between residualized industrial concentration in 1881 and residualized (log) wage in 2020.

Industrial concentration causes long-run decline The concentration of industries appears to be detrimental in the longer run. Figure 9 shows how industrial concentration in 1881 correlates with a measure of urban deprivation in the longer run, i.e., the share of low-skilled workers in 1971 (derived following Heblich et al., 2021, see panel a): even *before* the swift decline in manufacturing employment, specialized cities appear less attractive to skilled employment. Panel (b) shows how industrial concentration in 1881 correlates with a more recent measure of wage, namely labor income estimates for small areas based on the 2020 Family Resources Survey. The estimated gradients imply that less specialized cities in 1881, with a Herfindahl index around 0.05, had about 1.5 percentage points fewer unskilled workers in 1971 and 4% higher wages than more specialized cities with an index of 0.15.

We now use the exogenous variation in economic structure at the end of the nineteenth century to provide causal evidence on how early patterns of economic development shaped long-run city dynamics. We first shed light on these dynamics by regressing current outcomes in city c, y_{c2}, on urban development in 1881, $\mathbf{x}_{c1} = (h_{c1}, l_{c1})$,

$$y_{c2} = \alpha + \beta \mathbf{x}_{c1} + \gamma \mathbf{X}_c + \varepsilon_c,$$

while instrumenting $\mathbf{x}_{c1}$ with our exogenous predictors $\mathbf{p}_c = (\chi_c, \zeta_c)$ and conditioning on a large set of covariates $\mathbf{X}_c$. This specification differs from specification (3) and its subsequent structural estimation in two important dimensions. First, for ease of interpreta-

Table 3. The long-run effect of industrial concentration and city population—city-level estimates.

	Unskilled employment			Growth	Wage
	1971	1981	1991	1971	2020
Panel A: OLS					
Herfindahl (1881)	0.142	0.066	0.021	-2.530	-0.415
	(0.053)	(0.079)	(0.084)	(0.524)	(0.207)
Employment (1881)	0.020	0.040	0.069	0.046	-0.076
	(0.007)	(0.009)	(0.014)	(0.083)	(0.031)
	Unskilled employment			Growth	Wage
	1971	1981	1991	1971	2020
Panel B: TSLS					
Herfindahl (1881)	0.483	0.722	1.003	-3.459	**-2.338**
	(0.209)	(0.326)	(0.401)	(1.973)	(0.870)
	{18.45}	{18.45}	{18.45}	{18.45}	{18.45}
Employment (1881)	0.007	0.006	0.030	-0.101	**-0.248**
	(0.027)	(0.042)	(0.057)	(0.228)	(0.145)
	{18.60}	{18.60}	{18.60}	{18.60}	{18.60}
			Specification for the shifts		
Wage (2020)	All	Ex. 75km	Ex. 100km	Input	Trade
Panel C: Alternative shifts					
Herfindahl (1881)	-2.133	-2.416	-2.503	-3.631	-3.769
	(0.784)	(0.935)	(0.920)	(1.750)	(1.999)
	{22.43}	{16.73}	{16.50}	{12.32}	{10.72}
Employment (1881)	-0.251	-0.240	-0.248	-0.244	-0.245
	(0.143)	(0.147)	(0.147)	(0.176)	(0.176)
	{18.32}	{19.03}	{18.64}	{17.29}	{16.79}
			Additional controls		
Wage (2020)	Initial	Agricult.	Enclos.	Rateable	Manuf.
Panel D: Additional controls					
Herfindahl (1881)	-2.190	-2.485	-2.469	-2.731	-3.367
	(0.909)	(1.206)	(0.952)	(0.967)	(1.145)
	{14.94}	{12.77}	{13.16}	{17.26}	{14.17}
Employment (1881)	-0.245	-0.212	-0.218	-0.231	-0.401
	(0.168)	(0.177)	(0.161)	(0.152)	(0.207)
	{13.31}	{15.95}	{12.73}	{18.67}	{10.24}

Notes: A unit of observation [428] is a settlement around 1790–1820. Standard errors—clustered at the level of the closest city—are reported between parentheses; and projected F-statistics are reported in brackets (following Sanderson and Windmeijer, 2016). Panel **A** reports OLS estimates for the share of unskilled workers in 1971, 1981, and 1991 (following Heblich et al., 2021), employment growth between 1881–1971, and (log) average wage in 2020. Panel **B** reports TSLS estimates in which the two instruments are the shift-share predictor of industrial concentration (χ_c) and natural land fragmentation in the city fringe, ζ_c. Panel **C** varies the shifts used in the shift-share instrument, χ_c. While the set of baseline controls is the same as in Table 2, Panel **D** adds controls for initial conditions (agricultural buildings in 1750, Domesday buildings, manufacturing in 1817), agriculture within the expanded city fringe (caloric potential, and arable share), parliamentary enclosures within the settlement and within 1, 2, 3, 5, 10 kms (Heldring et al., 2022), land prices in 1815 (see Heblich et al., 2024), and the employment shares in manufacturing and transport in 1817.

tion, we adopt a linear specification in industrial concentration, with $h_{c1} = \sum_{j \in I} \left(\frac{L_{jc1}}{L_{c1}}\right)^2$. Second, the equation is estimated at the city level, implying that we cannot properly control for Marshall-Arrow-Romer externalities and for industry fixed effects—a caveat that we later address in firm- or industry-level specifications. The effect of industrial concentration on long-run city performance might reflect two distinct forces: nationwide industry decline might hurt cities specialized in those declining industries; and concentration might exert a direct effect on future city productivity, as suggested by Jacobs (1969). We isolate the latter effect by controlling for aggregate industry trends from 1881 to the present period in a shift-share design.

Table 3 shows that historical industrial concentration has adverse long-run consequences. Panel A first reports OLS estimates consistent with the visual patterns in Figure 9: contemporary productivity is negatively correlated with historical concentration, whether productivity is measured by current wages—our preferred reduced-form city-level outcome—the employment share of unskilled workers in 1971, 1981, and 1991, or employment growth between 1881 and 1971. Panel B then presents causal estimates from our **baseline** two-stage specification, in which the predicted shift-share concentration index (χ_c) uses leave-out sectoral growth as the shifts, $d_{j\,j \in I}$, excluding a 50-by-50-kilometer cell around each city. First, we find that higher historical industrial concentration (h_{c1}) predicts higher unskilled employment shares in 1971, 1981, and 1991, smaller city size in 1971, and substantially lower returns to labor in 2020. Second, although historical city size retains some predictive power, its estimated effects are an order of magnitude smaller and not statistically significant. Quantitatively, a 0.10 increase in the 1881 Herfindahl index is associated with 23% lower wages in 2020, whereas a 20% increase in city size in 1881 predicts only about 5% lower wages in 2020.

The implied variation in returns to labor associated with Jacobs externalities is economically large relative to standard agglomeration elasticities. For instance, a contemporaneous one-standard-deviation increase in city size would raise wages by about 7% (Graham and Gibbons, 2019). By contrast, our estimates imply that a one-standard-deviation increase in the 1881 Herfindahl index is associated with a 14% decline in wages.

Table 4 reports results from our firm-level analysis using data from 2008–2018. We aggregate all geographic variables to the NUTS-3 level (local administrative units) and replicate our baseline specification in a stacked regression framework, with (log) sales as the dependent variable. The regression is restrictive. It includes year fixed effects, (log) factor inputs, four-digit industry fixed effects (η_i), and the local share of turnover or employment in the firm's industry to account for Marshall-Arrow-Romer externalities (column 2). Under this specification, the coefficient of interest can be interpreted as the effect on firm-level total factor productivity net of industry-specific variation. Quantita-

Table 4. The long-run effect of industrial concentration and city population—firm-level estimates.

Turnover (ABS)	(1)	(2)
Herfindahl index (1881, h_{c1})	-3.378	**-2.376**
	(1.716)	(1.176)
Employment (1881, l_{c1})	-0.311	**-0.213**
	(0.043)	(0.029)
Observations	2,192,591	2,192,591
Local industrial share	No	Yes

Notes: A unit of observation is a firm/year in the Annual Business Survey (ABS). Standard errors are reported between parentheses and are clustered at the NUTS-3 level. The dependent variable is (log) annual sales/turnover. The main endogenous variables are the Herfindahl index of industrial concentration in 1881 (h_{c1}) and (log) employment in 1881 (l_{c1}). The two instruments are the shift-share predictor of industrial concentration (χ_c) and natural land fragmentation in the immediate fringe of urban settlements, ζ_c. The baseline controls are the same as in Table 2. In columns **(1)** and **(2)**, we control for year fixed effects, and (log) production factors (material, employment, capital). In column **(2)**, we control for SIC-4 fixed effects and the local share of turnover/employment in the firm industry.

tively, a 0.10 higher Herfindahl index in 1881 is associated with 24% lower productivity, whereas a 20% larger 1881 city is associated with only about 4% lower productivity—closely mirroring the city-level estimates.

Industrial concentration and patterns of innovation As discussed in Section 1, the long-run consequences of industrial concentration may operate through its contemporaneous effects on innovation. In Table 5, we replicate the baseline specification in Table 3 (B), replacing the long-run dependent variables with contemporaneous measures of innovation for 1883–1893: the (log) number of unique patents; the (log) number of unique inventors; the concentration of innovation; and the average *width* of patents—defined as the number of sub-industries, among 55 categories, appearing in the patent description.[15] An increase in the 1881 employment Herfindahl index is associated with substantially fewer patents (column 1) and inventors (column 2), consistent with the contrasting trajectories of Leeds and Bradford documented in Section 1.2 and Figure 5. Innovation intensity declines markedly in more specialized cities, but its composition changes as well: industrial concentration in employment is associated with an even sharper concentration of innovation, with a pass-through of approximately 1.84 between the two Herfindahl indices (column 3). One manifestation of this mechanism appears at the level

[15]We choose a 10-year window beginning in 1883 for two reasons: (i) for consistency, patenting measures are constructed after 1881; and (ii) the Patents, Designs, and Trade Marks Act of 1883 established the foundations of the modern intellectual property system through the formal examination of applications and improved documentation and dissemination of accepted patents.

of individual patents: a 0.10 increase in the 1881 Herfindahl index reduces the number of sub-industries referenced in patent descriptions (ranging from 1 to 4) by 0.62.

These patterns point to innovation—and the ability to adapt and reinvent—as a central mechanism linking industrial concentration to long-run local productivity.

Table 5. The effect of industrial concentration and city population on innovation (1883–1893).

Innovation (1883–1893)	Patents (1)	Innovators (2)	Concentration (3)	Width (4)
Herfindahl index (1881, h_{c1})	-34.050	-34.184	1.835	-6.254
	(15.776)	(14.207)	(1.049)	(2.985)
	{18.45}	{18.45}	{18.45}	{13.85}
Employment (1881, l_{c1})	-2.235	-1.330	0.087	0.750
	(2.277)	(2.133)	(0.166)	(0.468)
	{18.60}	{18.60}	{18.60}	{22.14}
Observations	428	428	428	381

Notes: The unit of observation is a settlement observed between 1790 and 1820. Standard errors, clustered at the level of the nearest city, are reported in parentheses; projected F-statistics are reported in brackets (following Sanderson and Windmeijer, 2016). We report TSLS estimates using two instruments: the shift-share predictor of industrial concentration (χ_c) and natural land fragmentation in the city fringe (ζ_c). The specification follows Panel B of Table 3. The dependent variables are defined as: **(1)** the log number of unique patents; **(2)** the log number of unique inventors; **(3)** the concentration of innovation; and **(4)** the average *width* of patents. Appendix A.4 reports separate patent estimates by one-digit industry.

Our empirical, reduced-form assessment of long-run externalities necessarily imposes restrictions on their spatial and sectoral scope. First, we abstract from heterogeneity in linkage intensity across sectors: some industries may be intrinsically more interconnected than others, potentially affecting the long-run impact of industrial concentration. Second, we restrict the spatial extent of externalities to within cities and ignore the industrial structure of neighboring cities. These choices reflect the limits imposed by our causal identification strategy: estimating spillovers across industries or across cities poses substantial empirical challenges. In the next section, we explore these dimensions further and examine the robustness of our conclusions.

3.2 Sensitivity analysis

Industrial concentration appears to be a key driver of the long-run underperformance of British cities. We now present a series of robustness checks, with additional detail in Appendix A.4, to support this conclusion.

Robustness of the industrial concentration effect Our identification strategy relies on leave-out sectoral growth measures that compute aggregate sectoral employment

shifters excluding a 50 × 50 kilometer cell around each city. Panel C of Table 3 shows that our results are stable when using alternative shift constructions: (i) including all locations; and (ii) excluding 75 × 75 kilometer or 100 × 100 kilometer cells. Panel C also reports specifications that rely on shift-share instruments more explicitly tied to specific forces affecting aggregate industrial dynamics: global supply factors operating through real input costs (column 4), and demand factors induced by trade with new partners (column 5). While these specifications are less statistically powered than our baseline, the qualitative conclusion that industrial concentration adversely affects long-run city-level productivity remains.

We interpret this industrial concentration effect as reflecting between-sector externalities à la Jacobs. Consistent with this interpretation, Appendix A.4 shows that our findings are orthogonal to secular structural transformation (Table A3) and are not driven by any specific nineteenth-century two-digit sector (Figure A11). The appendix further supports the shift-share design by allowing for cross-sector linkages—measured through occupational transitions in the 1851 and 1861 micro-censuses—and by estimating alternative parametric specifications commonly used in the literature (e.g., log Herfindahl indices, their inverse, or controls for the number of active industries; see Table A4).

Robustness of the city size effect Our identification narrative for the city size effect posits that land fragmentation constrains subsequent urban development by limiting land supply at the fringe of early settlements. Alternative mechanisms may also be at play, for example through differential agricultural productivity (Coeurdacier et al., 2022), agricultural mechanization (Caprettini and Voth, 2020) or the emergence of distinct informal institutions in areas with different land ownership structures (Heldring et al., 2022). To alleviate these concerns, our baseline specification controls for marginal land supply from the end of the nineteenth century onward; local suitability for arable production and potential crop yields (which capture exposure to the Grain Invasion; see Heblich et al., 2024); and access to natural resources, addressing the possibility that energy availability drives the rise and decline of British cities.[16] Panel D of Table 3 further adds controls for initial conditions, including agricultural productivity within the city fringe, parliamentary enclosures within the fringe, pre-1817 land prices, and employment shares in manufacturing and transport in 1817. For transparency, Appendix A.4 adopts the opposite approach, reporting more parsimonious specifications that omit baseline controls for connectedness, transport infrastructure, agricultural productivity, soil characteristics, and county fixed effects (Table A2).

[16] In unreported checks, we further show that the vast majority of cities expand beyond this narrow ring by the end of the nineteenth century, and that there are no systematic differences in zoning policies at the urban fringe—such as green belts or social housing—depending on their initial land fragmentation.

Spatial spillovers, heterogeneity, and sensitivity Appendix A.4 examines the spatial extent of Jacobs externalities and potential treatment heterogeneity, albeit in specifications that are less statistically powered than our baseline (Tables A5 and A6). We find that spatial spillovers are limited in a specification with three endogenous variables—population, local industrial concentration, and nearby industrial concentration—where nearby concentration and its instrument incorporate settlements within a 40-kilometer radius. The appendix also documents limited treatment heterogeneity across cities with differing shares of services, manufacturing, or primary-sector employment.

The appendix further reports sensitivity analyses that vary the construction of the land-fragmentation instrument (using fixed buffers or alternative spatial segmentations), inference procedures (to account for spatial correlation), and the cutoffs used to define urban settlements (Figure A12).

Overall, these robustness exercises leave our headline results unchanged. The stylized facts presented in this section provide evidence on the joint dynamics of urbanization and industrial diversity, highlighting that the long-run fate of cities is closely tied to their industrial structure. However, reduced-form estimates cannot account for general equilibrium forces and speak to the aggregate and distributional productivity and welfare implications of these externalities. The next section therefore adopts a structural approach by developing a quantitative model of cities and industries over time, capturing both spatial linkages across cities within a given period and intertemporal externalities.

4 A multi-sector dynamic spatial model

In this section, we develop a spatial, multi-sector, dynamic model of cities. The model involves a finite number of cities, $c \in \{1, \dots, C\}$, and industries, $i \in \{1, \dots, I\}$. Time is discrete and is indexed by t. Within each industry, every city produces its own variety that consumers view as different from varieties produced in other cities. There is an exogenous number of workers in the economy, $\bar{L}$. Each worker maximizes her utility from the consumption of varieties, is endowed with one unit of labor, and lives for one period.[17] The worker decides which industry to work for and which city to live in.

In what follows, we describe the four main building blocks of the model: workers' preferences, the production technology, the equilibrium within a time period t, and the dynamic process that links subsequent periods to each other.

[17] Each period corresponding to a century in the quantification, we view this as a realistic assumption. We present a version of the model with infinitely lived, forward-looking workers in Appendix B.2.

Preferences If a worker m who lives at time t decides to work in industry i and to reside in city c, she chooses her consumption levels to maximize her utility,

$$U_{ict}^m = \max_{\{q_{jdt}^m\}_j} \left\{ a_{ct}^m \left[\sum_{j=1}^{I} \left(\sum_{d=1}^{C} \left(q_{jdt}^m \right)^{\frac{\epsilon-1}{\epsilon}} \right)^{\frac{\epsilon}{\epsilon-1}\frac{\sigma-1}{\sigma}} \right]^{\frac{\sigma}{\sigma-1}} \right\}, \tag{4}$$

subject to the budget constraint,

$$\sum_{j=1}^{I} \sum_{d=1}^{C} p_{jdt} q_{jdt}^m \leq w_{ict} + R_{ct}, \tag{5}$$

where a_{ct}^m denotes the level of amenities enjoyed by the worker in city c, while the rest of the worker's utility is drawn from her consumption of varieties. Specifically, q_{jdt}^m denotes the worker's consumption of the city-d variety in industry j, p_{jdt} denotes the price of this variety, w_{ict} is the wage that prevails in the city-industry, and R_{ct} is the worker's share of land rents. When choosing her city, industry and consumption, the worker takes amenities, prices and wages as given. We assume that varieties are substitutes, and they are more substitutable within than across industries, implying $1 < \sigma < \epsilon$.

Amenities are a combination of three factors,

$$a_{ct}^m = \bar{a}_c L_{ct}^{-\nu} \varepsilon_{ct}^m, \tag{6}$$

where: $\bar{a}_c$ is the fundamental amenity level of city c, stemming from natural characteristics such as climate; $L_{ct}^{-\nu}$ is a congestion externality that makes cities with a larger population L_{ct} less pleasant places to live; and ε_{ct}^m is an idiosyncratic taste shock for city c that is drawn from the following Fréchet distribution,

$$Pr\left[\varepsilon_{ct}^m \leq z\right] = e^{-z^{-1/\eta}}, \tag{7}$$

and independently so across workers, cities and time periods. If η is high, then workers' utility is influenced to a large extent by their idiosyncratic tastes for cities; they are likely to settle in a city that they like, rather than in a city that offers them economic opportunities. The same would be true if workers faced high moving costs: η can also be interpreted as a parameter driving the severity of mobility frictions across cities.

Technology Varieties are produced by perfectly competitive firms. The representative firm produces the city-c variety in industry i at time t by combining workers (L_{ict}) and

land (H_{ict}) as follows,

$$Y_{ict} = \Gamma \mathcal{T}_{ict} L_{ict}^{\gamma} H_{ict}^{1-\gamma}, \tag{8}$$

where $\mathcal{T}_{ict}$ is the Total Factor Productivity (TFP) of industry i in city c at time t. The constant $\Gamma = \gamma^{-\gamma}(1-\gamma)^{-(1-\gamma)}$ is introduced to simplify the subsequent formulas.

Varieties can be traded across cities, but they are subject to iceberg trade costs. We denote the iceberg trade cost prevailing between cities c and d in industry i at time t by τ_{icdt}. We assume that trade costs are non-negative, which amounts to $\tau_{icdt} \geq 1$.[18]

Land is supplied in each city according to the supply function,

$$H_{ct} = r_{ct}^{\zeta_{ct}-1}, \tag{9}$$

where r_{ct} is the rent and $\zeta_{ct} - 1$ is the land supply elasticity. We let the exogenous parameter driving this elasticity, ζ_{ct}, vary both across cities and over time in order to mirror the heterogeneity across cities uncovered in the empirical analysis. It is natural to assume that $\zeta_{ct} \geq 1$, i.e., the supply function is never downward-sloping. Land rents are fully redistributed to workers who live in the city.

Within-period equilibrium Before we turn to presenting the dynamic evolution of TFP, we set up the equilibrium within a given time period t for a *given* distribution of TFP in that period. In this within-period equilibrium, we impose that the labor market clears in each city, the land market clears in each city,

$$\sum_{j=1}^{I} \frac{1-\gamma}{\gamma} w_{jct} L_{jct} = r_{ct} H_{ct}, \tag{10}$$

markets clear for each variety,

$$\left(w_{ict} + R_{ct}\right) L_{ict} = \sum_{d=1}^{C} \left(\frac{P_{idt}}{P_{dt}}\right)^{1-\sigma} \left(\frac{p_{ict}\tau_{icdt}}{P_{idt}}\right)^{1-\epsilon} \sum_{j=1}^{I} \left(w_{jdt} + R_{dt}\right) L_{jdt}, \tag{11}$$

where P_{idt} is the price index of industry-i varieties in city d,

$$P_{idt} = \left[\sum_{c=1}^{C} p_{ict}^{1-\epsilon} \tau_{icdt}^{1-\epsilon}\right]^{\frac{1}{1-\epsilon}}, \tag{12}$$

[18] We abstract from international trade in our baseline model. In Appendix B.2, we present an extension of the model that features the rest of the world as an additional location. We show in this appendix that 19th-century trade between Britain and the rest of the world does not influence our model-based estimates of dynamic externalities.

P_{dt} is the price index across all goods in city d,

$$P_{dt} = \left[\sum_{j=1}^{I} P_{jdt}^{1-\sigma} \right]^{\frac{1}{1-\sigma}}, \tag{13}$$

and each worker chooses the city and industry that offers them the highest utility.

Dynamic evolution of productivity We allow the productivity of each industry to be influenced by agglomeration externalities of the form,

$$\mathcal{T}_{ict} = T_{ict} L_{ct}^{\alpha} g_i \left(L_{c,t-1}, \left\{ L_{jc,t-1} \right\}_{j \in I} \right), \tag{14}$$

where T_{ict} is the exogenous fundamental productivity of industry i in city c at time t. Thus, agglomeration externalities depend on the current population of city c, as standard in the literature, but also on past population (as in Allen and Donaldson, 2020) and past sectoral composition.

We motivate a specific functional form for g_i as follows. As in the literature surveyed by Buera and Lucas (2018), knowledge creation arises from productive meetings between agents. Workers are endowed with one unit of time that they can devote to research. During this time, they randomly meet other workers in the same city c. We assume that the arrival rate of meetings is such that the overall number of meetings per worker is proportional to $L_{c,t-1}^{a}$, where a captures returns to scale in the meeting technology.

Meetings between two workers may generate new ideas, denoted $n_{c,t-1}$ per worker, and may also contribute to the obsolescence of existing ideas, denoted $d_{c,t-1}$ per worker. We assume that total factor productivity in period t depends on knowledge creation in period $t-1$ according to,

$$g_i \left(L_{c,t-1}, \left\{ L_{jc,t-1} \right\}_{j \in I} \right) \propto n_{c,t-1} \cdot d_{c,t-1}^{-b},$$

in which $b > 0$ governs the productivity impact of knowledge obsolescence. Each matching pair produces a new idea with probability p, which we normalize to one. However, we assume that meetings between workers from the same industry generate less novel ideas because their underlying knowledge is more similar. For simplicity, we assume that a new idea contributes to knowledge obsolescence with probability zero if the two workers belong to different industries, and with probability one if they belong to the same industry. Under these assumptions,

$$n_{c,t-1} = L_{c,t-1}^{a}, \quad d_{c,t-1} = L_{c,t-1}^{a} \sum_{j=1}^{I} \left(\frac{L_{jc,t-1}}{L_{c,t-1}} \right)^{2}$$

where $\left(\frac{L_{jc,t-1}}{L_{c,t-1}}\right)^2$ is the share of meetings involving two workers from industry j. Consequently, city-industry productivity evolves according to,

$$\mathcal{T}_{ict} = T_{ict} L_{ct}^{\alpha} L_{c,t-1}^{\rho} \left[\sum_j \left(\frac{L_{jc,t-1}}{L_{c,t-1}} \right)^2 \right]^{-\lambda}. \tag{15}$$

where $\lambda = b$, $\rho = a(1-b)$, and $T_{ict} L_{ct}^{\alpha}$ captures contemporaneous drivers of productivity.

This process, which links city-industry productivity to the spatial and sectoral distribution of employment in the previous period, generates the dynamics of the model and underlies the joint evolution of cities and industries. Equation (15) provides a flexible formulation of externalities that generalizes the process described in the one-sector model of Allen and Donaldson (2020).

Solving the model To solve the model, we exploit its recursive structure. In particular, we leverage the fact that the within-period equilibria of subsequent periods are only linked through the dynamic productivity process of Equation (15). This suggests the following strategy to solve the model from any period t: solve the within-period equilibrium of period t; obtain the productivity of each city-industry in period $t+1$ from Equation (15); solve the within-period equilibrium of period $t+1$; and so on. We provide the details of the solution algorithm in Appendix B.1.

5 Quantitative analysis

We now use the previous spatial model to quantify the role of local long-run externalities and their distributional consequences on the allocation of economic activity across space.

5.1 Parametrization, model inversion, and estimation

The quantification of our model requires: (i) a parametrization of key model elasticities; (ii) using its structure to recover unobserved city-specific fundamentals that rationalize the observed employment by city-industry and wages by city (a model inversion); and (iii) introducing the recovered productivities within a similar empirical framework as the one discussed in Section 2.3 to estimate Equation (15), i.e., the equation that drives the dynamic evolution of productivity.

Given its recursive structure, the model can be taken to the data in any period, and independently so. For reasons that will become clear later in this section, we primarily use contemporary data—covering the "long-run" or period 2—to estimate the model.

Parametrization and observable data We parametrize key elasticities from the empirical literature—focusing primarily on recent times (i.e., period 2). We set the elasticity of substitution across sectors, σ, to be equal to 4 (Bernard et al., 2003) and an elasticity of substitution across varieties, ϵ, equal to 5 (Simonovska and Waugh, 2014). Our modeling of productivity features a static agglomeration externality, as usual in quantitative models fitting a distribution of workers across cities of very different sizes (e.g., discussed as scale economies in Henderson, 1974). We consider a static agglomeration externality, α, of 0.07 (following Graham and Gibbons, 2019, which reports the latest available agglomeration-productivity elasticity estimates for the United Kingdom). The dispersion parameter of idiosyncratic location tastes, η, and the congestion parameter, ν, are tied together in the equilibrium conditions (see, for instance, Equations B.11 or B.12); they both serve as mitigation forces to limit differences in city sizes. We thus set $\nu + \eta$ to match an average migration elasticity of 2 (Head and Mayer, 2021). We use granular elasticities of housing supply at the Middle Layer Super Output Area (MSOA) level from Drayton et al. (2024) and map these estimates to the expanded urban area around our 435 cities in order to parametrize ζ_{c2} in each city c. These elasticities, obtained from a similar procedure as in Baum-Snow and Han (2024), are quite low, around 0.2 on average, illustrating the (recent) institutional constraints to development in cities of England and Wales. We also calibrate trade costs using data on the evolving transportation infrastructure (Appendix B.3).

Finally, our quantitative exercise requires a labor share in production, data on employment per industry and per city (L_{ict}), and data on wages at the city level w_{ct}. We rely on Feinstein (1972) and set a labor share of production at 0.77, arguably in the high range of such estimates. For employment by 2-digit industry (88 categories), we use the Business Register and Employment Survey in 2020 at the ward level and nest these estimates within our own geographies.[19] Finally, while we observe productivity, production factors, and wages at the firm level (as exploited in Section 3.1), we do so within a secure server where we cannot properly invert our very demanding model. For this reason, we rely on labor income estimates for small areas (Middle Layer Super Output Area, provided by the Office for National Statistics in 2020), which we nest within our geographies to measure wages at the city level. These quantities are key to recovering unobserved fundamentals that will be the inputs of our counterfactual: amenities and city-industry productivities.

Model inversion In this step, we recover the amenities, $\{\bar{a}_c\}_{c\in\{1,\dots,C\}}$, and productivities, $\left\{\overline{T}_{ic2}\right\}_{c,i}$, that rationalize observed wages (w_{c2}) and employment by city-industry

[19] Employment by 2-digit industry and city in the nineteenth century are available per Section 2.1.

in period 2 (L_{ic2}). The following theorem states that, given wages and employment per industry, there is a unique set of fundamentals that rationalize the data.

Theorem 1. *In each period and given the values of structural parameters, trade costs, and data on wages w_{c2} and employment by city-industry L_{ic2}, one can uniquely recover Total Factor Productivity levels $\overline{T}_{ic2}$ (up to scale) and amenities (relative to aggregate welfare, $\bar{a}_c/\overline{U}_2$).*

Proof. See Appendix B.3. □

Intuitively, the uniqueness result of Theorem 1 stems from the fact that the system of equations characterizing the equilibrium—Equations (B.7) to (B.9) in Appendix B.1—can be inverted to recover the values of fundamentals. The output of this procedure is a set of amenities $\mathcal{A} = \{\bar{a}_c\}_c$ and city-industry productivities $\mathcal{T} = \left\{\overline{T}_{ic2}\right\}_{i,c}$ across 435 cities—and 88 industries for the latter.[20]

Estimating long-run productivity spillovers Armed with the distribution of productivities, $\left\{\overline{T}_{ic2}\right\}_{i,c}$, we estimate the last block of our model, i.e., the equation characterizing the evolution of city-industry productivities:

$$\overline{T}_{ic2} = \mathcal{P}_{i2} \cdot L_{c1}^{\rho} \cdot \left[\sum_j \left(\frac{L_{jc1}}{L_{c1}}\right)^2\right]^{-\lambda} \cdot L_{ic2}^{\mu} \cdot \varepsilon_{ic2}. \tag{16}$$

Equation (16) can be estimated within an empirical setting that mirrors the one described in Section 2.3. Specifically, one can use exogenous land fragmentation ζ_c and the (log) predicted Herfindahl χ_c as instruments for period-1 (log) population and (log) industrial concentration. Equation (16) corresponds to the second stage of this two-stage procedure. Note that we split the term T_{ic2} of Equation (15) into two components in Equation (16): an aggregate industry trend $\mathcal{P}_{i2}$ and a structural error term ε_{ic2}. In effect, the term $\mathcal{P}_{i2}$ can be estimated as an industry fixed effect in Equation (16). Isolating these industry trends allows us to disentangle them from the long-run externalities.

In practice, we estimate the following specification,

$$\ln \overline{T}_{ic2} = \eta_i + \rho \ln L_{c1} - \lambda \ln \left[\sum_j \left(\frac{L_{jc1}}{L_{c1}}\right)^2\right] + \mu \ln L_{ic2} + \gamma \mathbf{X}_c + \varepsilon_{ic},$$

while instrumenting $\ln L_{c1}$ and $\ln \left[\sum_j \left(\frac{L_{jc1}}{L_{c1}}\right)^2\right]$ by our exogenous predictors $\mathbf{p}_c$; controlling for all variables used in Table 2 as well as county-level fixed effects and industry-level fixed effects; and clustering standard errors at the level of the closest city as of

[20] To implement the inversion procedure, we use an algorithm that we detail in Appendix B.3.

Table 6. The structural estimates for long-run externalities.

Productivity $\left(\ln \overline{T}_{ic2}\right)$	(1)	(2)	(3)
Herfindahl index ($h_{c1} = \ln \sum_j \left(L_{jc1}/L_{c1}\right)^2$)	-1.227	**-0.794**	-0.792
	(0.484)	(0.392)	(0.394)
	{18.40}	{18.56}	{18.59}
Employment ($l_{c1} = \ln L_{c1}$)	0.369	**-0.030**	-0.057
	(0.437)	(0.341)	(0.386)
	{22.63}	{22.54}	{21.02}
Observations	38,280	38,280	38,280
Static MAR	No	Yes	Yes
Long-run MAR	No	No	Yes

Notes: A unit of observation is a city/industry where a city is identified following our clustering procedure described in Section 2.2 and an industry is one of the 88 industrial categories (2-digit) present in the Business Register and Employment Survey. The specifications include the same controls as in Table 2, as well as 2-digit industry-level fixed effects. In column **(2)**, we control for the (log) local employment in the industry to account for Marshall-Arrow-Romer (MAR) externalities when such employment is not equal to zero. In column **(3)**, we further condition on long-run Marshall-Arrow-Romer (MAR) externalities. Standard errors are reported between parentheses and are clustered at the level of the closest city as of 2015; and projected F-statistics are reported in brackets (following Sanderson and Windmeijer, 2016).

2015. Table 6 shows that ρ is not statistically different from 0, consistent with Gibrat's law. By contrast, λ is statistically different from 0 and quite large: a 20% increase in the Herfindahl index, about half of a standard deviation on average, reduces overall productivity in a city by 16% (see columns 2 and 3 in which we control for static and long-run Marshall-Arrow-Romer externalities).[21]

5.2 Counterfactuals

We next use the estimated model to conduct counterfactual experiments. First, we assess the role of long-run Jacobs externalities in explaining the distribution of population and income across British cities. Second, we consider a stylized policy experiment in order to shed light on the arbitrage faced by a local planner willing to balance the short-run gains from specialization in a city's comparative advantage(s) against the subsequent productivity losses in the longer run.

[21] We provide some visual evidence for this negative relationship in Appendix B.3 and Appendix Figure B1. We also show that industrial concentration is *not* related to the recovered *amenities*—which we will assume to be fixed across periods and across our counterfactual experiments.

Neutralizing Jacobs externalities In this counterfactual, we offset long-run Jacobs externalities by changing the city-industry productivity levels of period 2 to,

$$\widetilde{T}_{ic2} = \overline{T}_{ic2} \left[\sum_j \left(\frac{L_{jc1}}{L_{c1}} \right)^2 \right]^{\lambda},$$

which amounts to eliminating the Herfindahl index from Equation (16) and simulating the evolution of an economy where industrial concentration does not negatively affect productivity in the subsequent "generation." Note that we solve for the equilibrium of counterfactual economies by using the procedure laid out in Section 4.

How does neutralizing Jacobs externalities affect the distribution of employment and income across cities? In the top panels of Figure 10, we show how employment (panel a) and wages (panel b) change as a function of their 19th-century industrial concentration. Cities with a lower (higher) degree of initial concentration lose (gain), and these effects are sizable: A city at the 20th percentile of the 19th-century Herfindahl distribution (with a Herfindahl index of 0.06) loses 25% of its employment and 20% of its wages, while a city at the 80th percentile (with a Herfindahl index of 0.13) would grow markedly and gain 12% in wages.

These redistributive effects are substantial, but best illustrated in space or in meaningful measures of (regional) inequalities. A marker of regional inequalities in Britain is the North/South divide, or how London, its hinterlands, and a few other Southern cities like Bristol, are richer than the great Northern cities of the past such as Liverpool, Manchester, Sheffield, Newcastle or Bradford. We use this divide as a way to see the redistributive effects of our counterfactual experiment. In Figure 10 panels (c)-(d), we nest cities using their Northing in the British National Grid (kilometers relative to a reference point within the projected coordinate system) and show the average population density and average wage along this latitude. For clarity, we draw lines corresponding to London and Manchester. One can see that there is indeed a north-south divide—with a productivity gap of about 35% between London and Manchester (panel d). Neutralizing long-run Jacobs externalities does not only reshuffle productivity gains (and employment) across cities; it does so along a (most) relevant north/south divide: the productivity gap is about 60% as large in the counterfactual experiment (20% between London and Manchester). A substantial part of contemporaneous regional inequalities in Britain is the legacy of past industrial concentration.[22]

[22]The remainder might be partly explained by the distribution of amenities and connectedness; it is however essentially the outcome of location-specific productivities interacted with the life cycles of industries. In short, Northern cities *also* have a comparative advantage in the wrong industries.

Figure 10. Neutralizing long-run Jacobs externalities.

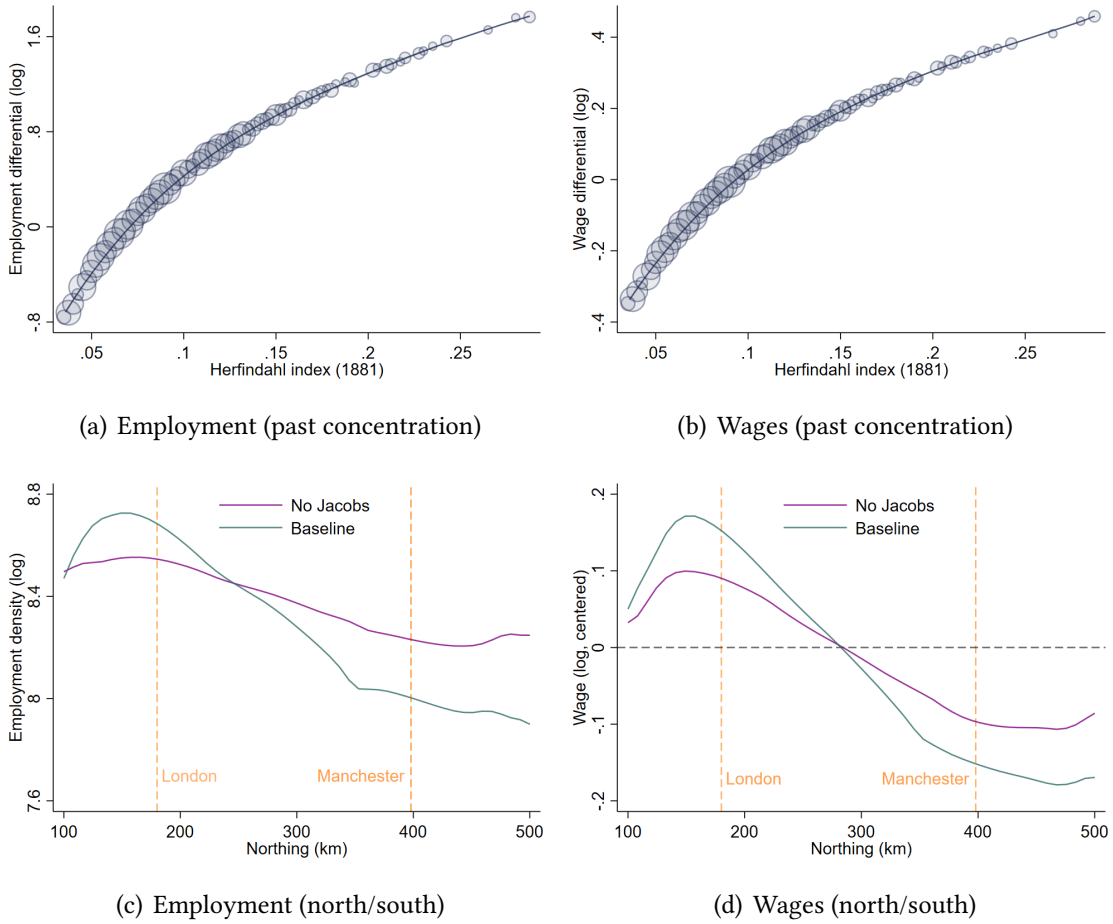

(a) Employment (past concentration)

(b) Wages (past concentration)

(c) Employment (north/south)

(d) Wages (north/south)

Notes: Panel **(a)** displays the relationship between industrial concentration in 1881 and the change in total employment from the period-2 data to the counterfactual equilibrium across our 435 cities. Panel **(b)** displays the same relationship between industrial concentration in 1881 and the change in nominal wages (per capita). Panels **(c)** and **(d)** nest cities along the "Northing" level in the British National Grid and display the best non-linear fit between average population density/wage against "Northing". For the sake of exposition, we display the Northing levels of London and Manchester as dashed (orange) lines. The baseline is represented by the green line; the counterfactual is the purple line.

Another "fundamental" trade-off? The preceding discussion of Jacobs externalities highlights a trade-off faced by local planners. A city may benefit from specializing according to its comparative advantage(s)—an insight at the heart of many place-based industrial policies. While such specialization may yield short-term gains, these gains might be offset by long-term productivity losses through the attenuation of cross-industry spillovers.

To capture the key trade-off, we introduce a stylized representation in which local policymakers can costlessly redistribute revenue-based total factor productivity across industries in their city according to:

$$\log\left(T^{*}_{ic2}\right) = \log\left(\overline{T}_{ic2}\right) + k\left[\log\left(\overline{T}_{ic2}\right) - \log\left(\overline{T}_{c2}\right)\right],$$

where $\overline{T}_{ic2}$ denotes productivity in industry i in city c at period 2, and $\overline{T}_{c2}$ is the unweighted average (log) productivity across all industries in city c. A policy with $k > 0$ increases the productivity of industries in which the city has a comparative advantage, mimicking policies that promote industrial concentration.

All local planners implement this costless policy and we evaluate outcomes using data for present-day England and Wales as the initial state. We then simulate the contemporaneous and long-term (period-3) distribution of economic activity—90 years later—keeping other city fundamentals, such as amenities, fixed. Welfare is measured across two generations of workers using expected indirect utilities, U_g, as:

$$\mathcal{V}(\beta) = U_2 + \beta^{90} \cdot U_3,$$

where $\beta \in (0, 1)$ is the (annual) social discount factor, and the economy grows at a constant annual rate of 2.1% (the annual growth of the UK over 1950–2015).

Figure 11. Policies affecting local industrial concentration.

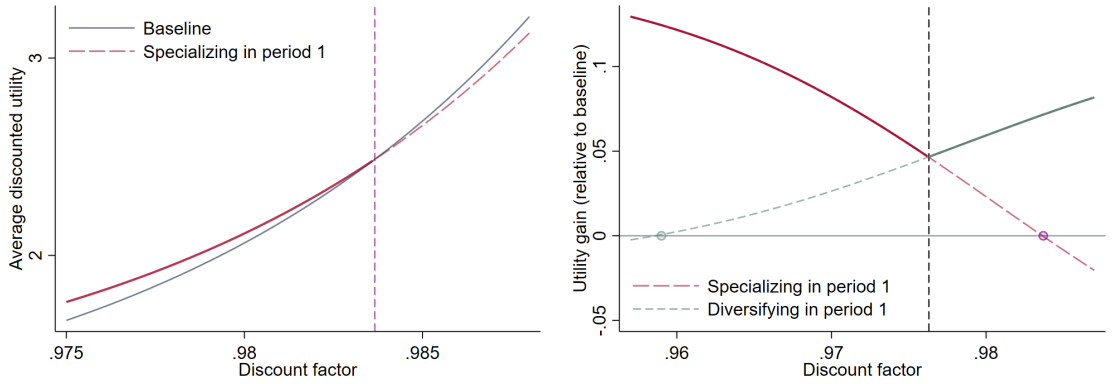

(a) Increasing industrial concentration

(b) Specializing/diversifying

Notes: Panel **(a)** displays welfare, $\mathcal{V}(\beta)$, in the baseline (blue line) and in a counterfactual economy where $k = 0.10$ redistributes productivity towards the productive industries in each city c (red line). A vertical dashed line marks the social discount factor below which such a (costless) policy would generate gains relative to the baseline economy. Panel **(b)** reports welfare in logarithmic terms relative to the baseline, $\log \mathcal{V}^f(\beta) - \log \mathcal{V}(\beta)$. We report: (i) a counterfactual economy where $k = 0.10$ redistributes productive gains towards the most productive industries (in red); and (ii) a counterfactual economy where $k = -0.10$ redistributes productive gains towards the least productive industries (in green). We highlight the range of discount factors β in which such policies would generate gains relative to the baseline economy by displaying a blue line corresponding to $y = 0$ (and dots in green and in red); the vertical dashed line separates the range of discount factors where the specializing/diversifying are preferred.

Figure 11 illustrates the trade-off between short-run gains from boosting comparative advantages and long-run losses from the resulting local industrial concentration. Panel (a) shows that a place-based industrial policy fostering industrial concentration across all cities is welfare-enhancing when the planner places relatively little weight on future generations. This could help explain the widespread adoption of such policies, particularly when planners are relatively impatient. Panel (b) complements this

insight by (i) providing a quantification of welfare gains relative to the baseline and (ii) showing the impact of a diversification policy ($k = -0.10$), in which productivities are redistributed away from stronger industries and towards weaker sectors in each city. In line with the previous insight, the diversification policy appeals more to patient planners, while the specialization policy is preferred by impatient ones. Interestingly, *both* policies improve welfare relative to the baseline within a range of discount factors, $\beta \in [0.96, 0.984]$, with minimum gains just under 4.5% at the point where the planner is indifferent between them.

The result points to a fundamental inter-temporal tension in the design of place-based policy. The weight a policymaker assigns to future generations is therefore central to evaluating any intervention that alters local industrial structure.

6 Concluding remarks

A large literature examines the rise and fall of cities, often focusing on prominent deindustrialized localities—such as Detroit or Manchester—or former factory towns. A separate body of work studies the sources of regional inequality and evaluates place-based versus people-based policies designed to address it. Our research lies at the intersection of these literatures by analyzing the *intertemporal* allocation of economic activity across space. We highlight a force that shapes both (i) the long-run dynamics of cities and (ii) the persistence of spatial inequality: industrial concentration and its effect on future productivity, particularly through cross-industry externalities à la Jacobs.

The presence of intertemporal spillovers introduces a dynamic trade-off for local policymakers. Specialization can raise short-run productivity by reinforcing local comparative advantage, but it may reduce industrial diversity and weaken long-run performance. This intertemporal trade-off complements the canonical static trade-off in urban economics between agglomeration benefits and crowding costs. How these intertemporal externalities shape optimal policy depends critically on how policymakers value the future. While both diversification and specialization may appear attractive, political incentives often favor short-term gains and place-based strategies that encourage concentration—implicitly placing lower weight on future productivity. Our framework makes this intertemporal tension explicit and quantifiable.

Our analysis models Jacobs externalities within a framework designed to study long-run urban dynamics rather than micro-level behavior. The precise channels through which these spillovers operate remain an open question. Do they operate primarily through technological innovation and cross-industry knowledge diffusion, through the accumulation of transferable human capital such as technical skills and entrepreneurial capabilities, or through broader institutional and organizational channels? Our evidence

on patenting activity provides suggestive support for innovation as one such mechanism, but identifying the relative importance of these channels remains an important task for future research.

References

Ahlfeldt, Gabriel M, Stephen J Redding, Daniel M Sturm, and Nikolaus Wolf, "The economics of density: Evidence from the Berlin Wall," *Econometrica*, 2015, *83* (6), 2127–2189.

Allen, Robert C., *The British Industrial Revolution in Global Perspective*, Cambridge University Press, 2009.

_ , "The Interplay among Wages, Technology, and Globalization: The Labor Market and Inequality, 1620-2020," in "The Handbook of Historical Economics," Elsevier, 2021, pp. 795–824.

Allen, Treb and Dave Donaldson, "Persistence and Path Dependence in the Spatial Economy," Technical Report, National Bureau of Economic Research 2020.

_ **, Costas Arkolakis, and Xiangliang Li**, "On the Equilibrium Properties of Network Models with Heterogeneous Agents," Technical Report, National Bureau of Economic Research 2020.

Alvarez-Palau, Eduard J, Dan Bogart, Max Satchell, and Leigh Shaw-Taylor, "Transport and urban growth in the First Industrial Revolution," *The Economic Journal*, 05 2025, *135* (668), 1191–1228.

Arribas-Bel, Daniel, M-À Garcia-López, and Elisabet Viladecans-Marsal, "Building (s and) cities: Delineating urban areas with a machine learning algorithm," *Journal of Urban Economics*, 2021, *125*, 103217.

Autor, David H, David Dorn, and Gordon H Hanson, "The China syndrome: Local labor market effects of import competition in the United States," *American economic review*, 2013, *103* (6), 2121–2168.

Bairoch, Paul and Gary Goertz, "Factors of urbanisation in the nineteenth century developed countries: a descriptive and econometric analysis," *Urban Studies*, 1986, *23* (4), 285–305.

Baum-Snow, Nathaniel and Lu Han, "The microgeography of housing supply," *Journal of Political Economy*, 2024, *132* (6), 1897–1946.

Bellefon, Marie-Pierre De, Pierre-Philippe Combes, Gilles Duranton, Laurent Gobillon, and Clément Gorin, "Delineating urban areas using building density," *Journal of Urban Economics*, 2021, *125*, 103226.

Berkes, Enrico, Matthew Lee Chen, and Matteo Tranchero, "300 years of British patents," *Research Policy*, 2026, *55* (1), 105347.

_ , **Ruben Gaetani, and Martí Mestieri**, "Cities and Technological Waves," Technical Report, mimeo 2021.

Bernard, Andrew B., Jonathan Eaton, J. Bradford Jensen, and Samuel Kortum, "Plants and Productivity in International Trade," *American Economic Review*, 2003, *93* (4), 1268–1290.

Boeri, Filippo and Olmo Silva, "Marshall at the times of Marshall," Technical Report 2025.

Borusyak, Kirill, Peter Hull, and Xavier Jaravel, "Quasi-experimental shift-share research designs," *The Review of Economic Studies*, 2022, *89* (1), 181–213.

Brinkman, Jeffrey C, "Congestion, agglomeration, and the structure of cities," *Journal of Urban Economics*, 2016, *94*, 13–31.

Broadberry, S. N., B. M. S. Campbell, Alexander Klein, Mark Overton, and Bas van Leeuwen, *British Economic Growth, 1270-1870*, New York: Cambridge University Press, 2015.

Buera, Francisco J and Robert E Lucas, "Idea Flows and Economic Growth," *Annual Review of Economics*, 2018, *10* (1), 315–345.

Cai, Jie and Nan Li, "Growth through inter-sectoral knowledge linkages," *The Review of Economic Studies*, 2019, *86* (5), 1827–1866.

Caliendo, Lorenzo, Maximiliano Dvorkin, and Fernando Parro, "Trade and labor market dynamics: General equilibrium analysis of the China trade shock," *Econometrica*, 2019, *87* (3), 741–835.

Caprettini, Bruno and Hans-Joachim Voth, "Rage against the machines: Labor-saving technology and unrest in industrializing England," *American Economic Review: Insights*, 2020, *2* (3), 305–20.

Carlino, Gerald and William R Kerr, "Agglomeration and innovation," *Handbook of regional and urban economics*, 2015, *5*, 349–404.

Clark, Gregory, "'The Industrial Revolution', in Aghion, P. and Durlauf, S.N. (eds.)," *Handbook of Economic Growth*, 2014. Elsevier.

_ , **Kevin Hjortshøj O'Rourke, and Alan M. Taylor**, "The Growing Dependence of Britain on Trade during the Industrial Revolution," *Scandinavian Economic History Review*, May 2014, *62* (2), 109–136.

Coeurdacier, Nicholas, Florian Oswald, and Marc Teignier, "Structural Change, Land Use and Urban Expansion," Technical Report 2022.

Combes, Pierre-Philippe and Laurent Gobillon, "The empirics of agglomeration economies," in "Handbook of regional and urban economics," Vol. 5, Elsevier, 2015, pp. 247–348.

_ , _ , **and Yanos Zylberberg**, "Urban economics in a historical perspective: Recovering data with machine learning," *Regional Science and Urban Economics*, 2022, *94*, 103711.

Crafts, Nicholas F. R., "British Industrialization in an International Context," *Journal of Interdisciplinary History*, 1989, *19* (3), 415.

Desmet, Klaus, David Krisztian Nagy, and Esteban Rossi-Hansberg, "The Geography of Development," *Journal of Political Economy*, 2018, *126* (3), 903–983.

Drayton, Elaine, Peter Levell, and David Sturrock, "The Determinants of Local Housing Supply in England," Technical Report, mimeo 2024.

Duranton, Gilles, "Urban Evolutions: The Fast, the Slow, and the Still," *American Economic Review*, March 2007, *97* (1), 197–221.

_ **and Diego Puga**, "Nursery cities: Urban diversity, process innovation, and the life cycle of products," *American Economic Review*, 2001, *91* (5), 1454–1477.

_ **and** _ , "Micro-foundations of urban agglomeration economies," in "Handbook of regional and urban economics," Vol. 4, Elsevier, 2004, pp. 2063–2117.

Eckart, Wolfgang, "On the land assembly problem," *Journal of Urban Economics*, 1985, *18* (3), 364–378.

Eckert, Fabian and Michael Peters, "Spatial Structural Change," Technical Report, mimeo 2023.

Faggio, Giulia, Olmo Silva, and William C. Strange, "Heterogeneous agglomeration," *Review of Economics and Statistics*, 2017, *99* (1), 80–94.

Fajgelbaum, Pablo and Stephen J Redding, "Trade, structural transformation, and development: Evidence from Argentina 1869–1914," *Journal of Political Economy*, 2022, *130* (5), 1249–1318.

Fajgelbaum, Pablo D. and Cecile Gaubert, "Place-Based Policies: Lessons from Theory," NBER Working Papers 33517, National Bureau of Economic Research, Inc February 2025.

Feinstein, C. H., *National Income, Expenditure and Output of the United Kingdom, 1855–1965*, Cambridge University Press, 1972.

Franck, Raphaël and Oded Galor, "Flowers of Evil? Industrialization and Long-Run Development," *Journal of Monetary Economics*, 2021, *117*, 108–128.

Gaubert, Cecile, Patrick M Kline, Damián Vergara, and Danny Yagan, "Place-Based Redistribution," Working Paper 28337, National Bureau of Economic Research January 2025.

Glaeser, Edward L., "Reinventing Boston: 1630–2003," *Journal of Economic Geography*, 2005, *5*, 119–153.

Glaeser, Edward L, Hedi D Kallal, Jose A Scheinkman, and Andrei Shleifer, "Growth in cities," *Journal of Political Economy*, 1992, *100* (6), 1126–1152.

Goose, Nigel, "Regions, 1700–1870," in Roderick Floud, Jane Humphries, and Paul Johnson, eds., *The Cambridge Economic History of Modern Britain*, second ed., Cambridge University Press, October 2014, pp. 149–177.

Graham, Daniel J. and Stephen Gibbons, "Quantifying Wider Economic Impacts of Agglomeration for Tranport Appraisal: Existing Evidence and Future Directions," *Economics of Transportation*, 2019, *19*, 100121.

Gregory, Ian N. and Jordi Martí Henneberg, "The Railways, Urbanization, and Local Demography in England and Wales, 1825-1911," *Social Science History*, 2010, *34* (2), 199–228.

Hanlon, W Walker, "The rise of the engineer: Inventing the professional inventor during the Industrial Revolution," Technical Report, National Bureau of Economic Research 2022.

_ , "The rise of the engineer: Inventing the professional inventor during the Industrial Revolution," *The Economic Journal*, 2025, *135* (670), 1749–1781.

_ **and Antonio Miscio**, "Agglomeration: A long-run panel data approach," *Journal of Urban Economics*, 2017, *99*, 1–14.

Harari, Mariaflavia, "Cities in bad shape: Urban geometry in India," *American Economic Review*, 2020, *110* (8), 2377–2421.

Harley, C. Knick and N. F. R. Crafts, "Simulating the Two Views of the British Industrial Revolution," *The Journal of Economic History*, 2000, *60* (3), 819–841.

Head, Keith and Thierry Mayer, "The United States of Europe: A Gravity Model Evaluation of the Four Freedoms," *Journal of Economic Perspectives*, 2021, *35* (2), 23–48.

Heblich, Stephan, Alex Trew, and Yanos Zylberberg, "East-side story: Historical pollution and persistent neighborhood sorting," *Journal of Political Economy*, 2021, *129* (5), 1508–1552.

_ **, Marlon Seror, Hao Xu, and Yanos Zylberberg**, "Industrial clusters in the long run: Evidence from Million-Rouble plants in China," *Review of Economic Studies*, 2026, *forthcoming*.

_ **, Stephen J Redding, and Yanos Zylberberg**, "The distributional consequences of trade: Evidence from the Grain Invasion," Technical Report, National Bureau of Economic Research 2024.

Heldring, Leander, James A Robinson, and Sebastian Vollmer, "The economic effects of the English Parliamentary enclosures," Technical Report, National Bureau of Economic Research 2022.

Henderson, J Vernon, "The sizes and types of cities," *The American Economic Review*, 1974, *64* (4), 640–656.

Henderson, Vernon, Ari Kuncoro, and Matt Turner, "Industrial development in cities," *Journal of Political Economy*, 1995, *103* (5), 1067–1090.

Herrendorf, Berthold, Richard Rogerson, and Akos Valentinyi, "Growth and Structural Transformation," in Philippe Aghion and Steven Durlauf, eds., *Handbook of Economic Growth*, Vol. 2 of *Handbook of Economic Growth*, Elsevier, 2014, chapter 6, pp. 855–941.

Hills, Sally, Ryland Thomas, and Nicholas Dimsdale, "The UK Recession in Context — What Do Three Centuries of Data Tell Us?," *Bank of England Quarterly Bulletin*, 2010, p. 15.

Hoskins, William G., *The Making of the English Landscape*, London: Hodder and Stoughton, 1988.

Hudson, Pat, "Industrial Organisation and Structure," in Paul Johnson and Roderick Floud, eds., *The Cambridge Economic History of Modern Britain: Volume 1: Industrialisation, 1700–1860*, Vol. 1, Cambridge: Cambridge University Press, 2004, pp. 28–56.

Ittmann, Karl, *Work, Gender and Family in Victorian England*, London: Palgrave Macmillan UK, 1995.

Jacks, David S, Kevin H O'rourke, and Jeffrey G Williamson, "Commodity price volatility and world market integration since 1700," *Review of economics and statistics*, 2011, *93* (3), 800–813.

Jacobs, Jane, *The Death and Life of Great American Cities*, New York: Random House, 1961.

_ , *The Economy of Cities*, New York: Vintage, 1969.

Kelly, Morgan, Joel Mokyr, and Cormac Ó Gráda, "The mechanics of the Industrial Revolution," *Journal of Political Economy*, 2023, *131* (1), 59–94.

Kline, Patrick and Enrico Moretti, "Local Economic Development, Agglomeration Economies, and the Big Push: 100 Years of Evidence from the Tennessee Valley Authority," *The Quarterly Journal of Economics*, 11 2014, *129* (1), 275–331.

_ **and** _ , "People, Places and Public Policy: Some Simple Welfare Economics of Local Economic Development Programs," *Annual Review of Economics*, 2014, *6* (1), 629–662.

Lane, Nathan, "Manufacturing revolutions: Industrial policy and industrialization in South Korea," *The Quarterly Journal of Economics*, 2025, p. qjaf025.

Lin, Jeffrey, "Technological adaptation, cities, and new work," *Review of Economics and Statistics*, 2011, *93* (2), 554–574.

Litvine, Alexis, Arthur Starzec, Rehmana Younis, Yannick Faula, Mickaël Coustaty, Leigh Shaw-Taylor, and Véronique Églin, "An Integrated Methodology for Extracting High-resolution Urban Footprints from Historical Maps," Technical Report 2023.

Matsuyama, Kiminori, "Agricultural productivity, comparative advantage, and economic growth," *Journal of Economic Theory*, 1992, *58* (2), 317–334.

Mendels, Franklin F., "Proto-Industrialization: The First Phase of the Industrialization Process," *The Journal of Economic History*, March 1972, *32* (1), 241–261.

Mokyr, Joel, *The Enlightened Economy: An Economic History of Britain 1700–1850*, Yale University Press, 2009.

_ , "Attitudes, Aptitudes, and the Roots of the Great Enrichment," in "The Handbook of Historical Economics," Elsevier, 2021, pp. 773–794.

Musson, Albert E., "Industrial Motive Power in the United Kingdom, 1800-70," *The Economic History Review*, 1976, *29* (3), 415–439.

Nagy, Dávid Krisztián, "Quantitative economic geography meets history: Questions, answers and challenges," *Regional Science and Urban Economics*, 2022, *94.*

Nagy, Dávid Krisztián, "Hinterlands, city formation and growth: Evidence from the US westward expansion," *Review of Economic Studies*, 2023.

Neeson, Jeanette M, *Commoners: common right, enclosure and social change in England, 1700-1820*, Cambridge University Press, 1996.

Ngai, L. Rachel and Christopher A. Pissarides, "Structural Change in a Multisector Model of Growth," *American Economic Review*, 2007, *97* (1), 429–443.

Nuvolari, Alessandro, Bart Verspagen, and Nick von Tunzelmann, "The Early Diffusion of the Steam Engine in Britain, 1700–1800: A Reappraisal," *Cliometrica*, October 2011, *5* (3), 291–321.

Ogilvie, Sheilagh, "Protoindustrialization," in "The New Palgrave Dictionary of Economics," London: Palgrave Macmillan UK, 2008, pp. 1–6.

Pierce, Justin R and Peter K Schott, "The surprisingly swift decline of US manufacturing employment," *American Economic Review*, 2016, *106* (7), 1632–62.

Redding, Stephen J. and Esteban Rossi-Hansberg, "Quantitative Spatial Economics," *Annual Review of Economics*, 2017, *9*, 21–58.

Saiz, Albert, "The geographic determinants of housing supply," *The Quarterly Journal of Economics*, 2010, *125* (3), 1253–1296.

Sanderson, Eleanor and Frank Windmeijer, "A weak instrument F-test in linear IV models with multiple endogenous variables," *Journal of econometrics*, 2016, *190* (2), 212–221.

Satchell, Max, Dan Bogart, and Leigh Shaw-Taylor, "Parliamentary Enclosures in England, 1606–1902," Technical Report 2017.

Shaw-Taylor, Leigh, "The Occupational Structure of Britain c.1379–1911 and the International Comparative History of Occupational Structure: An overview of findings and where to find them," Technical Report, The Cambridge Group for the History of Population and Social Structure 2019.

_ **and E. Anthony Wrigley**, "Occupational structural and population change. Chapter 2 in Floud, R., Humphries, J. and Johnson P.," *The Cambridge Economic History of Modern Britain: Volume 1, Industrialisation 1700-1860*, 2014. Cambridge University Press.

Simonovska, Ina and Michael E. Waugh, "The Elasticity of Trade: Estimates and Evidence," *Journal of International Economics*, 2014, *92* (1), 34–50.

Stokey, Nancy L., "A Quantitative Model of the British Industrial Revolution, 1780–1850," *Carnegie-Rochester Conference Series on Public Policy*, December 2001, *55* (1), 55–109.

Strange, William C., "Information, holdouts, and land assembly," *Journal of Urban Economics*, 1995, *38* (3), 317–332.

Thomas, Ryland and Nicholas Dimsdale, "A Millenium of Macroeconomic Data for the UK," 2018.

Trew, Alex, "Spatial Takeoff in the First Industrial Revolution," *Review of Economic Dynamics*, 2014, *17*, 707–25.

Trinder, Barrie, "Industrialising Towns 1700–1840," in Peter Clark, ed., *The Cambridge Urban History of Britain: Volume 2: 1540–1840*, Vol. 2 of *The Cambridge Urban History of Britain*, Cambridge: Cambridge University Press, 2000, pp. 805–830.

Wrigley, E. Anthony, "The PST System of Classifying Occupations," Technical Report 2010.

ONLINE APPENDIX—not for publication

This appendix **(A)** provides details about the data sources (complementing Section 2), descriptive statistics, and a sensitivity analysis of the reduced-form results (Section 3). The appendix **(B)** also provides complements to the quantitative model (Section 4) and its parametrization (Section 5).

A Data appendix

This section provides complements to Sections 2 and 3: we present our data sources, with a detailed description of our map digitization procedure; we discuss the land fragmentation algorithm underlying our exogenous predictor of city growth; we provide descriptive statistics about the rise of cities and their subsequent dynamics; and we discuss a series of robustness checks.

A.1 Data sources and construction

A large collection of county maps and Ordnance drawings We first collect and digitize early county maps from the North of England. Please find below the covered counties, with the map resolution, its date and its author(s): Northumberland, 1-inch map, 1769 (Andrew and Mostyn Armstrong); Durham, 1-inch map, 1768 (Thomas Jefferys and Andrew Armstrong), 1-inch map, 1820 (Christopher Greenwood); Cumberland, 1/2-inch map, 1773 (Joseph Hodskinson and Thomas Donald), 1-inch map, 1823 (Christopher and John Greenwood); Westmorland, 1-inch map, 1771 (Thomas Jefferys); Yorkshire, ca 4/5 inch, 1828 (Christopher Greenwood, et al.); Lancashire, not stated, 1768 (William Yates), 1 inch, 1818 (Christopher Greenwood, et al.), 4/5 inch, 1830 (G. Hennet); Cheshire, 3/4 inch, 1830 (William Swire and W.F. Hutchings), 5/4 inch, 1831 (Andrew Bryant); Derbyshire, 1-inch map, 1767/1791 (Peter Burdett); Nottinghamshire, not stated, 1794 (John Chapman), not stated, 1826 (Christopher and John Greenwood); Lincolnshire, ca. 1 inch, 1828 (Andrew Bryant), ca. 1 inch, 1830 (Christopher and John Greenwood). We carefully project these flat map tiles, which gives us an exhaustive coverage of the North of England, albeit at different dates and resolution between 1790–1830. To cover Southern England and Wales, we rely on about 350 Ordnance Survey drawings that were produced by the Ordnance Survey at the beginning of the nineteenth century and are usually referred to as the Old Series 1-inch maps. We keep the latest series when maps fully or partially overlap, leaving us with about 360 different map tiles produced between 1790–1820 for most of them.

Recognizing built-up from county maps and Ordnance drawings These different maps employ different annotations, symbols, colors, etc. County maps typically display built-up with dark rectangles, sometimes with dotted areas, but are otherwise quite clear and organized. The challenge is then to distinguish built-up from letters or dashed lines representing administrative boundaries. In stark contrast, Ordnance Survey drawings typically display built-up with red marks, but the drawings also contain the delineation of farms and topography (which is not represented using contour lines of similar alti-

tude, but rather "slope lines", i.e., the orthogonal lines indicating the typical course of water along the slope). In summary, our main object of interest (a building) is displayed across all maps, but with varying symbols. For these reasons, we identify built-up using supervised deep learning with a large training sample.

To recognize built-up and other land uses in historical maps, we develop a convolutional neural network frequently used in the biomedical literature to detect zones of interest within images (a "U-Net").[23] We train the algorithm using a manual labeling procedure with research assistants annotating images, and we complement our training sample with previous training data from French historical maps. We add basic transformations (i.e., flipping, zooms, rotations) to each training batch, such as to avoid overfitting and ensure invariance to the orientation and resolution of maps.

Figure A1. Recognizing roads.

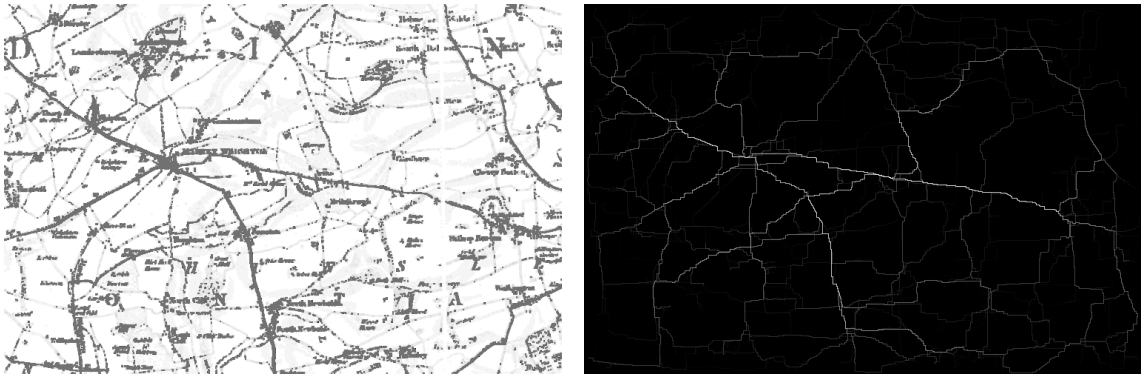

(a) "Travel" cost (b) Paths

Note: Panel **(a)** displays the input of the least cost path procedure to detect roads on a historical county map. Panel **(b)** displays the simulated least cost paths drawn between random departure and arrival points.

To identify roads, we develop a less standard approach: thin, non-straight lines are notoriously difficult to detect using computer vision. Our approach relies on the nature of roads: they are black lines on the map, but, in practice, they are designed to best facilitate transportation across space. In that respect, they markedly differ from all other black lines on the maps, e.g., the text or gradient lines in mountainous terrain. We exploit this discriminatory feature as follows: (i) we create a "stylized travel cost" matrix for each map, penalizing travel outside of darker, black pixels; (ii) we draw many random departure points from black pixels on the image and compute the least cost paths to each other pixels of the image for each draw; (iii) for each draw, we then randomize

[23]Two remarks in order: Litvine et al. (2023) employ a similar approach to extract urban footprints in Britain from these Ordnance Survey drawings and individual county maps; an alternative method is to consider an object-based classification which is standard in remote sensing but less common in map digitization (see, e.g., Combes et al., 2022, for a discussion of these methods).

many arrival points and start drawing the actual minimum paths between departure and arrival pixels.[24]

Figure A2. Consistent parishes across England and Wales.

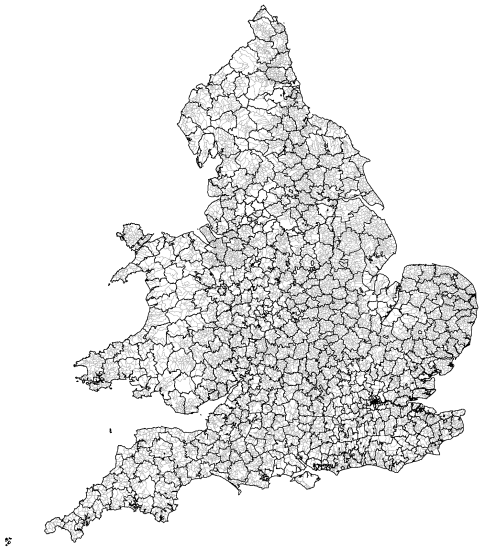

Notes: This Figure displays the output of the transitive closure algorithm implemented by the Cambridge Group for History of Population and Social Structure. Consistent mappable units based on parishes are displayed in gray; registration districts or poor law unions are displayed with black borders.

Consistent administrative units Our analysis relies on various levels of administration, spanning a long period. Section 2.3 describes how we identify and delineate cities

[24]Our approach relies on the nature of roads: roads are contiguous (impervious) areas which are designed to minimize travel cost between locations of interest. In practice, we can design a procedure to detect black lines, but we would then typically end up with many false positives (i.e., black lines that are not roads). Many of these black lines would, however, not fulfill the previous travel-cost minimization requirement: letters, gradient lines in mountainous terrain or farms are very inefficient patches of black pixels on which to travel between locations of interest. Others may be better suited, e.g., rivers, county boundaries, or railway tracks. We exploit the previous discriminatory feature as follows. We first transform the color map into a gray "travel cost" matrix by (i) filtering out non-gray colors, (ii) thickening black areas to create continuous lines from dashed lines, (iii) simplifying images by interpolating across pixels, and (iv) transforming the gray intensity through a power function in order to best calibrate the "cost" of traveling across pixels of different black intensity (with travel cost over a perfectly black pixel being 1, and travel cost over a perfectly white pixel being as high as possible). The output is the left panel of Figure A1. Second, we draw many random departure points from the subsample of black pixels on the image (as a proxy for the unobserved locations of interest) and we compute the least cost paths to all other pixels of the image for each draw. Roads are already more salient on this matrix. However, roads are designed to be used as "the" minimum cost path between locations: we randomize many arrival points for each departure point and start drawing the actual minimum paths between departure and arrival pixels on a black image. The output is a distribution of many minimum cost paths highlighting the most traveled roads more than the others (right panel of Figure A1). As shown by Figure A1, this algorithm not only identifies roads very well, but also their respective importance within the transportation network.

of the nineteenth century, a city shape that we use to nest economic outcomes in the recent period. These cities are the core administrative units of our study.

They are, however, not the only administrative divisions underlying our empirical analysis. First, our main specification (see, e.g., Tables 2 or 3) includes fixed-effects at the level of 39 ceremonial counties whose delineation is set in recent times. Second, in most of the empirical analysis, we report standard errors that are clustered at the level of the closest city as of 2015, a formal status attributed to only 55 cities. In this instance and in the previous one, we use recent geography to better control for spatial auto-correlation within contemporary administrative divisions. Third, while we nest most economic outcomes within the borders of our cities and expanded cities, census data and baptism records are originally provided at the parish level, and parishes are regularly redefined, merged or split over the course of the nineteenth century. To limit the importance of differential measurement error over time, we apply a preliminary "envelope" algorithm which considers the union of the different parishes covering the same points over time. For instance, if a parish is split into two parishes in 1891, we would group the two sub-parishes from 1891 onward to create a consistent, unique parish from 1801 to the current day. This grouping is less relevant at the level of higher administrative divisions, as none of these re-compositions of lowest administrative units significantly affect the allocation of administrative units across higher divisions. The output of the procedure is shown in Figure A2, with about 11,500 consistent parishes across England and Wales.

Transportation, travel time, and trading costs Both the derivation of stylized facts and the quantification of our model rely on transportation infrastructure in the nineteenth century and in recent times. Our dynamic characterization of historical transportation relies on transportation infrastructure from the Cambridge Group for the History of Population and Social Structure (including the roads in 1830, density of train lines in 1851, and waterways around 1820, all used to condition the main empirical specification). The data is best described in Alvarez-Palau et al. (2025). The transportation infrastructure is integrated into a network in order to derive a few important controls used, e.g., in Table 3: the travel times to major ports (London, Liverpool, Plymouth, Portsmouth) and resources.

The transportation network is also important to derive the trading costs in the quantitative model. We describe this derivation in greater detail in Appendix B.3.

Other geographic variables The derivation of stylized facts and the identification of dynamic Jacobs externalities hinge on numerous geographic factors, either to extract ex-

Figure A3. Travel cost and distance to coal across England and Wales, as computed around 1817.

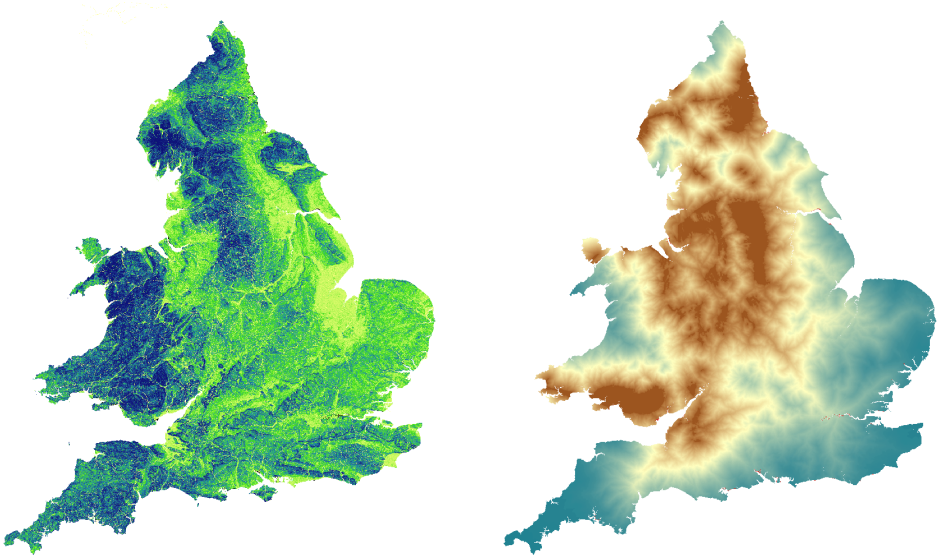

(a) Travel cost (b) Distance to coal

Notes: Panel **(a)** displays the raster of transport costs as calculated using the transport network at the beginning of the 19th century, and a penalization accounting for the local elevation gradient (yellow: low, green: medium, blue: high). Panel **(b)** displays the minimum travel time from the nearest coal field (red: low, blue/green: high).

ogenous variation in city growth or to condition the analysis on important confounders. First, we consider the following topographic characteristics: elevation (Open Land Map, 30m resolution), used as a main control and as input in the land fragmentation algorithm together with the derived slope; soil organic carbon content (Open Land Map, 250m resolution), used in a sensitivity analysis; soil bulk density (Open Land Map, 250m resolution), used in a sensitivity analysis; a detailed soil classification (from The National Soil Map and Soil Classification, produced by the National Soil Resources Institute); and a dataset of all rivers and smaller streams in England and Wales (OS Open Rivers). Second, we combine our city identification and delineation (Section 2.3) with geographic characteristics to derive the area/latitude/longitude of the initial city outline, the predicted expanded area in 1881, and the built-up density within 1, 2, 3, 5, 10 kms of the initial city outline. Third, we measure agricultural productivity around our cities by extracting the suitability to grow wheat, oat, grass, and rye from the Global Agro-Ecological Zones produced by the Food and Agriculture Organization of the United Nations—we use the rain-fed, high-input model specification. Fourth, we use a measure of baseline share of arable agriculture (extracted from the Tithe survey, see Heblich et al., 2024) for a similar purpose, i.e., controlling for initial agricultural production within the city hinterlands. Fifth, we collect information on historical factors possibly anchoring hu-

man settlements and the distribution of land ownership across space, most notably the presence of Domesday settlements (1086) extracted from the revision of the Phillimore edition of Domesday Book (1975–1986) and enclosures within 1, 2, 3, 5, 10 kms of the initial city outline (Satchell et al., 2017; Heldring et al., 2022).

A.2 Land fragmentation

Our land fragmentation algorithm consists of the following steps. In a first step, we extract fine-grained terrain characteristics including elevation, ruggedness, time-invariant soil attributes and water bodies from Google Earth Engine. We then store these characteristics in an "image", i.e., a 2D array where the value at each pixel (x, y) is a vector of attributes $(a_1, \ldots, a_m)$—a standard color image is often stored as a 2D array where the value at each pixel is a triplet RGB. We then normalize the different attributes to be between 0 and 1. The output is a multi-band raster covering England and Wales at a resolution of 30m (bands: normalized elevation, normalized slope, normalized bulk, soil classes).

The second step produces superpixels to isolate contiguous zones of the image that are homogeneous in their attributes. There are several image segmentation algorithms, e.g., SLIC, Quickshift, Felzenszwalb or watershed.[25] We opt for Quickshift, which allows for a grouping of pixels that is more flexible in their proximity in actual space (i.e., along the physical distance) versus the color space. Applied to this peculiar setting, the algorithm relies on a standard "orthogonal" distance between the n-dimensional vectors that are stored in every pixel as the "distance in the color space" or "value distance." The algorithm maximizes a weighted sum of the two target distances within constituted superpixels, with a weight allocated to physical distance relative to the previously-defined "value distance." We parameterize the algorithm by choosing the scale parameter, the maximum physical distance, and the relative weight between distance in the color-space and physical distance in order to best capture the shape of agricultural parcels. A superpixel with similar values is, here, a reasonably-compact patch of land with homogeneous topography and soil characteristics: a typical agricultural parcel.

In a third step, we calculate: (i) a Herfindahl measure of superpixel concentration at the parish level, which can be benchmarked against the actual Herfindahl concentration of farm ownership as collected from micro-census records in 1851 across 11,500 parishes of England and Wales (see Figure 8); and (ii) the predicted density of farms at the fringe of each city—a measure of predicted land fragmentation. The variation in predicted land fragmentation is very local; we do however see aggregate patterns due to overall topography (mountainous terrain in Central England or Wales, hilly terrain in Cornwall) or

[25] See, e.g., a description of these segmentation algorithms.

Figure A4. Predicted land fragmentation.

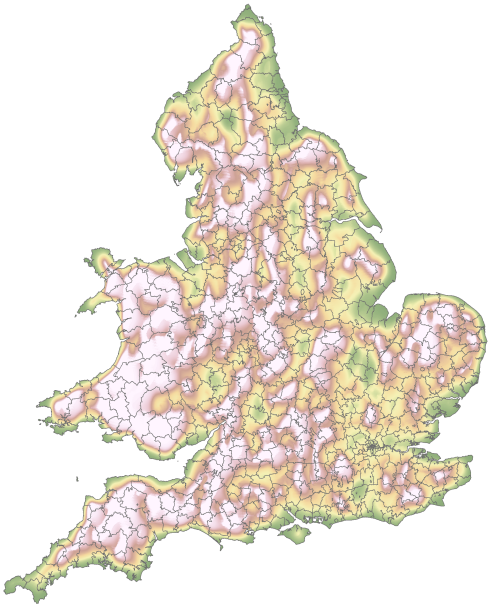

Note: This Figure displays an interpolated, aggregated raster map of predicted land fragmentation. The color scheme is an elevation color scheme: from green (low) to yellow, red and white (high). One can see that mountainous areas are typically more fragmented, but the low-lying hills of Cornwall or Cotswold, or the soil heterogeneity in Norfolk also generates significant land fragmentation.

soil composition (e.g., in Norfolk). We illustrate these aggregate patterns in Figure A4.

A.3 Descriptive statistics

In this section, we provide complements to Section 2.2 by focusing on the (nature of the) rise of cities.

The rise of (different) cities Figure A5 shows the distribution of city growth and industrial concentration across our urban settlements. We see that the median settlement grows by a factor of about 3. The growth rate for the top decile (in purple) is above 300% (panel a). The large heterogeneity in employment growth is also reflected in a large heterogeneity in industrial concentration. Most of the fastest-growing cities become more specialized (panel b), an effect which is explained by the fact that fast-growing cities are initially specialized across the few key sectors that flourish over the course of the nineteenth century. Importantly, most cities of similar size in 1817 have Herfindahl indices that could differ by up to 0.20 in 1881—equivalent to the difference between a city with employment equally distributed across 3 (2-digit) sectors and a city with employment equally distributed across 10 such sectors.

We illustrate the role of initial industries, as proxies for initial location advantages, in panels (c) and (d) of Figure A5 where we compare the actual employment growth and

Figure A5. Growth, industrial concentration, and the role of the initial industrial mix.

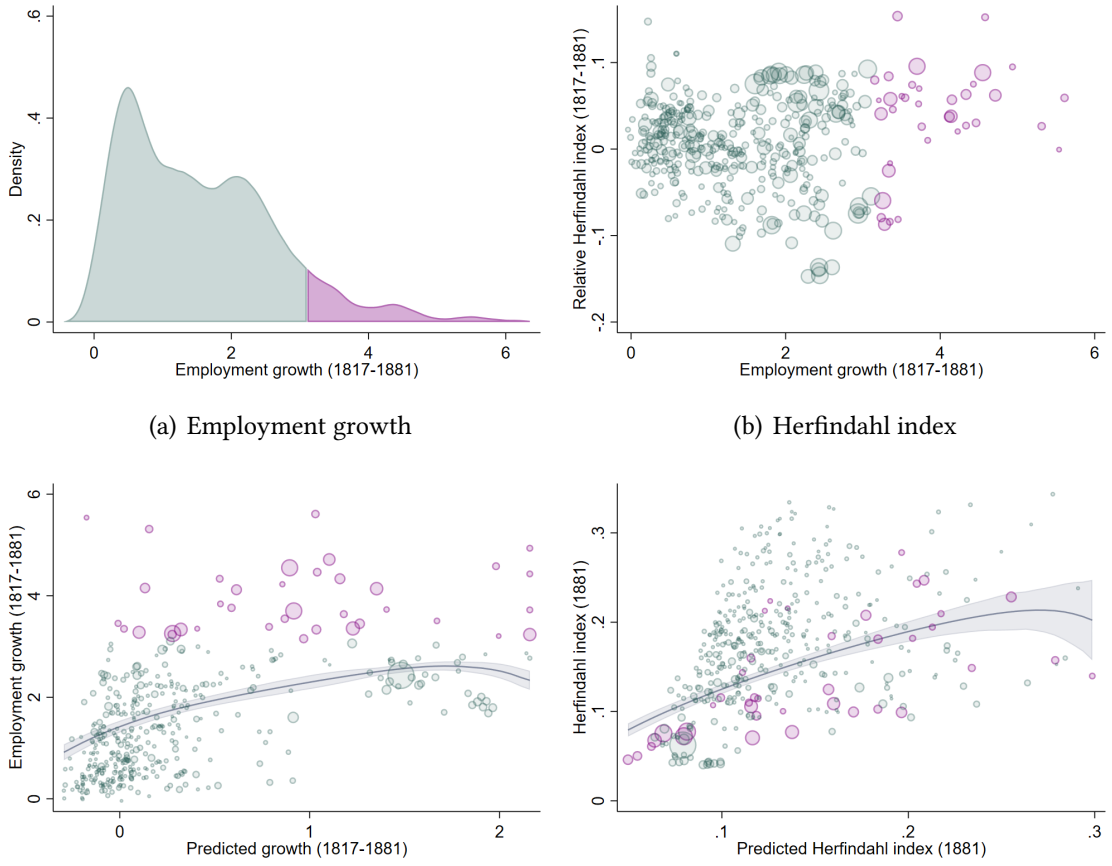

(a) Employment growth

(b) Herfindahl index

(c) Predicted employment growth

(d) Predicted Herfindahl index

Notes: panel **(a)** displays the distribution of employment growth, $\frac{L_c^{81}-L_c^{17}}{L_c^{17}}$, within the boundaries of 435 potential cities. The top decile of growing settlements between 1817–1881 is highlighted in purple. In panel **(b)**, we show the relationship between employment growth and the evolution of industrial concentration, $\sum_j \left(s_{jc}^{81}\right)^2 - \sum_j \left(s_j^{81}\right)^2$, across urban areas—where s_{ic}^{81} is the employment share in industry i and city c, and s_i^{81} is the aggregate employment share in industry i. Panel **(c)** displays the measure of predicted employment growth, g_c, against the actual employment growth across our 435 potential cities. The top decile of growing settlements are highlighted in purple. The line is a locally weighted regression on all observations, with employment in 1817 as weight. Panel **(d)** repeats the same exercise with the actual and predicted Herfindahl index, χ_c.

industrial concentration in 1881 with their predictions, g_c and χ_c, as computed using a "shift-share" design based on initial industries in 1817. We find that the initial industrial mix does predict employment growth within urban areas but also, and more significantly, industrial concentration.

Both our actual and predicted indices of industrial concentration are based on 2-digit industries. We now shed additional light on the role of 1-digit sectors in cities' changing industrial composition as opposed to the more granular variation within these 1-digit sectors. In Figure A5, we display the relationship between the 1881 Herfindahl index of industrial concentration computed at the 2-digit level and a predicted measure, also

Figure A6. The role of the initial industrial mix—robustness checks.

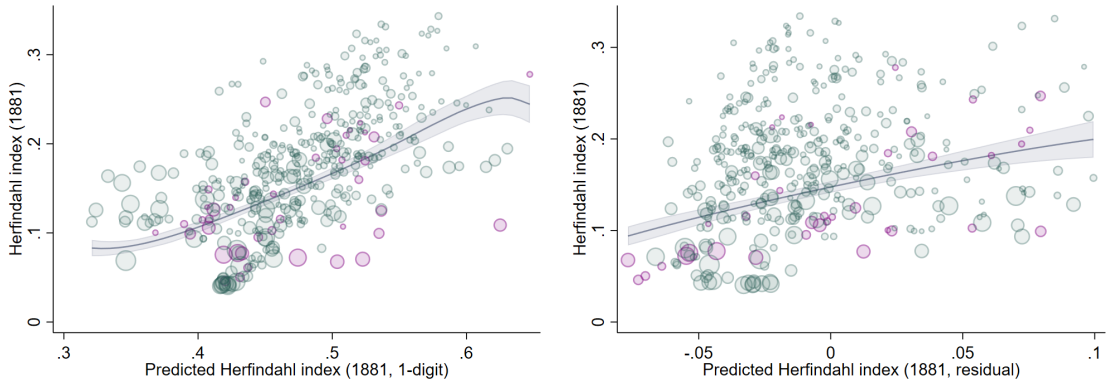

(a) Herfindahl index (1881, 1-digit)

(b) Herfindahl index (1881, residual)

Notes: Panel **(a)** displays the measure of predicted industrial concentration computed at the 1-digit level against the actual industrial concentration. The top decile of growing settlements are highlighted in purple. The line is a locally weighted regression on all observations. Panel **(b)** repeats the same exercise with a residualized measure of predicted industrial concentration that is (i) computed at the 2-digit level and (ii) cleaned for the role of the previous 1-digit measure of predicted industrial concentration. The slope is about 60% to that of Figure A5 (panel d).

computed at the 2-digit level. In Figure A6, we decompose this relationship into (i) the part explained by predicted industrial concentration at the 1-digit level (panel a) and (ii) the residual of the 1-digit prediction, thus exploiting within-sector variation only (panel b). We can see that the relationship remains strong in panel (b); the slope is about 60% to that of Figure A5.

Figure A7. Specialization of cities—prediction and residual Herfindahl.

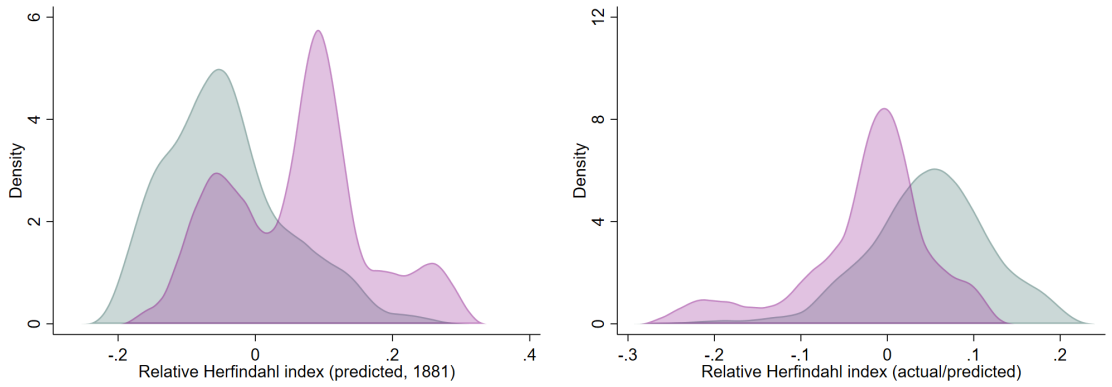

(a) Predicted Herfindahl index

(b) Residual Herfindahl index

Notes: This Figure shows the distribution of predicted industrial concentration χ_c (see Section 2.3, panel **a**) and residual industrial concentration $h_c - \chi_c$ (panel **b**). The top decile of growing settlements are highlighted in purple.

The previous evidence shows that fast-growing cities become more specialized. We

better qualify this observation in Figure A7 where we decompose industrial concentration h_c (as shown in Figure A5) into predicted industrial concentration χ_c and residual industrial concentration $h_c - \chi_c$. We then plot the distribution of these two objects for the top decile in terms of employment growth during 1817–1881 (in purple) and the rest (in teal). We see that the specialization of fast-growing cities is entirely predicted from their initial industry mix: fast-growing cities are initially specialized across a few key sectors that flourish over the course of the nineteenth century.

Figure A8. A balance test for urban settlements with different land fragmentation in their immediate fringe.

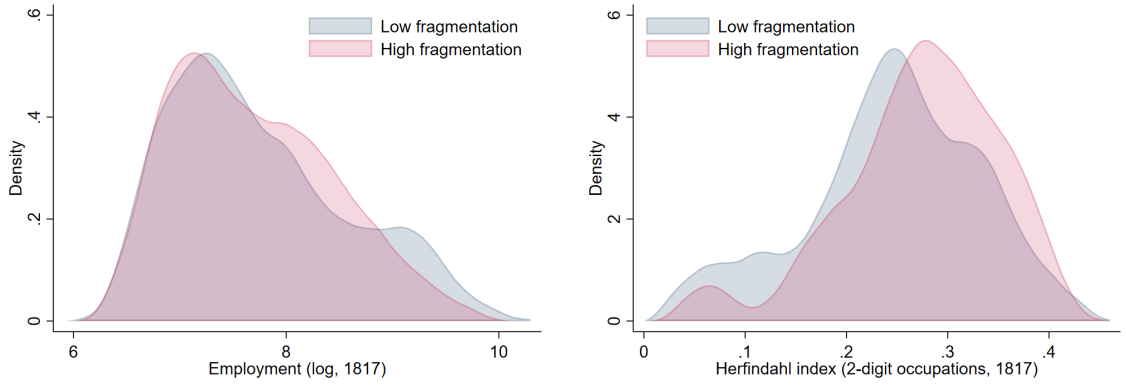

(a) Employment (1817)

(b) Herfindahl index (1817)

Notes: This Figure displays the distribution of population density (panel **a**) and industrial concentration (calculated as a Herfindahl index across 2-digit occupations, panel **b**) for cities with above- (red) and below-median (blue) predicted land fragmentation in their immediate fringe.

Exogenous variation in city size To isolate exogenous variation in late nineteenth century population, we use a proxy for land ownership fragmentation in the immediate fringe of urban settlements. In this appendix, we provide a balance test by illustrating the correlation between settlement characteristics at the beginning of the nineteenth century and predicted land fragmentation in these settlements' immediate fringe. We find that settlements with above- (red) and below-median (blue) predicted land fragmentation are very similar in population density and industrial concentration in 1817 (see Figure A8).

City population and city growth This section presents additional evidence about the distribution of city populations and growth over time. In Figure A9, we display the relationship between cities' average yearly growth and initial employment. Panel (a) shows this relationship in the nineteenth century. Initially large cities grow slightly faster during this period. Panel (b) repeats the analysis for the twentieth century. Over this period,

Figure A9. Gibrat's law.

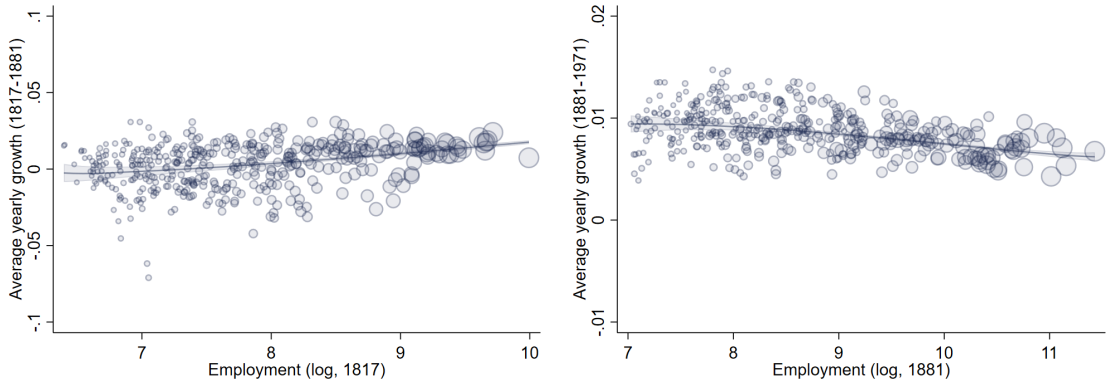

(a) Gibrat's law, 1817–1881 (b) Gibrat's law, 1881–1971

Notes: This Figure shows the relationship between cities' (log) initial employment and subsequent yearly growth. Panel **(a)** conducts the analysis for the period 1817–1881, while panel **(b)** conducts it for the period 1881–1971.

the relationship becomes flat, even slightly negative: that is, large cities lose their advantage in terms of growth. This is in line with the empirical findings of Section 3.1: larger population does not confer a significant advantage in terms of long-run growth. It is also in line with the urban literature documenting a typically flat relationship between city size and growth (Gibrat's Law).

Figure A10. Zipf's law.

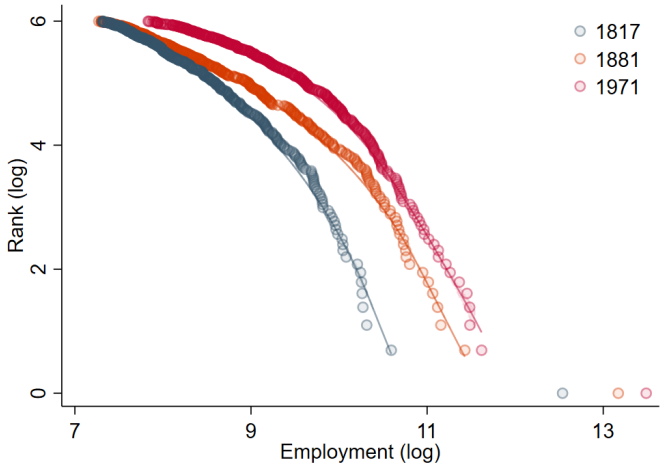

Notes: This Figure shows the relationship between cities' (log) rank in 1817 (blue), 1881 (orange) and 1971 (purple) and their (log) employment. The estimated slope is -1.20 in 1817, -0.95 in 1881, and -1.03 in 1971.

We also provide support for another empirical regularity characterizing the distribution of city size: the Zipf law relating the rank of cities to their size. In Figure A10, we

plot the relationship between the (log) rank and the (log) employment across our cities in 1817 (blue), 1881 (orange) and 1971 (purple). One can see that the relationship is close to linear in all years; and the estimated slope is -1.20 in 1817, -0.95 in 1881, and -1.03 in 1971. In summary, we find that the Zipf's law of city size holds reasonably well over the course of two centuries for Great British cities.

A.4 Robustness checks

In this section, we provide a sensitivity analysis for our main findings of Section 3.1.

Table A1. The effect of industrial concentration and city population on innovation across industries (1883–1893).

Patents (1883–1893)	Food (1)	Mining (2)	Construct. (3)	Metal (4)	Power (5)
Herfindahl index	-21.981	-1.444	-13.578	-6.336	-29.154
	(11.665)	(8.639)	(9.537)	(7.861)	(10.668)
	{18.45}	{18.45}	{18.45}	{18.45}	{18.45}
Employment	-1.379	-0.540	0.017	-0.237	-1.462
	(1.579)	(1.025)	(1.448)	(1.129)	(1.681)
	{18.60}	{18.60}	{18.60}	{18.60}	{18.60}
Observations	428	428	428	428	428
Patents (1852–1899)	Electr. (6)	Textile (7)	Chemic. (8)	Transport (9)	Instrum. (10)
Herfindahl index	-14.375	-31.386	-8.825	-18.976	-15.590
	(12.178)	(14.098)	(5.307)	(11.482)	(11.357)
	{18.45}	{18.45}	{18.45}	{18.45}	{18.45}
Employment	-0.859	-1.751	-0.667	-1.896	-1.054
	(1.471)	(2.013)	(0.967)	(1.643)	(1.422)
	{18.60}	{18.60}	{18.60}	{18.60}	{18.60}
Observations	428	428	428	428	428

Notes: A unit of observation is a settlement around 1790–1820. Standard errors, clustered at the level of the nearest city, are reported in parentheses; projected F-statistics are reported in brackets (following Sanderson and Windmeijer, 2016). We report TSLS estimates using two instruments: the shift-share predictor of industrial concentration (χ_c) and natural land fragmentation in the city fringe (ζ_c). The specification follows Panel B of Table 3 (column 1), with the dependent variables defined as the log number of unique patents (1883–1893) in: **(1)** Food and agriculture; **(2)** Mining and minerals; **(3)** Construction; **(4)** Metallurgy; **(5)** Power and general machinery; **(6)** Electrical and communications; **(7)** Textile; **(8)** Chemicals; **(9)** Transport; and **(10)** Instrument making. We omit household appliances and other/unclassified patents.

Industrial concentration and contemporaneous innovation Section 3.1 and Table 5 document strong contemporaneous effects of industrial concentration on inno-

vation, whether measured by the number of unique patents or unique inventors. Table A1 extends the analysis to 10 industries—excluding household appliances and unclassified patents—and shows that the negative effects of concentration are present in food and agriculture; power and general machinery; electrical and communications; textiles; chemicals; and transport. Although all estimates are negative, they are substantially smaller in magnitude for mining, minerals, and metallurgy, possibly reflecting more limited cross-industry spillovers in these sectors.

Table A2. The long-run effect of industrial concentration and population—more parsimonious specification(s).

Wage (2020)	(1)	(2)	(3)	(4)	(5)
Herfindahl index (1881, h_{c1})	-2.695	-2.869	-2.391	-2.383	-4.402
	(1.059)	(1.045)	(0.931)	(0.866)	(1.257)
	{10.57}	{23.02}	{13.23}	{20.94}	{11.25}
Employment (1881, l_{c1})	-0.195	-0.228	-0.244	-0.255	-0.123
	(0.185)	(0.170)	(0.164)	(0.154)	(0.199)
	{9.11}	{16.79}	{13.59}	{14.44}	{9.12}
Observations	428	428	428	428	428
Omitting...	Travel	Transport	Agr. prod.	Soil	County

Notes: A unit of observation is a cluster of settlements around 1790-1820—following the procedure in Section 2.2. Standard errors are reported between parentheses and are clustered at the level of the closest city as of 2015; and projected F-statistics are reported in brackets (following Sanderson and Windmeijer, 2016). The dependent variable is the (log) wage in 2020 (labor income estimates for small areas based on the Family Resources Survey). The two instruments are the "shift-share" predictor of industrial concentration (χ_c) defined in Section 2.3 and natural land fragmentation in the immediate fringe of urban settlements, ζ_c. Columns **(1)**-**(5)** reports the estimates of more parsimonious specifications than Panel B of Table 3, excluding: **(1)** travel time to the closest market town, to each major port (London, Liverpool, Plymouth, Portsmouth), and distance to the shore; **(2)** density of roads (1830), train lines (1851), and waterways; **(3)** suitability to grow wheat, barley, oat, grass, and rye; **(4)** share of heavy soil and clay (NSRI); and **(5)** fixed-effects at the level of 39 counties.

Sensitivity analysis In our baseline specification, we show that land fragmentation affects urban growth even when controlling for competing mechanisms—specifically, general agricultural productivity (Coeurdacier et al., 2022) and the exposure to the repeal of the Corn Laws (Heblich et al., 2024). For the sake of transparency, Table A2 reports a more parsimonious set of specifications that sequentially remove groups of geographic controls. Column (1) excludes "connectedness" variables—travel time to each major port (London, Liverpool, Plymouth, Portsmouth), and distance to the shore. Column (2) omits "transportation" variables (road density in 1830, railway density in 1851, and local waterway density). Column (3) drops agricultural suitability to grow wheat, barley, oat, grass, and rye. Column (4) drops soil characteristics (the local share of heavy soil and the local share of clay). Finally, column (5) removes the fixed effects at the level

of 39 counties. Across all these specifications, the coefficients on the Herfindahl index and employment remain remarkably stable.

Table A3. The long-run effect of industrial concentration and population—sensitivity to industry controls.

Wage (2020)	(1)	(2)	(3)	(4)	(5)
Herfindahl index (1881, h_{c1})	-3.604	-3.142	-2.606	-5.396	-2.851
	(1.763)	(1.386)	(1.200)	(2.307)	(1.071)
	{7.12}	{17.04}	{11.86}	{6.60}	{18.69}
Employment (1881, l_{c1})	-0.282	-0.199	-0.248	-0.148	-0.170
	(0.172)	(0.164)	(0.150)	(0.212)	(0.154)
	{17.86}	{18.51}	{19.39}	{9.22}	{20.68}
Observations	428	428	428	428	428
Additional controls	Herf. (1d)	Agri.	Service	Manu.	Num. ind.

Notes: A unit of observation is a cluster of settlements around 1790-1820—following the procedure in Section 2.2. Standard errors are reported between parentheses and are clustered at the level of the closest city as of 2015; and projected F-statistics are reported in brackets (following Sanderson and Windmeijer, 2016). The dependent variable is the (log) wage in 2020 (labor income estimates for small areas based on the Family Resources Survey). The two instruments are the "shift-share" predictor of industrial concentration (χ_c) defined in Section 2.3 and natural land fragmentation in the immediate fringe of urban settlements, ζ_c. Column **(1)** adds a control for a Herfindahl index predicted as in Section 2.3, but with 1-digit sectors (agriculture, manufacturing, services, transport, public); column **(2)** adds a control for the agricultural employment share in 1881; column **(3)** adds a control for the service employment share in 1881; column **(4)** adds a control for the manufacturing employment share in 1881; and column **(5)** adds a control for the number of active industries in 1881.

Our interpretation is that the industrial concentration effect arises through intertemporal externalities à la Jacobs—that is, the (lack of) diversity of geographically proximate industries—rather than through secular changes in agricultural or manufacturing employment. Table A3 confirms this by conditioning the baseline specification on measures capturing structural transformation: a predicted Herfindahl index using 1-digit sectors, and the agricultural, service, and manufacturing employment shares in 1881. We also control for the number of active industries in 1881. Our results remain qualitatively unchanged.

We next examine whether our findings are driven by any single *major* nineteenth-century industry. Re-estimating the baseline specification of Table 3 (Panel B) and excluding each of the 16 major industries one at a time, we find that the negative effect of industrial concentration on long-run wages remains negative and highly stable. No single industry drives the main result (see Figure A11).

We then conduct additional robustness checks varying (i) the land fragmentation instrument—using fixed buffers of 1/2 kilometers or SLIC rather than Quickshift to segment space into potential agricultural parcels; (ii) inference methods accounting for spatial correlation—clustering at the level of registration districts or poor law unions, at the level of counties, at the level of Travel-to-Work Area; and (iii) the population threshold

Figure A11. The long-run effect of industrial concentration—dropping industries one by one.

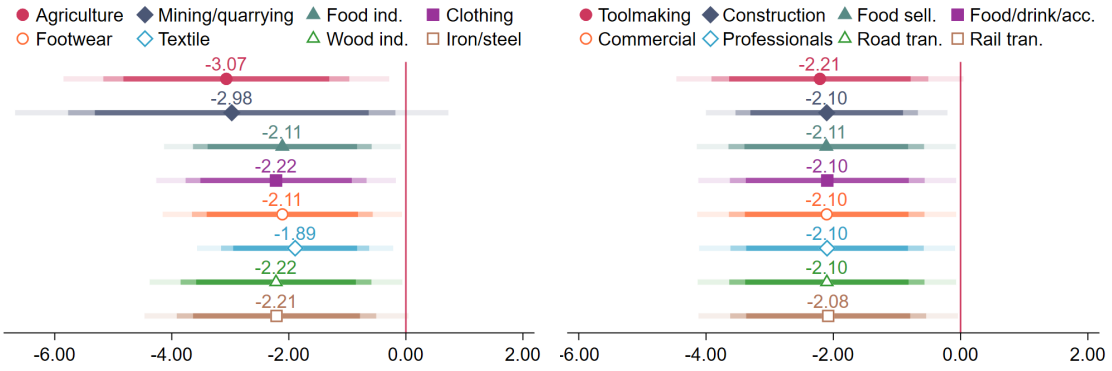

Notes: This Figure shows the estimated effect of 1881 industrial concentration on the 2020 (log) wage in specifications in which we drop each of the 16 major nineteenth-century industries one by one from the actual and predicted Herfindahl indices.

Figure A12. The long-run effect of industrial concentration—instrument, city selection, and clustering.

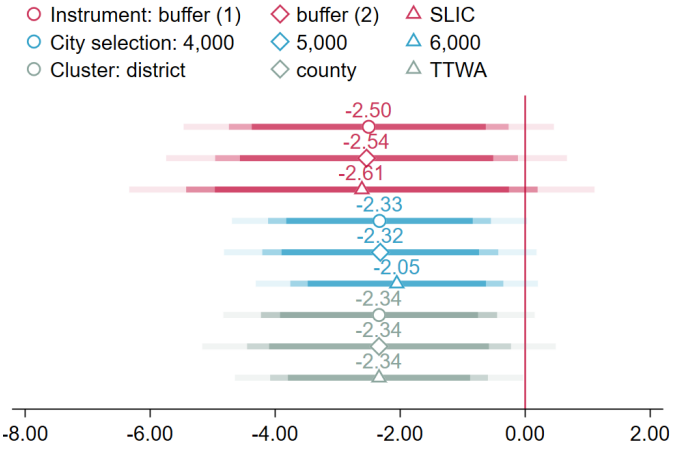

Notes: This Figure shows the estimated effect of 1881 industrial concentration on the 2020 (log) wage in the following robustness checks: we consider a sensitivity analysis around our baseline specification changing the land fragmentation instrument, computed with fixed buffers (1 and 2 kilometers, respectively "buffer(1)" and "buffer(2)"), using SLIC rather than Quickshift to segment space into potential agricultural parcels ("SLIC"); with different cut-offs to define urban settlements (4000, 5000, 6000 inhabitants around 1820); with different inference to account for spatial correlation (clustering at the level of registration districts or poor law unions, at the level of counties, at the level of Travel-to-Work Area.

defining urban settlements (4000, 5000, 6000 inhabitants around 1820). Across these variations, the negative effect of industrial concentration on long-run wages—and associated confidence interval—is reported in Figure A12.

Alternative indices of industrial concentration We probe the robustness of our results to alternative instruments and indices of industrial concentration in Table A4. Table A4 first probes the robustness of our estimates to the exact specification, e.g., using

Table A4. The long-run effect of industrial concentration and population—alternative indices for industrial concentration.

Wage (2020)	(1)	(2)	(3)	(4)
Herfindahl index (1881, log)	-0.432			
	(0.145)			
	{26.20}			
Herfindahl index (1881, inverse)		0.127		
		(0.049)		
		{21.04}		
Herfindahl index (1881, linkages)			-1.768	
			(0.631)	
			{70.65}	
Krugman index (1881, log)				-0.076
				(0.374)
				{15.76}
Employment (1881, l_{c1})	-0.277	-0.296	-0.268	-0.322
	(0.147)	(0.149)	(0.162)	(0.218)
	{17.30}	{17.31}	{15.70}	{13.86}
Observations	428	428	428	428

Notes: A unit of observation is a cluster of settlements around 1790-1820—following the procedure in Section 2.2. Standard errors are reported between parentheses and are clustered at the level of the closest city as of 2015; and projected F-statistics are reported in brackets (following Sanderson and Windmeijer, 2016). The dependent variable is the (log) wage in 2020 (labor income estimates for small areas based on the Family Resources Survey). The two instruments are the "shift-share" predictor of industrial concentration (χ_c) defined in Section 2.3 and natural land fragmentation in the immediate fringe of urban settlements, ζ_c. Column **(1)** uses the logarithms of the Herfindahl index (1881, h_{c1}) and its instrument; column **(2)** transforms the Herfindahl index (1881, h_{c1}) and its instrument through an inverse ($f(x) = 1/(0.05 + x)$); column **(3)** constructs a weighted Herfindahl index where cross-sectoral weights are parametrized on the occupational transitions for employed males in the micro-censuses of 1851 and 1861; and column **(4)** uses instead the logarithm of distance to the average national portfolio ($\sum_j |s_{jc1} - s_{j1}|$). In column **(3)**, we add the link-weighted Herfindahl index in 1817 as an additional control.

the logarithms of the Herfindahl index (1881, h_{c1}) or its inverse (as discussed in Combes and Gobillon, 2015). We perform these robustness checks in column (1) and (2): a 20% higher Herfindahl index is associated with a 8% lower wage; and a 1.8 higher value for the index of industrial diversity (a standard deviation in the inverse transformation of the Herfindahl index) is associated with a 23% higher wage.

Column (3) relies instead on Herfindahl indices (actual and predicted) with cross-sectoral weights. More specifically, letting α_{ij} denote the symmetric transition probability between sectors i and j for employed males linked through the micro-censuses in 1851 and in 1861, one can define a Herfindahl index as $h_c = \sum_{i,j} \alpha_{ij} s_{ic} s_{jc}$, both in 1881 and in 1817, or based on predicted shares for the instrument. Intuitively, this measure coincides with our baseline measure when the matrix $\mathbf{A} = \left(\alpha_{ij}\right)_{i,j}$ is the identity matrix. The

main take-away messages are that the negative effect of industrial concentration resists these alternative specifications. For instance, a 0.10 increase in the weighted Herfindahl index is associated with 18% lower wages in 2020.

Finally, column (4) considers a different concept—local industrial "specialization"—measuring local industrial shares against those of the country-wide portfolio: $h_{c1} = \sum_j |s_{jc1} - s_{j1}|$. Under this specification of specialization (and its associated instrument based on predicted shares), we do not find a negative long-run effect. Industrial *concentration* causes long-run decline, rather than generic deviations from a synthetic aggregate economy.

Table A5. The long-run effect of industrial concentration and population—spatial spillovers.

	Wage (2020)
Herfindahl index (1881, h_{c1})	-2.240
	(1.055)
	{16.94}
Herfindahl index in nearby cities (1881, h^d_{c1})	2.691
	(2.526)
	{5.03}
Employment (1881, l_{c1})	-0.363
	(0.185)
	{8.53}
Observations	428

Notes: A unit of observation is a cluster of settlements around 1790-1820—following the procedure in Section 2.2. Standard errors are reported between parentheses and are clustered at the level of the closest city as of 2015; and projected F-statistics are reported in brackets (following Sanderson and Windmeijer, 2016). The dependent variable is the (log) wage in 2020 (labor income estimates for small areas based on the Family Resources Survey). The three instruments are the "shift-share" predictor of industrial concentration (χ_c) defined in Section 2.3, the "shift-share" predictor of industrial concentration using buffers of 40 kilometers around the city, and natural land fragmentation in the immediate fringe of urban settlements, ζ_c. The variable h^d_{c1} is an industrial concentration index using a buffer 40 kilometers around the city.

Spatial spillovers and treatment heterogeneity Our quantitative model allows for inter-city linkages through factor flows and trade but does not incorporate Jacobs externalities *across* cities. In Table A5, we provide support for this hypothesis by adding a measure of industrial concentration within 40 kilometers around each city, and instrumenting the latter with a "shift-share" predictor of industrial concentration based on initial employment within the same buffers. We find that Jacobs externalities mostly operate within a few kilometers around each city—we have 435 cities in our baseline dis-

tributed over more than 100,000 square kilometers such that a limited number of those cities would fall into 10-kilometer buffers around other cities.

Table A6. The long-run effect of industrial concentration and population—treatment heterogeneity.

Interaction with ...	Serv. (1881)	Manu. (1881)	Prim. (1881)
Wage (2020)	(1)	(2)	(3)
Herfindahl index (1881, h_{c1})	-2.738	-2.267	-3.404
	(1.108)	(1.074)	(1.811)
	{12.42}	{14.71}	{7.15}
Employment (1881, l_{c1})	-0.254	-0.200	-0.216
	(0.195)	(0.141)	(0.156)
	{4.04}	{13.92}	{21.10}
Herfindahl (1881) × Int.	0.045	-0.763	1.367
	(0.917)	(0.948)	(1.294)
	{3.83}	{7.51}	{5.91}
Observations	428	428	428

Notes: A unit of observation is a cluster of settlements around 1790-1820—following the procedure in Section 2.2. Standard errors are reported between parentheses and are clustered at the level of the closest city as of 2015; and projected F-statistics are reported in brackets (following Sanderson and Windmeijer, 2016). The dependent variable is the (log) wage in 2020 (labor income estimates for small areas based on the Family Resources Survey). The three instruments are the "shift-share" predictor of industrial concentration (χ_c) defined in Section 2.3, natural land fragmentation in the immediate fringe of urban settlements, ζ_c and its interaction with the different interacted variables.

Table A6 analyzes treatment heterogeneity with respect to the sectoral composition of cities in 1881: the incidence of services (column 1), manufacturing (column 2), and the primary sector (column 3). Interacted variables are standardized for ease of interpretation: the estimate in front of the interaction can be understood as the extent to which one standard deviation in the interacted variable affects the treatment effect. Cities that were more service-intensive exhibit a slightly weaker specialization curse, whereas manufacturing-intensive cities exhibit a slightly stronger one. These differences, however, are small, indicating limited treatment heterogeneity.

B Theory appendix

This appendix provides complements to the model (Section 4) and its quantification (Section 5). First, we provide details on how we solve the model. Next, we present model extensions that generalize the baseline model to accommodate infinitely lived agents and international trade. Finally, we provide further details on the model's parameterization and estimation: on the quantification of trade costs; on the theorem behind the model inversion (Theorem 1) and the numerical procedure; and on how the city amenities and productivities recovered in the inversion relate to past industrial concentration.

B.1 Solving the model

In this section, we propose an algorithm to solve for the equilibrium of the model forward in time, starting in any given period t. This is what allows us to solve for the counterfactual results of Section 5.2. The algorithm relies on reducing the within-period equilibrium conditions to a system of $3 \times I \times C$ equations. To obtain this system, note first that nominal wages equalize across industries within each city as workers are freely mobile across industries:

$$w_{ict} = w_{ct}.$$

Plugging this result into Equation (10), we obtain total land rents in city c as,

$$R_{ct}L_{ct} = r_{ct}H_{ct} = \frac{1-\gamma}{\gamma} w_{ct}L_{ct},$$

from which we obtain,

$$w_{ct} + R_{ct} = \frac{1}{\gamma} w_{ct}. \tag{B.1}$$

Also, from Equation (9), we get

$$r_{ct} = \left(\frac{1-\gamma}{\gamma}\right)^{1/\zeta_{ct}} w_{ct}^{1/\zeta_{ct}} L_{ct}^{1/\zeta_{ct}}. \tag{B.2}$$

Given perfect competition, the price of each variety c in industry i at the factory gate is equal to its marginal cost of production in equilibrium,

$$p_{ict} = \mathcal{T}_{ict}^{-1} w_{ct}^{\gamma} r_{ct}^{1-\gamma} = \left(\frac{1-\gamma}{\gamma}\right)^{\frac{1-\gamma}{\zeta_{ct}}} \mathcal{T}_{ict}^{-1} L_{ct}^{\frac{1-\gamma}{\zeta_{ct}}} w_{ct}^{\gamma+\frac{1-\gamma}{\zeta_{ct}}}, \tag{B.3}$$

where we used Equation (B.2). As a result, we can write the price index of industry i,

Equation (12), as,

$$P_{idt} = \left[\sum_{c=1}^{C} \left(\frac{1-\gamma}{\gamma} \right)^{-\frac{1-\gamma}{\zeta_{ct}}(\epsilon-1)} \mathcal{T}_{ict}^{\epsilon-1} L_{ct}^{-\frac{1-\gamma}{\zeta_{ct}}(\epsilon-1)} w_{ct}^{-\left(\gamma+\frac{1-\gamma}{\zeta_{ct}}\right)(\epsilon-1)} \tau_{icdt}^{1-\epsilon} \right]^{\frac{1}{1-\epsilon}}, \tag{B.4}$$

and market clearing condition (11) as,

$$w_{ct} L_{ict} = \left(\frac{1-\gamma}{\gamma} \right)^{-\frac{1-\gamma}{\zeta_{ct}}(\epsilon-1)} \tilde{T}_{ict}^{\epsilon-1} L_{ct}^{-\frac{1-\gamma}{\zeta_{ct}}(\epsilon-1)} w_{ct}^{-\left(\gamma+\frac{1-\gamma}{\zeta_{ct}}\right)(\epsilon-1)} \sum_{d=1}^{C} P_{dt}^{\sigma-1} P_{idt}^{\epsilon-\sigma} w_{dt} L_{dt} \tau_{icdt}^{1-\epsilon}, \tag{B.5}$$

where we also use Equation (B.1).

By the Fréchet distribution of idiosyncratic city tastes, the probability that a worker chooses city c equals,

$$Pr\left[U_{ct}^{m} \geq U_{dt}^{m},\ \forall d\right] = \frac{\left(\bar{a}_c \frac{w_{ct}+R_{ct}}{P_{ct}} L_{ct}^{-\nu}\right)^{1/\eta}}{\sum_{d=1}^{C} \left(\bar{a}_d \frac{w_{dt}+R_{dt}}{P_{dt}} L_{dt}^{-\nu}\right)^{1/\eta}} = \frac{\left(\frac{1}{\gamma}\bar{a}_c \frac{w_{ct}}{P_{ct}} L_{ct}^{-\nu}\right)^{1/\eta}}{\sum_{d=1}^{C} \left(\frac{1}{\gamma}\bar{a}_d \frac{w_{dt}}{P_{dt}} L_{dt}^{-\nu}\right)^{1/\eta}}.$$

In equilibrium, the fraction of workers choosing to live in c becomes equal to this probability:

$$\frac{L_{ct}}{\bar{L}} = \frac{\left(\frac{1}{\gamma}\bar{a}_c \frac{w_{ct}}{P_{ct}} L_{ct}^{-\nu}\right)^{1/\eta}}{\sum_{d=1}^{C} \left(\frac{1}{\gamma}\bar{a}_d \frac{w_{dt}}{P_{dt}} L_{dt}^{-\nu}\right)^{1/\eta}},$$

from which:

$$P_{ct} = \left(\gamma \overline{U}_t\right)^{-1} \bar{a}_c w_{ct} L_{ct}^{-(\nu+\eta)}, \tag{B.6}$$

where:

$$\overline{U}_t = \left[\frac{\sum_{d=1}^{C} \left(\frac{1}{\gamma}\bar{a}_d \frac{w_{dt}}{P_{dt}} L_{dt}^{-\nu}\right)^{1/\eta}}{\bar{L}} \right]^{\eta}.$$

Plugging this result into Equations (13) and (B.5) and rearranging Equation (B.4), we obtain the following system of equations:

$$P_{ict}^{1-\epsilon} = \sum_{d=1}^{C} \left(\frac{1-\gamma}{\gamma} \right)^{-\frac{1-\gamma}{\zeta_{dt}}(\epsilon-1)} \overline{T}_{idt}^{\epsilon-1} L_{dt}^{-\left(\frac{1-\gamma}{\zeta_{dt}}-\alpha\right)(\epsilon-1)} w_{dt}^{-\left(\gamma+\frac{1-\gamma}{\zeta_{dt}}\right)(\epsilon-1)} \tau_{idct}^{1-\epsilon} \tag{B.7}$$

$$\bar{a}_c^{1-\sigma} w_{ct}^{1-\sigma} L_{ct}^{(\nu+\eta)(\sigma-1)} = \left(\gamma \overline{U}_t\right)^{1-\sigma} \sum_{i=1}^{I} P_{ict}^{1-\sigma} \tag{B.8}$$

$$\left(\frac{1-\gamma}{\gamma}\right)^{\frac{1-\gamma}{\zeta_{ct}}(\epsilon-1)} w_{ct}^{1+\left(\gamma+\frac{1-\gamma}{\zeta_{ct}}\right)(\epsilon-1)} L_{ct}^{1+\left(\frac{1-\gamma}{\zeta_{ct}}-\alpha\right)(\epsilon-1)} =$$
$$\left(\gamma \overline{U}_t\right)^{1-\sigma} \sum_{i=1}^{I}\sum_{d=1}^{C} \overline{T}_{ict}^{\epsilon-1} P_{idt}^{\epsilon-\sigma} \bar{a}_d^{\sigma-1} w_{dt}^{\sigma} L_{dt}^{1-(\nu+\eta)(\sigma-1)} \tau_{icdt}^{1-\epsilon} \tag{B.9}$$

where:

$$\overline{T}_{ict} = T_{ict} f_i\left(L_{c,t-1}, \left\{L_{jc,t-1}\right\}_{j\in I}\right),$$

is the part of Total Factor Productivity that is exogenous in period t.

Applying the change in variables

$$\begin{aligned} x_{ict}^1 &= P_{ict}^{1-\epsilon} \\ x_{ict}^2 &= w_{ict}^{1-\sigma} L_{ct}^{(\nu+\eta)(\sigma-1)} \\ x_{ict}^3 &= w_{ict}^{1+\left(\gamma+\frac{1-\gamma}{\zeta_{ct}}\right)(\epsilon-1)} L_{ct}^{1+\left(\frac{1-\gamma}{\zeta_{ct}}-\alpha\right)(\epsilon-1)} \end{aligned} \tag{B.10}$$

and recalling that $w_{ict} = w_{ct}$, Equations (B.7), (B.8) and (B.9) can be rewritten as the following system of $3 \times I \times C$ equations:

$$\begin{aligned} x_{ict}^1 &= \sum_{j=1}^{I}\sum_{d=1}^{C} \left(x_{jdt}^2\right)^{\frac{\alpha+\gamma}{\kappa_{dt}}\frac{\epsilon-1}{\sigma-1}} \left(x_{jdt}^3\right)^{-\left(1-\frac{1+\nu+\eta}{\kappa_{dt}}\right)} K_{icjdt}^1 \\ x_{ict}^2 &= \sum_{j=1}^{I}\sum_{d=1}^{C} \left(x_{jdt}^1\right)^{\frac{\sigma-1}{\epsilon-1}} K_{icjdt}^2 \\ x_{ict}^3 &= \sum_{j=1}^{I}\sum_{d=1}^{C} \left(x_{jdt}^1\right)^{-\frac{\epsilon-\sigma}{\epsilon-1}} \left(x_{jdt}^2\right)^{-\left(1-\frac{\alpha+\gamma}{\kappa_{dt}}\frac{\epsilon-1}{\sigma-1}\right)} \left(x_{jdt}^3\right)^{\frac{1+\nu+\eta}{\kappa_{dt}}} K_{icjdt}^3 \end{aligned} \tag{B.11}$$

where

$$\kappa_{dt} = 1 + \nu + \eta + \left[\frac{1-\gamma}{\zeta_{dt}} - \alpha + \left(\gamma + \frac{1-\gamma}{\zeta_{dt}}\right)(\nu+\eta)\right](\epsilon-1) \tag{B.12}$$

is a combination of structural parameters, and K_{icjdt}^1, K_{icjdt}^2 and K_{icjdt}^3 are the following functions of exogenous variables:

$$K_{icjdt}^1 = \begin{cases} \left(\frac{1-\gamma}{\gamma}\right)^{-\frac{1-\gamma}{\zeta_{dt}}(\epsilon-1)} \overline{T}_{jdt}^{\epsilon-1} \tau_{jdct}^{1-\epsilon} & \text{if } i = j \\ 0 & \text{otherwise} \end{cases}$$

$$K_{icjdt}^2 = \begin{cases} \left(\gamma \overline{U}_t\right)^{1-\sigma} \bar{a}_c^{\sigma-1} & \text{if } c = d \\ 0 & \text{otherwise} \end{cases}$$

$$K_{icjdt}^3 = \left(\gamma \overline{U}_t\right)^{1-\sigma} \left(\frac{1-\gamma}{\gamma}\right)^{-\frac{1-\gamma}{\zeta_{dt}}(\epsilon-1)} \overline{T}_{jct}^{\epsilon-1} \bar{a}_d^{\sigma-1} \tau_{jcdt}^{1-\epsilon}$$

where,

$$\overline{T}_{ict} = T_{ict} L_{c,t-1}^{\rho} \left[\sum_{j} \left(\frac{L_{jc,t-1}}{L_{c,t-1}} \right)^{2} \right]^{-\lambda} \tag{B.13}$$

is the productivity component which is exogenous in period t.

We propose the following solution algorithm to solve this system starting in a given period t. First, guess an initial distribution of x_{ict}^1, x_{ict}^2 and x_{ict}^3 in period t. Next, insert the guesses on the right-hand side of system (B.11) to obtain an updated guess of x_{ict}^1, x_{ict}^2 and x_{ict}^3, and iterate on system (B.11) until convergence. With the equilibrium values of x_{ict}^1, x_{ict}^2 and x_{ict}^3 in hand, express period-t price indices, wages, population and sectoral employment levels by inverting the system (B.10). Finally, obtain TFP in period $t+1$ from Equation (B.13) and repeat the procedure for subsequent periods.

B.2 Extensions

We now provide two extensions to the baseline model: one in which workers live forever instead of just one period; and one in which British cities engage in international trade.

A model with infinitely-lived workers We now present a version of the model in which workers are infinitely lived and make forward-looking decisions about their locations, subject to migration costs across periods.

We assume that a worker m who resided in city c_{t-1} at the end of period $t-1$ chooses her city c_t for the next period to maximize her total discounted stream of future utilities. This implies that her value function is given by,

$$v_{c_{t-1},t}^{m} = \max_{c_t} \left\{ \max_{i_t} \ln U_{i_t,c_t,t}^{m} - \ln m_{c_{t-1},c_t} + \beta \mathbf{E}_t \left[v_{c_t,t+1}^{m} \right] \right\},$$

where $U_{i_t,c_t,t}^{m}$ is the amenity-adjusted real income in period t, given by Equation (4), and m_{c_{t-1},c_t} is the cost of moving from city c_{t-1} to city c_t. The last term, $\mathbf{E}_t \left[v_{c_t,t+1}^{m} \right]$, is the worker's continuation value, which is discounted by a factor $\beta \in [0,1)$. The continuation value includes an expectation because the future taste shocks for cities, given by Equation (7), are not yet realized in period t. The model presented in Section 4 can be viewed as a special case of this more general model, with $\beta = 0$ and $m_{c,d} = 1$ for all cities c and d.

Given the Fréchet distribution of idiosyncratic city tastes, it can be shown that the expected value of a city c at time t, $V_{ct} = e^{\mathbf{E}_t \left[v_{c,t+1}^{m} \right]}$, evolves according to the equation,

$$V_{ct} = \sum_{d=1}^{C} \left(\bar{a}_d \frac{w_{d,t+1} + R_{d,t+1}}{P_{d,t+1}} L_{d,t+1}^{-\nu} m_{cd}^{-1} V_{d,t+1}^{\beta} \right)^{1/\eta}, \tag{B.14}$$

while the fraction of workers who choose to move from city c to city d between periods $t-1$ and t equals,

$$\mu_{c,d,t-1} = \frac{\left(\bar{a}_d \frac{w_{dt}+R_{dt}}{P_{dt}} L_{dt}^{-\nu} m_{cd}^{-1} V_{dt}^{\beta}\right)^{1/\eta}}{\sum_{d'=1}^{C}\left(\bar{a}_{d'} \frac{w_{d',t}+R_{d',t}}{P_{d',t}} L_{d',t}^{-\nu} m_{c,d'}^{-1} V_{d',t}^{\beta}\right)^{1/\eta}}.$$

As a consequence, the population of a city d evolves according to the equation,

$$L_{dt} = \sum_{c=1}^{C} \frac{\left(\bar{a}_d \frac{w_{dt}+R_{dt}}{P_{dt}} L_{dt}^{-\nu} m_{cd}^{-1} V_{dt}^{\beta}\right)^{1/\eta}}{\sum_{d'=1}^{C}\left(\bar{a}_{d'} \frac{w_{d',t}+R_{d',t}}{P_{d',t}} L_{d',t}^{-\nu} m_{c,d'}^{-1} V_{d',t}^{\beta}\right)^{1/\eta}} L_{c,t-1}. \tag{B.15}$$

Equations (B.14) and (B.15), together with Equations (11), (13) and (15), determine the equilibrium of the model with infinitely-lived workers. Note that Equation (15), which we use to estimate the strength of dynamic externalities, is unchanged in this more general model.

A model with international trade Next, we present a version of the model in which British cities trade with foreign markets, subject to international trade costs.

We assume that, besides the C British cities, there exists an additional location $C+1$ that represents the rest of the world. City c can trade with the rest of the world at an iceberg cost $\tau_{i,c,C+1,t} \geq 1$ in period t. Note that international trade costs are allowed to vary by industry i, city c and time t. Just like locations within Britain, the rest of the world is endowed with exogenous amenities $\bar{a}_{C+1}$, fundamental industry productivities $\bar{T}_{i,C+1,t}$, and land supply elasticity $\zeta_{C+1,t} - 1$.

Given these assumptions, this model can be viewed as a special case of our baseline model in which the rest of the world is one of the cities. As a consequence, the model's equilibrium is still determined by Equations (15) and (B.11), except that the index c runs from 1 to $C+1$. Note that Equation (15), which we use to estimate the strength of dynamic externalities, is unchanged in the model with international trade. This means that a model with trade between British cities and the rest of the world in the 19th century would yield the same estimates for dynamic externalities in British cities as our baseline model in which 19th-century international trade is not explicitly modeled.

B.3 Complements to the model parametrization and estimation

In this section, we provide further details on the model's quantification. First, we describe how we compute trade costs. Next, we prove the main theorem behind the model

inversion (Theorem 1) and describe the numerical procedure applied to run the inversion. Finally, we show how the city amenities and productivities recovered in the inversion relate to British cities' past industrial concentration.

Trading costs over time To compute trading costs over time, we follow Alvarez-Palau et al. (2025) and combine the main transport modes at the time. Specifically, we combine information on: (i) the road network that was represented by turnpike roads; (ii) waterways consisting of rivers, canals and coastal routes; and (iii) the railway network and railway stations observed in 1880 (Gregory and Henneberg, 2010) in a multi-modal transport network and calculate the least cost path between all city-centroids of our sample. We connect the different transport modes and city-centroids with direct linear routes. Straight-line distances between points are calculated using the Manhattan distance metric, which reflects the reality that roads typically do not follow direct, 'as-the-crow-flies' paths. We consider the following straight-line connections:

- Every city-centroid located within a 15km radius is interconnected through direct linear routes.
- Every city-centroid located within 10km from the nearest river is interconnected through linear routes.
- Every city-centroid located within 10km from the nearest turnpike road to the east, south, west and north is interconnected through linear routes.
- Every city-centroid located within 10km from the nearest port is interconnected through linear routes.
- Every city-centroid located within 10km from the nearest 1880 railway station is interconnected through linear routes.
- Every seaport located within 10km from the nearest river is connected through linear routes.
- Every seaport located within 10km from the nearest turnpike road is interconnected through linear routes.
- Every seaport located within 10km from the nearest railway station is interconnected through linear routes.
- Every railway station located within 10km from the nearest river is interconnected through linear routes.

- Every railway station located within 10km from the nearest turnpike road is interconnected through linear routes.

All other distances are calculated along the specific transport network path. To translate distances into costs, we consider the following transport costs in ascending order: (i) cost of shipping goods on coastal waterways: 0.003 per mile; (ii) cost of shipping goods on rail: 0.027 per mile; (iii) cost of shipping goods on rivers or canals: 0.036 per mile; (iv) cost of shipping goods on roads: 0.213 per mile. In addition, we assume fixed transshipment costs between road and railway, waterways, or coastal routes of 1.895. Lastly, we assume that transport between the city-centroid and the nearest sea or river port, railway station or turnpike road is not distance dependent, i.e., we assume that actual production locations within cities are directly connected to relevant transport modes. This is on line with reality where we see that canals meander through Manchester, connecting different production locations, and we also see railways branching out to industrial districts.

Proof of Theorem 1 Rearranging the period-2 version of Equations (B.7) to (B.9) yields:

$$P_{ic2}^{1-\epsilon} = \sum_{d=1}^{C} \left(\frac{1-\gamma}{\gamma}\right)^{-\frac{1-\gamma}{\zeta_{d2}}(\epsilon-1)} \overline{T}_{id2}^{\epsilon-1} L_{d2}^{-\left(\frac{1-\gamma}{\zeta_{d2}}-\alpha\right)(\epsilon-1)} w_{d2}^{-\left(\gamma+\frac{1-\gamma}{\zeta_{d2}}\right)(\epsilon-1)} \tau_{idc2}^{1-\epsilon} \tag{B.16}$$

$$\left(\frac{\bar{a}_c}{\overline{U}_2}\right)^{1-\sigma} w_{c2}^{1-\sigma} L_{c2}^{(\nu+\eta)(\sigma-1)} = \gamma^{1-\sigma} \sum_{i=1}^{I} P_{ic2}^{1-\sigma} \tag{B.17}$$

$$\begin{aligned} &\left(\frac{1-\gamma}{\gamma}\right)^{\frac{1-\gamma}{\zeta_{c2}}(\epsilon-1)} w_{c2}^{1+\left(\gamma+\frac{1-\gamma}{\zeta_{c2}}\right)(\epsilon-1)} L_{c2}^{\left(\frac{1-\gamma}{\zeta_{c2}}-\alpha\right)(\epsilon-1)} \overline{T}_{ic2}^{1-\epsilon} L_{ic2} = \\ &\gamma^{1-\sigma} \sum_{d=1}^{C} P_{id2}^{\epsilon-\sigma} \left(\frac{\bar{a}_d}{\overline{U}_2}\right)^{\sigma-1} w_{d2}^{\sigma} L_{d2}^{1-(\nu+\eta)(\sigma-1)} \tau_{icd2}^{1-\epsilon} \end{aligned} \tag{B.18}$$

from which we obtain the following system of $3IC$ equations:

$$\begin{aligned} \widehat{x}_{ic}^{1} &= \sum_{j=1}^{I} \sum_{d=1}^{C} \left(\widehat{x}_{jd}^{3}\right)^{-1} \widehat{K}_{icjd}^{1} \\ \widehat{x}_{ic}^{2} &= \sum_{j=1}^{I} \sum_{d=1}^{C} \left(\widehat{x}_{jd}^{1}\right)^{\frac{\sigma-1}{\epsilon-1}} \widehat{K}_{icjd}^{2} \\ \widehat{x}_{ic}^{3} &= \sum_{j=1}^{I} \sum_{d=1}^{C} \left(\widehat{x}_{jd}^{1}\right)^{-\frac{\epsilon-\sigma}{\epsilon-1}} \left(\hat{x}_{jd}^{2}\right)^{-1} \widehat{K}_{icjd}^{3} \end{aligned}$$

where $\widehat{x}_{ic}^{1} = P_{ic2}^{1-\epsilon}$, $\widehat{x}_{ic}^{2} = \left(\frac{\bar{a}_c}{\overline{U}_2}\right)^{1-\sigma}$, and $\widehat{x}_{ic}^{3} = \overline{T}_{ic2}^{1-\epsilon}$.

The solution to this system exists and is unique if the largest eigenvalue of matrix $\mathbf{A}$ is less or equal to one in absolute value (Allen et al., 2020) (up to scale if the eigenvalue

is equal to one), where $\mathbf{A}$ is:

$$\mathbf{A} = \begin{bmatrix} 0 & 0 & 1 \\ \left|\frac{\sigma-1}{\epsilon-1}\right| & 0 & 0 \\ \left|\frac{\epsilon-\sigma}{\epsilon-1}\right| & 1 & 0 \end{bmatrix}.$$

One can easily verify that, under the assumption $\epsilon > \sigma > 1$, the largest eigenvalue of $\mathbf{A}$ is equal to 1.

Numerical procedure to invert the model The challenge involved in solving Equations (B.16) to (B.18) is that the system is homogeneous of degree one in unobserved fundamentals. While iteration can be proven to work in similar systems if the degree of homogeneity is below one (Allen et al., 2020), this is no longer necessarily true if it is equal to one.

To circumvent this issue, we borrow from Desmet et al. (2018) and approximate the system in the following way:

$$P_{ic2}^{1-\epsilon} = \sum_{d=1}^{C} \left(\frac{1-\gamma}{\gamma}\right)^{-\frac{1-\gamma}{\zeta_{d2}}(\epsilon-1)} \overline{T}_{id2}^{(\epsilon-1)(1-\delta)} L_{d2}^{-\left(\frac{1-\gamma}{\zeta_{d2}}-\alpha\right)(\epsilon-1)} w_{d2}^{-\left(\gamma+\frac{1-\gamma}{\zeta_{d2}}\right)(\epsilon-1)} \tau_{idc2}^{1-\epsilon} \tag{B.19}$$

$$\left(\frac{\bar{a}_c}{\overline{U}_2}\right)^{1-\sigma} w_{c2}^{1-\sigma} L_{c2}^{(\nu+\eta)(\sigma-1)} = \gamma^{1-\sigma} \sum_{i=1}^{I} P_{ic2}^{1-\sigma} \tag{B.20}$$

$$\begin{aligned} &\left(\frac{1-\gamma}{\gamma}\right)^{\frac{1-\gamma}{\zeta_{c2}}(\epsilon-1)} w_{c2}^{1+\left(\gamma+\frac{1-\gamma}{\zeta_{c2}}\right)(\epsilon-1)} L_{c2}^{\left(\frac{1-\gamma}{\zeta_{c2}}-\alpha\right)(\epsilon-1)} \overline{T}_{ic2}^{1-\epsilon} L_{ic2} = \\ &\gamma^{1-\sigma} \sum_{d=1}^{C} P_{id2}^{\epsilon-\sigma-\delta} \left(\frac{\bar{a}_d}{\overline{U}_2}\right)^{\sigma-1} w_{d2}^{\sigma} L_{d2}^{1-(\nu+\eta)(\sigma-1)} \tau_{icd2}^{1-\epsilon} \end{aligned} \tag{B.21}$$

where the only difference relative to Equations (B.16) to (B.18) is that the parameter δ appears in Equations (B.19) and (B.21). As $\delta \to 0$, this system becomes identical to (B.16) to (B.18).

Intuitively, for any small but positive δ, the system (B.19) and (B.21) is homogeneous to a degree below one. Therefore, it can be solved by iteration. In practice, we start with a $\delta = 0.128$ and gradually lower δ to get closer and closer to the original system. We stop when δ is low enough that the solution of the model under the recovered amenities $\{\bar{a}_c\}_c$ and city-industry productivities $\left\{\overline{T}_{ic2}\right\}_{i,c}$, computed as in Section 4, is sufficiently close to the data.

The structural estimates for dynamic spillovers Section 5.1 describes (i) how we recover the distribution of city amenities $\bar{a}_c$ and city-industry productivities $\overline{T}_{ic2}$ around 2020 from wages w_{c2} and employment by city-industry L_{ic2} and (ii) the empirical estima-

tion of Equation (16) (see, e.g., Table 6).

Figure B1. The structural estimates for dynamic spillovers—an illustration.

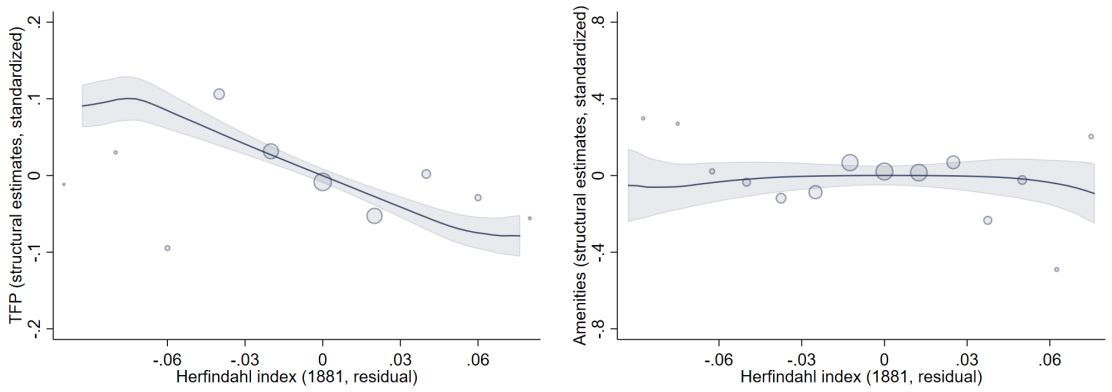

(a) Productivity (b) Amenity

Notes: Panel **(a)** displays the relationship between industrial concentration in 1881 and standardized productivities $\overline{T}_{ic2}$ across our 435 cities and 88 industries; both measures are cleaned for all controls used in Table 2 and industry fixed effects. Panel **(b)** displays the relationship between industrial concentration in 1881 and standardized amenities $\bar{a}_c$; the x-axis and y-axis variables are then cleaned for all controls used in Table 2.

In this Appendix, we provide an illustration of the effect of dynamic spillovers in the spirit of Figure 9: we residualize city-industry (standardized) productivities $\overline{T}_{ic2}$ and (standardized) amenities $\bar{a}_c$, and we show their dependence on industrial concentration in 1881. One can see that industrial concentration is negatively associated with future city productivity, but not with the estimated city amenities—consistent with the assumptions underlying our counterfactual experiments.